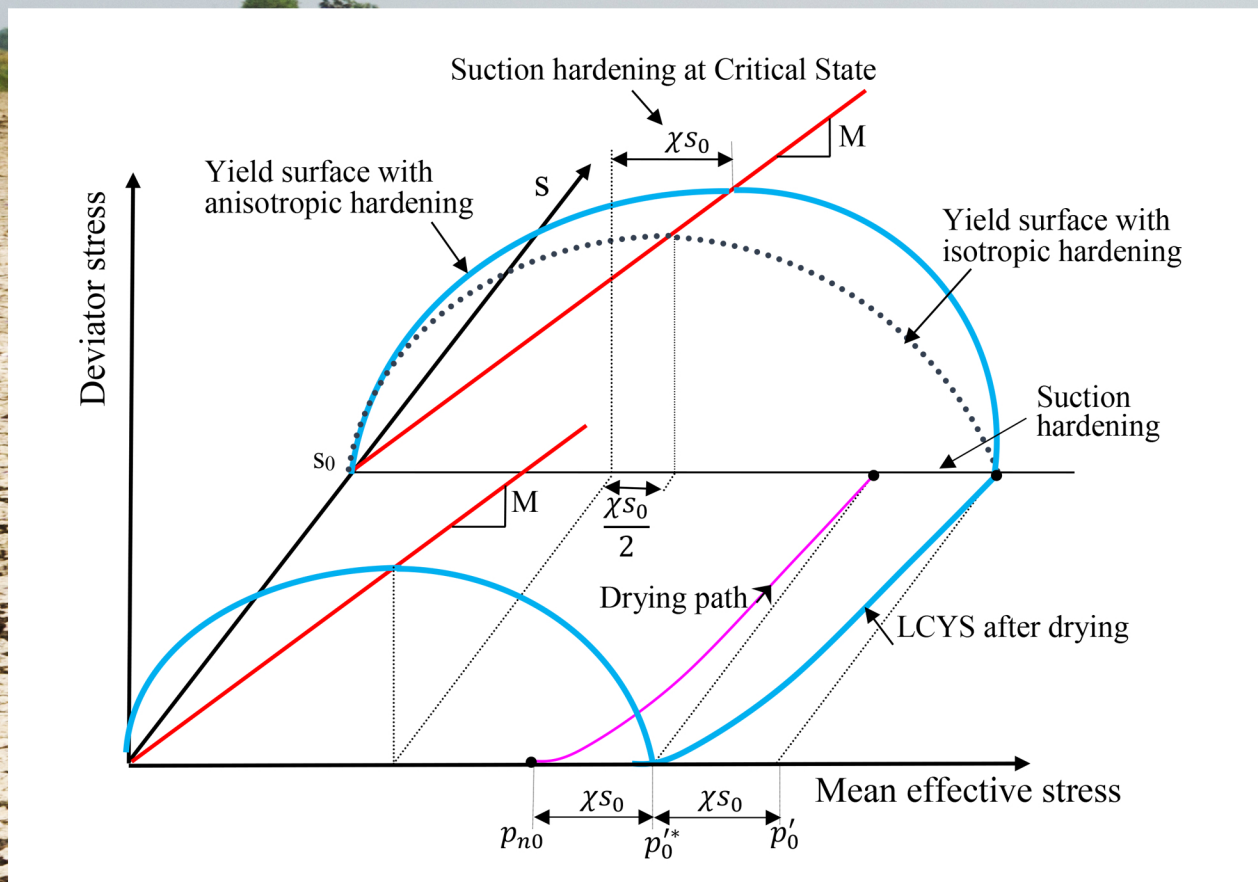


Towards a Unified Soil Mechanics Theory

The Use of Effective Stresses in Unsaturated Soils

Third Edition



Eduardo Rojas

Bentham Books

**Towards a Unified Soil
Mechanics Theory:
The Use of Effective Stresses in
Unsaturated Soils
(Third Edition)**

Authored by

Eduardo Rojas

*Universidad Autónoma de Querétaro
México*

Towards a Unified Soil Mechanics Theory: The Use of Effective Stresses in Unsaturated Soils (Third Edition)

Author: Eduardo Rojas

ISBN (Online): 978-981-5050-35-6

ISBN (Print): 978-981-5050-36-3

ISBN (Paperback): 978-981-5050-37-0

© 2022, Bentham Books imprint.

Published by Bentham Science Publishers Pte. Ltd. Singapore. All Rights Reserved.

First published in 2022

BENTHAM SCIENCE PUBLISHERS LTD.

End User License Agreement (for non-institutional, personal use)

This is an agreement between you and Bentham Science Publishers Ltd. Please read this License Agreement carefully before using the ebook/echapter/ejournal (“**Work**”). Your use of the Work constitutes your agreement to the terms and conditions set forth in this License Agreement. If you do not agree to these terms and conditions then you should not use the Work.

Bentham Science Publishers agrees to grant you a non-exclusive, non-transferable limited license to use the Work subject to and in accordance with the following terms and conditions. This License Agreement is for non-library, personal use only. For a library / institutional / multi user license in respect of the Work, please contact: permission@benthamscience.net.

Usage Rules:

1. All rights reserved: The Work is the subject of copyright and Bentham Science Publishers either owns the Work (and the copyright in it) or is licensed to distribute the Work. You shall not copy, reproduce, modify, remove, delete, augment, add to, publish, transmit, sell, resell, create derivative works from, or in any way exploit the Work or make the Work available for others to do any of the same, in any form or by any means, in whole or in part, in each case without the prior written permission of Bentham Science Publishers, unless stated otherwise in this License Agreement.
2. You may download a copy of the Work on one occasion to one personal computer (including tablet, laptop, desktop, or other such devices). You may make one back-up copy of the Work to avoid losing it.
3. The unauthorised use or distribution of copyrighted or other proprietary content is illegal and could subject you to liability for substantial money damages. You will be liable for any damage resulting from your misuse of the Work or any violation of this License Agreement, including any infringement by you of copyrights or proprietary rights.

Disclaimer:

Bentham Science Publishers does not guarantee that the information in the Work is error-free, or warrant that it will meet your requirements or that access to the Work will be uninterrupted or error-free. The Work is provided "as is" without warranty of any kind, either express or implied or statutory, including, without limitation, implied warranties of merchantability and fitness for a particular purpose. The entire risk as to the results and performance of the Work is assumed by you. No responsibility is assumed by Bentham Science Publishers, its staff, editors and/or authors for any injury and/or damage to persons or property as a matter of products liability, negligence or otherwise, or from any use or operation of any methods, products instruction, advertisements or ideas contained in the Work.

Limitation of Liability:

In no event will Bentham Science Publishers, its staff, editors and/or authors, be liable for any damages, including, without limitation, special, incidental and/or consequential damages and/or damages for lost data and/or profits arising out of (whether directly or indirectly) the use or inability to use the Work. The entire liability of Bentham Science Publishers shall be limited to the amount actually paid by you for the Work.

General:

1. Any dispute or claim arising out of or in connection with this License Agreement or the Work (including non-contractual disputes or claims) will be governed by and construed in accordance with the laws of Singapore. Each party agrees that the courts of the state of Singapore shall have exclusive jurisdiction to settle any dispute or claim arising out of or in connection with this License Agreement or the Work (including non-contractual disputes or claims).
2. Your rights under this License Agreement will automatically terminate without notice and without the

need for a court order if at any point you breach any terms of this License Agreement. In no event will any delay or failure by Bentham Science Publishers in enforcing your compliance with this License Agreement constitute a waiver of any of its rights.

3. You acknowledge that you have read this License Agreement, and agree to be bound by its terms and conditions. To the extent that any other terms and conditions presented on any website of Bentham Science Publishers conflict with, or are inconsistent with, the terms and conditions set out in this License Agreement, you acknowledge that the terms and conditions set out in this License Agreement shall prevail.

Bentham Science Publishers Pte. Ltd.

80 Robinson Road #02-00

Singapore 068898

Singapore

Email: subscriptions@benthamscience.net



CONTENTS

FOREWORD	i
PREFACE	iii
DEDICATION	vi
CHAPTER 1 INTRODUCTION	1
1.1. DIFFERENT APPROACHES FOR UNSATURATED SOILS	1
1.2. EFFECTIVE STRESSES	4
CHAPTER 2 THE EFFECTIVE STRESS EQUATION	10
2.1. INTRODUCTION	10
2.2. THE EFFECTIVE STRESS EQUATION	11
CHAPTER 3 THE POROUS-SOLID MODEL	22
3.1. INTRODUCTION	22
3.2. DIFFERENT POROUS-SOLID MODELS	23
3.2.1. Distinct Element Models.....	26
3.2.2. Random Models.....	30
3.2.3. Network Models	40
3.3. THE NETWORK MODEL	43
3.4. MECHANISMS OF WETTING AND DRYING	46
3.4.1. Main Drying Curve.....	47
3.4.2. Main Wetting Curve	47
3.4.3. Secondary and Scanning Curves.....	48
3.5. EFFECTIVE STRESS PARAMETERS	49
CHAPTER 4 THE PROBABILISTIC POROUS-SOLID MODEL	56
4.1. INTRODUCTION	56
4.2. THE PROBABILISTIC MODEL	57
4.3. MAIN WETTING CURVE	59
4.4. MAIN DRYING CURVE	63
4.5. SATURATED AND DRY VOLUMES	65
4.6. SCANNING CURVES	72
4.6.1. Drying –Wetting Cycle.....	73
4.6.2. Wetting-Drying Cycle.....	74
4.7. ASSESSMENT OF THE PROBABILISTIC MODEL	77
4.8. PARAMETRIC ANALYSIS	80
CHAPTER 5 APPLICATIONS OF THE POROUS-SOLID MODEL	83
5.1. INTRODUCTION	83
5.2. MERCURY INTRUSION POROSIMETRY TESTS	84
5.3. SOIL-WATER RETENTION CURVES	88
5.4. OBTAINING THE PORE SIZE DISTRIBUTION	99
CHAPTER 6 COMPRESSION STRENGTH OF SOILS	104
6.1. INTRODUCTION	104
6.2. NUMERICAL AND EXPERIMENTAL COMPARISONS	105
CHAPTER 7 TENSILE STRENGTH	112
7.1. INTRODUCTION	112
7.2. TENSILE TESTS	113
CHAPTER 8 VOLUMETRIC BEHAVIOR	118
8.1. INTRODUCTION	118
8.2. PROPOSED EQUATION	121
8.3. ELASTOPLASTIC FRAMEWORK	125
8.4. NUMERICAL AND EXPERIMENTAL COMPARISONS	130
8.4.1. Tests by Fleureau <i>et al.</i>	130
8.4.2. Tests by Futai and Almeida	134

8.4.3. Tests by Cunningham <i>et al.</i>	140
8.4.4. Tests by Thu <i>et al.</i>	144
CHAPTER 9 COLLAPSE UPON WETTING	147
9.1. INTRODUCTION	147
9.2. VOLUMETRIC ELASTOPLASTIC FRAMEWORK	151
9.3. COMPACTED SOILS	156
9.4. NUMERICAL AND EXPERIMENTAL COMPARISONS	160
CHAPTER 10 EXPANSIVE SOILS	171
10.1. INTRODUCTION	171
10.2. BACKGROUND	172
10.3. EXTENDED ELASTOPLASTIC FRAMEWORK	176
10.4. EXPERIMENTAL AND NUMERICAL COMPARISONS	183
10.4.1. Tests by Romero <i>et al.</i>	183
10.4.2. Tests by Alonso <i>et al.</i>	194
CHAPTER 11 HYDRO-MECHANICAL COUPLING	203
11.1. INTRODUCTION	203
11.2. PROCEDURE	208
11.3. NUMERICAL AND EXPERIMENTAL COMPARISONS	210
11.3.1. Tests by Chiu and Ng.....	210
11.3.2. Tests by Ng and Pang	214
11.3.3. Tests by Sun <i>et al.</i>	217
CHAPTER 12 A FULLY COUPLED CRITICAL STATE MODEL	222
12.1. BACKGROUND	222
12.2. CRITICAL STATE	224
12.3. GENERAL ELASTOPLASTIC FRAMEWORK	226
12.4. MECHANICAL MODEL	230
12.5. NUMERICAL AND EXPERIMENTAL COMPARISONS	237
12.5.1. Tests by Futai and Almeida	238
12.5.2. Tests by Cui and Delage	241
12.5.3. Tests by Garakani <i>et al.</i>	247
CHAPTER 13 RETENTION CURVES IN DEFORMING SOILS	254
13.1. INTRODUCTION	254
13.2. PROCEDURE	256
13.3. MODELING THE SWRC	257
13.3.1. Tests by Gao <i>et al.</i>	258
13.3.2. Tests by Salager <i>et al.</i>	264
CHAPTER 14 UNDRAINED TESTS	270
14.1. INTRODUCTION	270
14.2. NUMERICAL AND EXPERIMENTAL COMPARISONS	272
14.2.1. Tests by Jotisankasa <i>et al.</i>	272
14.2.2. Tests by Sun <i>et al.</i>	275
CHAPTER 15 COMPACTED SOILS	284
15.1. INTRODUCTION	284
15.2. ELASTOPLASTIC FRAMEWORK	288
15.3. NUMERICAL AND EXPERIMENTAL COMPARISONS	296
15.3.1. Tests by Sun <i>et al.</i>	296
15.3.2. Tests by Jotisankasa <i>et al.</i>	300
15.3.3. Tests by Tarantino and De Col	302
CHAPTER 16 HYDRAULIC CONDUCTIVITY	312
16.1. INTRODUCTION	312
16.2. CAPILLARY FLOW	316
16.3. NUMERICAL AND EXPERIMENTAL COMPARISONS	319
REFERENCES	329
SUBJECT INDEX	350

FOREWORD

As rightly suggested by Prof. Serge Leroueil in the preface to a previous edition of the present version of Prof. Eduardo Rojas' book, a thorough elucidation of the essential features of the hydro-mechanical behavior of unsaturated soils, still a rather elusive endeavor, has been closely linked with efforts to isolate the relevant, effective stress fields governing their mechanical response. This book is a commendable attempt at demonstrating the suitability of the effective stress principle in defining a unified theoretical framework within which the most essential features of unsaturated soil behavior can be explained, and thus experimentally demonstrated, when the key constitutive relationships are presented as an extension of classical saturated soil mechanics, particularly in its three traditional categories: permeability and seepage, shear strength, and volume change.

In the present edition of the book, further elaboration on some of the contents of the original 12 chapters of the book is presented, including additional experimental evidence substantiating the appropriateness of a network porous-solid model postulated by Prof. Rojas that considers both micropores and macropores, and their inherent interconnections, for either dry, partially saturated, or saturated soils. The network model presents several outstanding features, including its apparent ability to reasonably reproduce the structure of the test soil based on grain and pore-size distributions, simulate soil-water retention curves and assess Bishop's effective stress parameter. Furthermore, a probabilistic solid-porous model is introduced to considerably reduce the memory storage requirements during the explicit integration of all constitutive equations *via* computational drivers. Finally, a unified elastoplastic framework for expansive, collapsible, and compacted soil materials is introduced.

Four additional chapters have been added to the present edition of the book, including a simulation of soil-water retention curves *via* the porous-solid model as the test soil deforms (Chapter 13); simulation of undrained triaxial testing on unsaturated soils *via* a fully coupled hydromechanical constitutive model (Chapter 14); simulation of volumetric behavior of compacted soils under different stress paths *via* a coupled model (Chapter 15); and, finally, application of the probabilistic porous network model to establish an analytical equation for the relative hydraulic conductivity (Chapter 16). Results from well-thought-out experimental efforts reported by fellow scholars in the literature have demonstrated the potential of these frameworks in capturing, to a very promising extent, the hydromechanical response of unsaturated soils.

In his preface to the previous edition, Prof. Leroueil asked himself whether it was necessary to put all this information together into one single eBook, and his answer was a grammatically resounding “yes,” highlighting the subtle continuity and congruence of topics in one single document, from schematically thorough physical models to the equivalent effective stress equation and its practical applications. I could not agree more, and hence would like to emphasize another critical dimension to Prof. Eduardo Rojas’ scholarly work: its manifest potential as invaluable reference material in our quest to overcome the persistent challenge to change in the advancement of unsaturated soil mechanics in undergraduate education and civil engineering practice.

Laureano R. Hoyos
University of Texas at Arlington,
Arlington, Texas, U.S.A.

PREFACE

With the introduction of the effective stress concept, the behavior of saturated soils could be clearly understood, and the basic principles of saturated soil mechanics could be established. The effective stress principle states that the strength and volumetric behavior of saturated materials are exclusively controlled by effective stresses. Constitutive models for saturated materials of different types are all based on the effective stress principle. Later, based on the principles of thermomechanics, the Critical State theory combined the strength and volumetric behavior of saturated soils in a simple and powerful constitutive model. A great number of models for saturated soils are based on the Critical State theory.

Things did not go so smoothly for unsaturated materials. More than fifty years ago, Alan W. Bishop proposed an equation for the effective stresses of unsaturated soils. However, this equation was widely criticized because it could not explain by itself the phenomenon of collapse upon wetting of soils. In addition, Bishop's effective stress parameter χ showed to be extremely elusive and difficult to determine experimentally. Given these difficulties, the use of the so-called independent stress variables (mainly net stress and suction) became common in unsaturated soil mechanics. Different equations for the strength and volumetric behavior of soils were proposed based on these variables. Then, the theory for unsaturated soils became distant from that of saturated materials. The Barcelona Basic Model represents one of the simplest and most accomplished models within this trend. The Barcelona Basic Model enhanced the Critical State theory to include unsaturated materials and give a plausible explanation to the phenomenon of collapse upon wetting. This model proved that this phenomenon could only be modeled if, in addition to a volumetric equation, a proper elastoplastic framework was included. However, the simulation of some particular phenomena related to the strength and volumetric behavior of unsaturated soils, appeals for the inclusion of the hysteresis of the soil-water retention curve and the hydro-mechanical coupling observed in unsaturated materials. The difficulties met in introducing these aspects into the independent stress variables models made it clear that a different approach should be considered. Then, gradually elastoplastic models based on Bishop's effective stress equation started to appear, showing their superiority by including the hysteresis of the soil-water retention curve and the hydromechanical coupling of unsaturated soils. And finally, the debate about the appropriateness of Bishop's equation to represent the effective stresses for unsaturated soils is slowly coming to an end. This transformation in the construction of constitutive models for unsaturated soils is also leading towards a unified soil mechanics theory.

This book shows how the effective stress principle can be applied to simulate the strength and volumetric behavior of unsaturated soils employing the same equations commonly used for saturated materials. The book initiates with an analysis of the stresses transmitted to the different phases of an unsaturated soil when it is loaded. Contrary to other analyses, and based on the simulation of wetting-drying processes in porous media, it is considered here that unsaturated soils may exhibit three different fractions: an unsaturated fraction represented by medium size pores, a saturated fraction represented by micropores, and eventually, a dry fraction represented by very large pores. Each one of these fractions is linked to a different effective stress equation. The analysis results in an expression for the stresses carried by the solid skeleton of the material. This expression can be written in the same terms as Bishop's effective stress equation and leads to an analytical expression for Bishop's effective stress parameter χ . However, the variables required to obtain this parameter χ cannot be experimentally determined. For that purpose, a network solid-porous model is developed. This network model can approximately reproduce the structure of soils based on the grain and pore size distributions of the material and is capable of determining the allocation of water into the pores of the soil and thus simulating the soil-water retention curves of the material, including the scanning curves. It is also possible to obtain the required parameters to determine the value of Bishop's parameter χ and therefore compute the current effective stress. Nevertheless, the use of a network solid-porous model requires a large memory storage capacity that cannot be presently found in common computers. Furthermore, the time required to run a network model with only one million elements becomes excessive and is not a practical option. For that reason, a probabilistic solid-porous model that reduces the storage requirements and speeds of the simulations has been developed. Additionally, a unified elastoplastic framework to account for the volumetric behavior of unsaturated soils, including expansive, collapsible and compacted materials, has been developed. This framework explains some phenomena that could not be explained using the independent stress variables approach. All these developments lead to a general framework for the strength and volumetric behavior of soils based on the Critical State theory and the bounding surface concept resulting in a simple, fully coupled model that accounts for the behavior of both saturated and unsaturated materials, including compacted and expansive soils. Each one of these developments has been confronted with experimental results showing the appropriateness of this approach. In that sense, a unified soil mechanics theory is presently on its way.

CONSENT FOR PUBLICATION

Not applicable.

CONFLICT OF INTEREST

The author declares no conflict of interest, financial or otherwise.

ACKNOWLEDGEMENT

Declared none.

Eduardo Rojas
Universidad Autónoma de Querétaro
México

DEDICATION

*To Silvia, my loving wife, and my son and daughter:
Carlos Javier and Sonia Itzel, who have shown me
the pleasure of shearing.*

CHAPTER 1**Introduction**

Abstract: The use of the effective stress principle led to a general theory for the strength and volumetric behavior of saturated soils. Presently, all constitutive models for saturated soils are based on this principle. In 1959, Bishop proposed an equation for the effective stress of unsaturated soils. However, it was severely criticized because it could not explain by itself the phenomenon of collapse upon wetting. Moreover, an analytical expression for the determination of its main parameter χ was not provided, and in addition, its value could not be easily determined in the laboratory. Since then, several equations to determine the value of parameter χ have been proposed. Sixty years later, it is acknowledged that Bishop's effective stress equation can be employed to simulate the behavior of unsaturated soils when it is complemented with a proper elastoplastic framework.

Keywords: Air pressure, Collapse, Constitutive model, Effective stress parameter, Effective stress, Elastoplastic framework, Independent stress variables, Pore water pressure, Saturated soil, Shear strength, State surface, Suction, Total stress, Unsaturated soil, Volumetric behavior.

1.1. DIFFERENT APPROACHES FOR UNSATURATED SOILS

Even though the idea of using effective stresses in the study of unsaturated materials is old, the incapacity of providing an explanation to the phenomenon of collapse upon wetting (among other reasons) made this approach to be abandoned for about forty years. During that time, some other approaches to study the behavior of unsaturated soils were used. The state or constitutive surfaces [1], as the one represented in Fig. (1), were used for some time. In these plots, the behavior of a certain state variable, such as the void ratio, is plotted as a function of two independent stress variables, mainly the mean net stress ($p = p - u_a$) and suction ($s = u_a - u_w$), where p represents the total mean stress and u_a and u_w are the air and water pressures, respectively. This procedure aimed to establish mathematical relationships between the void ratio or the degree of saturation with the independent stress variables, as Hung, Fredlund and Pereira [2] have done. This method represented to some researchers the acceptance of the inexistence of an effective stress equation for unsaturated materials (see, for example, [3]). However, state surfaces soon showed their limitations. For example, unicity could only be ensured under certain conditions, especially because of the hysteresis of the soil-water retention curve (SWRC), the hydro-mechanical coupling, and the dependency of

soil behavior on the stress path. In any case, this task would have been formidable and complex because the behavior of unsaturated materials depends not only on the mean net stress and suction but also on the degree of saturation and the structure of soils. Recently, Zhang and Lytton [4] proposed a modified state-surface approach under isotropic stress conditions that can be applied to the study of the volumetric behavior of unsaturated soils, including collapsing and expansive soils.

Sometime later, the independent stress variables approach was employed to study the behavior of unsaturated soils. The independent stress state variables were defined as those stresses controlling the strength and volumetric behavior of soils. By performing the analysis of the equilibrium of an elemental volume of unsaturated soil, Fredlund and Morgenstern [5] proved that the use of two out of three possible combinations of the stress variables represented by the total stress (σ), the air pressure, and the water pressure, were sufficient to completely define the state of stresses of an unsaturated sample. The three possible combinations are: $(\sigma - u_w)$ with $(u_a - u_w)$; $(\sigma - u_a)$ with $(\sigma - u_w)$; and $(\sigma - u_a)$ with $(u_a - u_w)$. Being this last combination, net stress ($\bar{\sigma} = \sigma - u_a$) and suction, the most employed to study the behavior of unsaturated soils.

This theoretical analysis co-validated the experimental observations made by Bishop and Donald [6] in 1961. These researchers performed a series of triaxial tests where the confining stress (σ_3), the air, and the water pressures were all independently controlled during the loading of the sample. In this way, the values of the net confining stress ($\sigma_3 - u_a$) and suction could be maintained constant throughout the test while the independent pressures could change. These results showed that the independent variations of σ_3 , u_a and u_w had no effect on the stress-strain curve whenever the confining net stress and suction remained constant. However, a variation in these values resulted in marked changes in the stress-strain curve of the sample.

With the use of the independent stress variables, the representation of the failure surface for unsaturated soils is required, in addition to the normal net stress ($\sigma_n - u_a$) and the shear stress (τ) axes, the inclusion of the suction axis as indicated in Fig. (2). This figure shows the failure lines for a saturated material (indicated by the friction angle φ) and for an unsaturated one (indicated by the friction angle φ_s) where for the last, the cohesion (c) appears as a strength parameter.

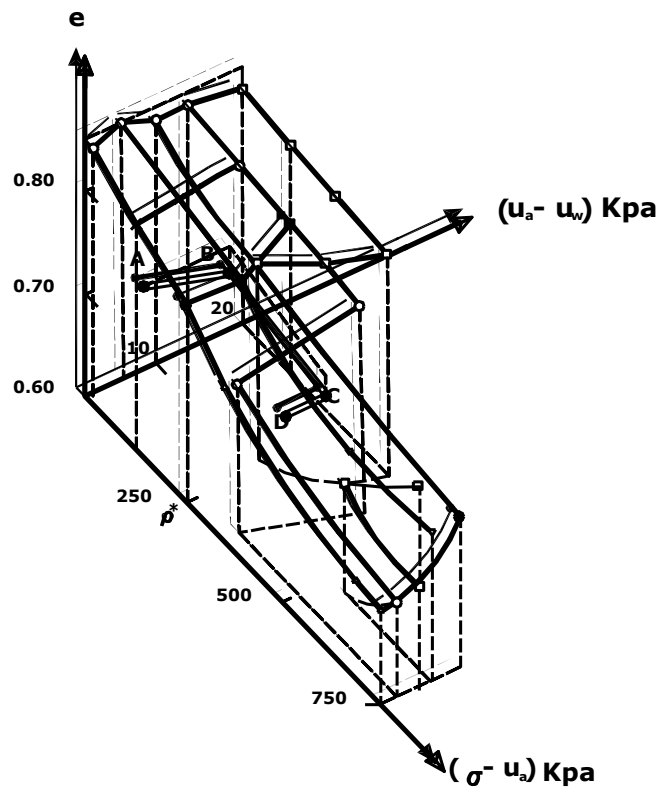


Fig. (1). State surface for the void ratio (adapted from [1]).

Following this tendency, Alonso, Gens and Josa [7] developed a constitutive model for unsaturated soils based on the modified Cam-Clay model (MCCM) developed by Roscoe and Burland [8]. Known as the Barcelona Basic Model (BBM), it is the simplest model to simulate the behavior of unsaturated soils, including collapsing materials. It has also been extended for the case of expansive soils. One of the main contributions attributed to the BBM is that it clearly explains the phenomenon of collapse upon wetting by introducing the loading collapse yield surface (LCYS) as illustrated in Fig. (3). This phenomenon occurs when a saturated sample is dried (path AB in Fig. (3)), then loaded by increasing the net stress (path BC), and finally wetted up to saturation (path CD).

The Effective Stress Equation

Abstract: Based on the analysis of the equilibrium of solid particles of an unsaturated sample subject to a certain suction, it is possible to establish an analytical expression for Bishop's parameter χ . With this parameter, the effective stress can be evaluated and used to predict the shear strength and volumetric behavior of unsaturated soils. For the determination of parameter χ , three elements are required: the saturated fraction, the unsaturated fraction, and the degree of saturation of the unsaturated fraction of the sample. The equation established for parameter χ clarifies some features of the strength of unsaturated soils that, up to now, had no apparent explanation. A drawback to this expression is that the three required parameters for the determination of χ cannot be obtained from current experimental procedures.

Keywords: Equilibrium, Total stress, Effective stress, Suction, Volumetric behavior, Shear strength, Effective stress parameter, Saturated fraction, Unsaturated fraction, Dry fraction, Degree of saturation of the unsaturated fraction, Microstructure, Macrostructure, Water menisci, Homogeneous material.

2.1. INTRODUCTION

Most natural soils show a bimodal structure consisting of a microstructure and a macrostructure [32]. On the one hand, the microstructure can be formed by packets of fine particles that flocculate and remain attached to each other. These packets or aggregates contain the intra-aggregate pores, which are pores of small size. On the other hand, the macrostructure is represented by the arrangement of these packets of fine particles sometimes mixed with solid grains the size of silt or sand that show the inter-aggregate and inter-particle (when solid grains are present) pores which are pores of larger size. In such a case, the size of pores usually ranges from $500\mu\text{m}$ to $0.01\mu\text{m}$. The smallest pores are close to the thickness of the adsorbed water layer, meaning that these pores never dry. This phenomenon accounts for the difference in the consistency of fine and coarse materials when dry. When suction applied to the soil is low, a great part of the macrostructure and the totality of the microstructure remain saturated. When suction increases, the saturated soil volume decreases in such a way that some solids are now completely surrounded by dry pores while others are only partially surrounded by saturated pores. Instead, most of the microstructure is still saturated. Finally, for very high suction, the saturated soil volume tends to disappear while the dry fraction increases. In the case of coarse materials, the saturated fraction may completely disappear, while for clayey soils,

this never happens because of the existence of intra-aggregated voids filled with layers of adsorbed water. Therefore, it can be said that, in general, an unsaturated soil consists of a saturated fraction, where soil particles are completely surrounded by water, an unsaturated fraction, where solid particles are linked together by water menisci and a dry fraction where solids are completely surrounded by air. In some cases, the bimodal structure may not appear, for example, in the case of homogeneous dense sands. In that case, the transit from the saturated to the dry condition happens very fast, and the saturated fraction completely disappears at small values of suction while the dry fraction increases rapidly. This behavior reflects the characteristics of the soil-water retention curves (SWRCs) of each material, as will be shown later.

If a soil sample is confined in a closed environment at a constant temperature during an appropriate period of time to reach equilibrium, then it can be admitted that the relative humidity is the same everywhere in the sample, and therefore, the value of suction is constant throughout the soil. Thus, air and water pressures in the saturated zones are the same as in the unsaturated ones. This implies that all saturated zones are surrounded by menisci of water, showing the same radius of curvature as the unsaturated zones.

2.2. THE EFFECTIVE STRESS EQUATION

Consider a homogenous and isotropic soil showing a bimodal structure where pores are randomly distributed, as shown in Fig. (1). The term homogenous means that a representative elementary volume can be used to model the whole material as this volume adequately reflects both the microstructure and macrostructure of the system. The term isotropic means that the mechanical and geometrical properties are the same in all three directions, including the spatial distribution of menisci.

The solid particles constituting both the macro and the microstructure can be observed in Fig. (1). Also, the water menisci and gas phases are included. In general, it is considered that the solid particles of the microstructure are grouped in the form of packets. In this case, the influence of the contractile skin is ignored as both Haines [33] and Murray [34] demonstrated that its influence could be neglected for practical purposes. Also, the water vapor, adsorbed water, and dissolved air are disregarded as Murray [34] has proved that their influence is also minimal. Finally, the contact areas between solids will be neglected as implicitly considered in Terzaghi's effective stress equation. Based on a Disturbed State Model, Desai and Wang [35] performed an analysis of the effective stress on saturated soils, which includes the effect of the variation of the contact area of

solids. A similar procedure could be used for unsaturated materials if the contact area of solids was not neglected.

For this analysis, the following notation is used: a superindex indicates the fraction being referred to: s for the saturated, u for the unsaturated, and d for the dry fraction of the soil. A subindex indicates the phase being referred: \bar{s} for solids, w for water, and a for air. A double subindex indicates the influence of one phase to another; for example, $A_{\bar{s}a}$ and $A_{\bar{s}w}$ represent the area of solids subjected to air and water pressure, respectively.

Considering a unitary thickness of the soil section shown in Fig. (1), it can be established that the total area (A) of the cross-section B-B', results from the addition of the saturated (A^s), the unsaturated (A^u) and the dry fractions (A^d) of the sample, that is to say $A = A^s + A^u + A^d$. Also, the total area of the saturated fraction results from the addition of the area where water directly reacts (A_w^s) plus that occupied by solids ($A_{\bar{s}}^s$), in the form $A^s = A_w^s + A_{\bar{s}}^s$. Moreover, the solid particles on the saturated fraction are only in contact with water and other solids. If the contact area between solids is neglected, then all the horizontal projection of the area of solids of the saturated fraction (aggregates) represented in section B-B' is subject to the water pressure; that is to say $A_{\bar{s}}^s = A_{\bar{s}w}^s$. Therefore, the total area of the saturated fraction can be written as the sum of the areas where water directly reacts and the horizontal projection of solids pushed by water; that is to say:

$$A^s = A_w^s + A_{\bar{s}w}^s \quad (2.1)$$

On the other hand, the total area of the unsaturated fraction results from the sum of the areas where the solid ($A_{\bar{s}}^u$), liquid (A_w^u) and gas (A_a^u) phases react, that is to say $A^u = A_{\bar{s}}^u + A_w^u + A_a^u$. Additionally, the solids also are in contact with the three phases. If the contact area between solids is ignored, then the horizontal projection of the solids of the unsaturated fraction on section B-B' results from the addition of the areas of solids where the pressures of liquid ($A_{\bar{s}w}^u = (A_{\bar{s}w}^u)_1 + (A_{\bar{s}w}^u)_2$) and air ($A_{\bar{s}a}^{ui}$) react:

$$A_{\bar{s}}^u = A_{\bar{s}w}^u + A_{\bar{s}a}^{ui} \quad (2.2)$$

The Porous-Solid Model

Abstract: Based on the analysis of the equilibrium of solid particles in a soil sample subject to a certain suction, an analytical expression for the value of Bishop's parameter χ was established in the previous chapter. This parameter can be written as a function of the saturated fraction, the unsaturated fraction, and the degree of saturation of the unsaturated fraction of the soil. However, the determination of these three parameters cannot be made from current experimental procedures. Therefore, a porous-solid model simulating the structure of soils is proposed herein and used to determine these parameters. The data required to build up the porous-solid model are the void ratio of the sample and their grain and pore size distributions.

Keywords: Porous-solid model, Soil structure, Macropores, Micropores, Sites, Cavities, Bonds, Connectors, Network porous models, Random models, Distinct element method, Pore size distribution, Grain size distribution, Soil-water retention curves, Pore shrinkage.

3.1. INTRODUCTION

Only recently it has been acknowledged that Bishop's effective stress equation ($\sigma' = \bar{\sigma} + \chi s$) may lead to more realistic and simple constitutive models for unsaturated soils (see, for example, [27, 29, 30]). However, the problem of a proper determination of parameter χ still subsists, as it has been experimentally recognized that the approximation $\chi \approx S_w$ is not always satisfactory, especially for soils showing bimodal structure.

In the previous chapter, an analysis of stresses in the skeleton of an unsaturated soil showing a bimodal structure resulted in an effective stress equation for unsaturated materials (Eq. 2.13). Unfortunately, the parameters required for the determination of the effective stress f^s , f^u and S_w^u cannot be obtained from current laboratory procedures.

An alternative method for the determination of these parameters is the use of a porous-solid model able to simulate the distribution of water in the pores of soils and hence reproduce the soil-water retention curves (SWRCs).

Some simplified porous models have already been developed to study different phenomena such as capillary condensation and evaporation [51], and activated

chemical absorption in heterogeneous surfaces [52]. Also, Fredlund and Xing [53] proposed an equation that defines the SWRC based on the pore size distribution (PSD). More recently, Simms and Yanful [54] proposed a porous network that correctly simulates the PSD, the SWRC, the relative hydraulic conductivity, and the volume change. However, these latter models do not account for hysteresis.

One way to include hysteresis and observe in detail the influence of water menisci on the deformation and volumetric behavior of unsaturated soils is by making use of micromechanical models. This type of model is more complex because, besides simulating the porous structure, they also simulate the solid skeleton of the material and can include the phenomenon of shrinkage of macropores during drying or loading. These models require a porous structure formed by pores of different sizes placed at random in order to correctly simulate the phenomenon of hysteresis. A model with these characteristics can also be used to determine the values of parameters f^s , f^u and S_w^u required to compute the effective stress for unsaturated soils and even include hydro-mechanical coupling in constitutive relationships. Three of these models are described below.

3.2. DIFFERENT POROUS-SOLID MODELS

The accurate description of real porous media, such as soils, is quite a complicated task, if only because they include millions or billions of pores per gram with sizes ranging from 0.01 to 500 micrometers. Another problem is the phenomenon of hysteresis. In 1929, Haines [33] postulated that the main drainage SWRC occurs at higher suctions than the main wetting curve because the latter is controlled by the largest pores while the former is controlled by the smallest. Additionally, when load or suction increases, there is a reduction in the size of pores. The shrinkage of macropores with suction has been analyzed by Simms and Yanful [55], measuring the PSD change of a glacial till. They observed that the pore volume related to the pore size exhibits two crests, as shown in Fig. (1). The first crest is located at a diameter of pores of approximately 0.1 μm and corresponds to the micropores, *i.e.*, those that maintain their size when suction increases. The other crest is located at a diameter of pores of approximately 6 μm and corresponds to the macropores, which shrink with increasing suction. Simms and Yanful [55] observed that for this particular soil, practically all macropores experienced a progressive shrinkage as suction increased. For suctions of the order of 2.5 MPa, practically all macropores had shrunk, and their size diminished by approximately one order of magnitude as they reduced their mean size from 6 to 0.6 μm . The same type of behavior was observed for other soils. Additionally, there is the shrinkage of pores with loading. Simms and Yanful [56] performed a series of PSD tests on different soils subject to

different confining stresses. These results show a general trend for all cavities to reduce their size and displace their peak on the PSD curves to the left-hand side with increasing confining stresses, although the reduction in the size of macropores is much larger than that of micropores.

Accordingly, a simplified description of soils that captures the phenomena described above can be made with four elements: the macrocavities, the microcavities, the bonds, and the solids. Cavities (C) contain most of the volume of voids. The microcavities are those pores of small size. The macrocavities are the largest pores in the soil and differ from the microcavities in that the former shrink with increasing suction or load. The bonds or connectors (B) are the elements that link together two cavities. These pores are smaller than cavities and are subdivided into microbonds and macrobonds. The volume contained by the bonds is negligible when compared to that of cavities. Finally, the solids are included in the spaces left by the pores and form the skeleton of the material. If an analogy is made between the porous structure of soil and a building, then the rooms and corridors of the building represent the cavities while the doors and windows represent the bonds. Additionally, the solid structure of the building represents the skeleton of the soil.

Each one of these elements possesses its own size distribution however, its spatial distribution is strongly correlated given the geometrical restrictions to be fulfilled. These interactions with their neighbors allow reproducing, in a simplified manner, the structure of soils. Therefore, a solid-porous network built with these elements can simulate the most important aspects of the wetting-drying phenomena, such as the hydraulic hysteresis of the SWRC and the shrinkage of macropores. For this purpose, the model must comply with certain conditions to correctly describe the main phenomena of real soils. These conditions are:

- a) Heterogeneity of sizes. All elements (macrocavities, microcavities, macrobonds, microbonds, and solids) show their own size distribution.
- b) Compressibility of the network. This can be accomplished by allowing the shrinkage of macropores with loading or suction increase.
- c) Size correlation between neighbors. There is a statistical correlation between the sizes of the different elements meeting at a certain place, such as cavities with bonds and cavities with solids.
- d) Non-uniform connectivity, as the number of bonds converging at one cavity, may change from site to site.
- e) Geometrical restrictions, in order to guarantee that the bonds connecting to one cavity do not intersect one another.

The Probabilistic Porous-Solid Model

Abstract: In the previous chapter, a computational network porous-solid model was developed to simulate the hydraulic behavior of unsaturated soils. However, important computational constraints make this model unpractical. In this chapter, a probabilistic porous-solid model is developed to overcome these constraints. The probabilistic model is an alternative to the use of computational network models and shows important advantages. This model is built from the probability of a certain pore to be filled or remain filled with water during a wetting or drying process, respectively. The numerical results of the probabilistic model are compared with those of the computational network model showing only slight differences. Then the model is validated by making some numerical and experimental comparisons. Finally, a parametric analysis is presented.

Keywords: Probabilistic model, Network models, Basic unit, Hydro-mechanical coupling, Solids, Cavities, Bonds, Saturated fraction, Unsaturated fraction, Dry fraction, Degree of saturation of the unsaturated fraction, Retention curves, Bishop's parameter, Relative volume, Porosimetry tests, Macropores, Micropores, Effective stresses.

4.1. INTRODUCTION

Recently, Bishop's effective stress equation has been used for the development of simpler and more realistic constitutive models for unsaturated soils [24, 27-30], not only because it can estimate approximately the strength of soils but also because it takes into account the hysteresis and hydro-mechanical coupling observed in unsaturated soils. The importance of hysteresis becomes evident by the fact that the degree of saturation affects the stiffness and strength of soil samples subject to the same value of suction. This phenomenon shows that for a single value of suction, a large range of values for the degree of saturation is possible; therefore, this phenomenon affects the value of the effective stress. Hydromechanical coupling is related to the shift of SWRCs on the suction axis produced by the volumetric deformation of the sample during loading or suction increase which in turn affects the value of the effective stress. Both phenomena need to be considered by the porous-solid model.

The analysis presented in Chapter 2 shows that Bishop's effective stress equation for unsaturated soils (Eq. (1.1), Chapter 1) can be expressed as in Eq. (2.13) with parameter χ defined as in Eqs. (2.15) or (2.16). According to this last equation,

Eduardo Rojas

All rights reserved-© 2022 Bentham Science Publishers

parameter χ depends not only on the degree of saturation (S_w) of the sample but also on the void ratio and the structure of the soil as experimentally observed by Bishop and Donald [6]. The main problem with the use of Bishop's equation lays precisely in the determination of parameter χ . In this chapter, a probabilistic porous-solid model is developed for the determination of this parameter during wetting-drying processes.

4.2. THE PROBABILISTIC MODEL

Based on the framework of the computational network model developed in Chapter 3, it is possible to develop a probabilistic solid-porous model [82]. The model is based on the concept of basic units, which allow the introduction of the solid phase in the network. This, in turn, allows the quantification of parameters f^s , f^u and S_w^u required to determine the value of χ . Initially, a basic unit for cavities and bonds is defined, and the equations for the main boundary curves at wetting and drying are established.

The procedure used to develop the probabilistic model was the following: first, an infinite 2D or 3D network made of cavities, bonds, and solids is considered. Thereafter, the conditions for a pore (cavity or bond) to drain or saturate during a drying or wetting process are established. Then, based on the size distribution of each element, it is possible to write the above conditions in the form of probabilistic equations. These equations can then be simultaneously solved, and the probability for a pore of a certain size to drain or saturate during a drying or wetting process can be determined. Subsequently, it is possible to establish a ratio between the dried and saturated pores and thus obtain the degree of saturation of the material to finally plot the SWRCs at wetting and drying.

This process requires the distributions of the relative volumes of cavities (V_{RC}) and bonds (V_{RB}) as a function of their size. The relative volume is defined as the volume of the elements of a certain size, divided by their total volume. These distributions can be obtained from the results of porosimetry tests. Once these distributions are known, it is possible to define the relative volume of cavities $C(R_c)$ and bonds $B(R_c)$ smaller or equal to the critical radius R_c in the form,

$$C(R_c) = \int_0^{R_c} V_{RC}(R) dR \quad (4.1)$$

$$B(R_c) = \int_0^{R_c} V_{RB}(R) dR \quad (4.2)$$

The critical radius R_c is defined as the maximum size of the pore that can be intruded by water at certain suction. When these integrals are solved for the full range of sizes, the result is unity, which means that these functions, in fact, represent the distribution of probabilities for cavities and bonds, respectively, as a function of their size. These functions are represented in Figs. (1a and b) for wetting and drying paths, respectively.

Using the above equations, it is possible to determine the volume of pores of a certain size. For example, if $V_C(R_c)$ represents the volume of cavities whose sizes range from zero to R_c , this parameter is given by the relationship $V_C(R_c) = \int_0^{R_c} V_C(R) V_{RC}(R) dR$, where $V_C(R)$ represents the volume of cavities of size R . Similarly, the volume of bonds for sizes ranging between zero and R_c is given by the relationship $V_B(R_c) = \int_0^{R_c} V_B(R) V_{RB}(R) dR$, where $V_B(R)$ represents the volume of bonds of size R .

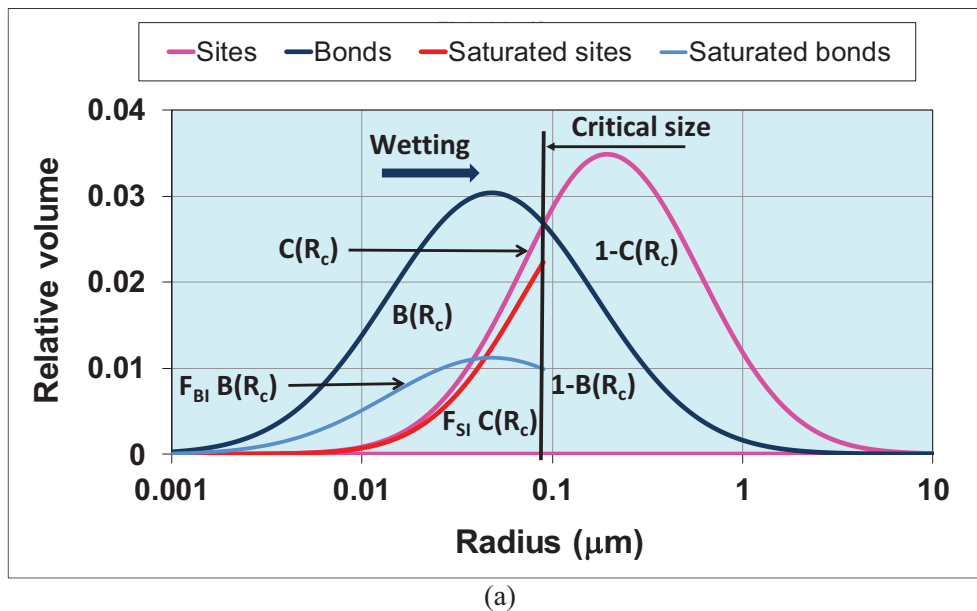


(Fig. 1) contd....

CHAPTER 5**Applications of the Porous-Solid Model**

Abstract: In the previous chapter, a probabilistic porous-solid model with the ability to simulate both branches of the soil-water retention curve, was developed. In this chapter, the model is used to interpret more realistically the results of mercury intrusion porosimetry tests. Moreover, it is used to obtain the pore size distribution of soils employing both branches of the soil-water retention curve as data. The numerical and experimental comparisons for different soils show that the model approximately reproduces the pore size distributions obtained from mercury intrusion porosimetry tests. Finally, a procedure to fit the numerical with the experimental soil-water retention curves in order to obtain the pore size distribution of soils is presented.

Keywords: Mercury intrusion porosimetry tests, Scanning electron micrographs, Pore size distribution, Grain size distribution, Superficial tension, Contact angle, Soil-water retention curve, Critical radius, Relative volume, Macrocavities, Microcavities, Micropores, Hydro-mechanical coupling, Soil mixtures, Logarithmic normal distribution, Mean size, Standard deviation.

5.1. INTRODUCTION

One of the most popular methods to obtain the pore size distribution (PSD) of soils is the mercury intrusion porosimetry (MIP) test. MIP tests are made in pressure chambers filled with mercury (which is a non-wetting fluid), where a moisture-free soil sample is immersed. Then, the pressure in the chamber is progressively increased while the volume of intruded mercury in the pores of soil is recorded. The diameter of the intruded pores at a certain pressure is obtained from the Young-Laplace equation (Eq. (3.2), Chapter 3), using the appropriate parameters of surface tension for the air-mercury interface and the contact angle between mercury and solid particles. Finally, a graph showing the relative intruded volume *versus* the size of pores is generated. With these results, the sizes of macrocavities and microcavities can be established. However, the unrealistic hypotheses made to determine the sizes of pores, together with the impossibility to measure the whole range of sizes [56], as well as doubts related to the deleterious effect of high mercury pressures on the size of pores for loose soils [81], in addition to some inconsistencies on the application of data to correctly reproduce the soil water retention curves (SWRCs) [89], require these results to be taken with caution and to be considered only as an approximation to the real PSD of the material.

5.2. MERCURY INTRUSION POROSIMETRY TESTS

Recently, the use of the MIP test to ascertain the PSD of soils has become quite popular in unsaturated soil mechanics, primarily because of its simplicity. To perform this test, a sample of around 1 cm^3 is introduced into a cell filled with mercury. The sample has been previously dried by means of different techniques, two of them the most frequently used: oven-drying and freeze-drying. In general, the freeze-drying method is preferred as it is associated with a smaller disturbance of the original structure of the soil due to the rapid rate of freezing. Once the sample has been placed in the cell, the pressure of mercury is gradually increased, and the volume of intruding mercury is measured. The radii of the intruded pores are obtained from the Young-Laplace equation involving the superficial tension of mercury, the contact angle between mercury and solid particles, and the mercury pressure. The main hypothesis employed to interpret these results is to assume that only those pores size of the critical radius (determined from the Young-Laplace equation for the current mercury pressure) are intruded at each increment of mercury pressure. Then, a graph showing the relative volume of pores (in cm^3 per gram) for each pore size is produced. More details of the equipment and procedure required to obtain the PSD of soils by MIP can be consulted in Simms and Yanful [55].

However, the hypothesis made to interpret MIP tests is clearly unrealistic. It supposes that only equally sized pores are interconnected, while there is no interconnection between pores of different sizes. In fact, it has been acknowledged that MIP tests exaggerate the frequency of small pores and underestimate that of large pores [90]. This is a result of the intrusion of mercury in the bonds, matching that of the cavity connected to this bond. This is explained by the fact that larger pores are the first ones to be intruded when mercury pressure increases. Then, because bonds and cavities are interconnected, and bonds are smaller than cavities, in order to intrude a cavity, mercury pressure has to be increased to produce the intrusion of one of its connecting bonds.

Considering a porous-solid model as the one described in Chapter 3, it is possible to generate a better interpretation of MIP tests. The invasion of mercury (which is a non-wetting fluid) is similar to a drying process where pores are invaded by air (which is also a non-wetting fluid), forcing the water to drain out of the sample. In both cases, the largest pores are the first to fill in with air or mercury, as indicated in Fig. (1).

When mercury pressure increases, only a fraction of pores, which size is equal to or larger than the critical radius, saturate while the rest remain blocked by smaller bonds. This occurs because of the interconnection of pores of all sizes. Some larger pores saturate during this increase of mercury pressure because at least one of their interconnected bonds belongs to those that saturate during this last increment.

The mechanism of mercury invasion is sketched in Fig. (1). Considering that the critical radius reduces from R_{c1} to R_{c2} due to the increase in mercury pressure, the blank zone in the figure represents the volume of pores that still have not yet been invaded by mercury. The single shadow zone represents the volume of pores already invaded by mercury before the new pressure increment. Finally, the double shadow zone represents the volume of pores filled in during the last pressure increment.

For MIP tests, the appropriate values of contact angle and surface tension are needed. According to Eq. (3.2) in Chapter 3, the ratio between the suctions in pores filled with water (s_w) and mercury (s_m) is given by the relationship:

$$\frac{s_w}{s_m} = \frac{T_{sw} \cos \theta_w}{T_{sm} \cos \theta_m} \quad (5.1)$$

where T_{sw} and T_{sm} represent the surface tension for water and mercury, respectively, while θ_w and θ_m are the contact angles for water and mercury with the soil minerals, respectively.

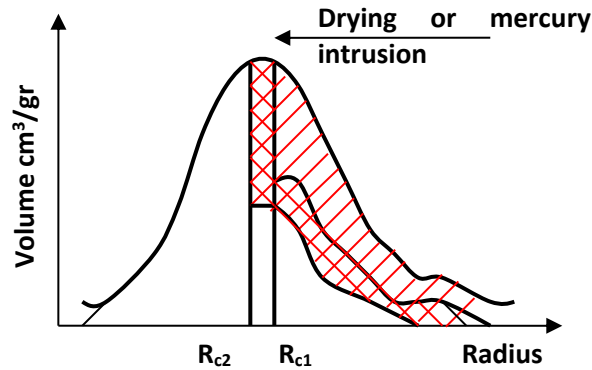


Fig. (1). Pores invaded by mercury (shaded zone) during a MIP test.

Compression Strength of Soils

Abstract: In this chapter, the probabilistic porous-solid model is used to determine the mean effective stress of soils at failure. The plots of the deviator stress against the mean effective stress show a unique failure line for a series of triaxial tests performed at different confining net stress and suctions for both wetting and drying paths. This result confirms that the proposed effective stress equation is adequate to predict the shear strength of unsaturated soils. It also results in different strengths for wetting and drying paths, as the experimental evidence indicates.

Keywords: Shear strength, Effective stress, Net stress, Triaxial tests, Confining stress, Axis translation technique, Constant volume test, Friction angle, Wetting path, Drying path, Porous-solid model, Soil-water retention curve, Logarithmic normal distribution, Critical state, Pore size distribution, Grain size distribution.

6.1. INTRODUCTION

The probabilistic porous-solid model can be used to obtain the mean effective stress at failure for a soil following any stress path. These results can be plotted against the deviator stress to determine the failure surface of the material. In this chapter, the experimental results of the Speswhite kaolin, as reported by Wheeler and Sivakumar [111], are used. These researchers performed a series of triaxial tests with different stress paths. With these results, some points of the soil-water retention curve (SWRC) at wetting could be obtained. Also, the pore size distributions (PSDs) of samples statically compacted at different vertical pressures and water contents have been reported by Thom, Sivakumar, Sivakumar, Murray and Mackinnon [112]. Finally, the grain size distribution (GSD) of this material was reported by Espitia [113].

At this stage, the strength equations do not consider volume changes or hydromechanical coupling, and for that reason, only those paths involving no volume change of the sample during shearing were considered for the numerical comparisons. For the same reason, the experimental results were considered in three different groups depending on the confining stress applied to the sample. These groups correspond to the confining pressures of 0.1 (three tests), 0.2 (two tests), and 0.3 MPa (one test). Each group corresponds to a different PSD resulting in three different sets of SWRCs and three different groups of curves for parameters f^s , f^u and S_w^u . Accordingly, numerical and experimental comparisons were made independently for each group.

Eduardo Rojas

All rights reserved-© 2022 Bentham Science Publishers

6.2. NUMERICAL AND EXPERIMENTAL COMPARISONS

All samples tested in the triaxial cell, as well as those used for the determination of the PSD and the SWRC, were prepared by static compaction at a water content of 25% (4% less than the optimal). These samples were compacted in nine layers at a constant displacement of 1.5 mm/min and a maximum vertical total stress of 0.4 MPa. This procedure provided samples with a dry density of 1.2 g/cm³, a specific volume of 2.21, and a degree of saturation of 54%. Prior to the loading stage, all samples were subject to an isotropic net stress of 0.050 MPa with suctions ranging from 0 to 0.3 MPa in the triaxial cell. At these levels of suction, all samples increased their water content. In addition, those samples subject to suctions of 0 and 0.1 MPa experienced volumetric collapse. Once equilibrium was accomplished, the isotropic net stress was increased to reach a final value ranging between 0.1 and 0.3 MPa. Because all samples increased their water content during the equilibrium stage, this means that all these results correspond to the wetting branch of the SWRC.

The GSD of the Speswhite kaolin reported by Espitia [113] is shown in Fig. (1a). The same figure shows the adjusted numerical curve obtained from a double logarithmic normal distribution. Even though, small differences between these two curves subsist, the numerical fitting is sufficiently accurate.

The experimental points (Ex) of the SWRCs for the confining pressures of 0.1, 0.2, and 0.3 MPa are shown in Fig. (1b). These points were obtained from the results of controlled suction triaxial tests with no volume change performed by Sivakumar [114]. They correspond to the value of the degree of saturation at a critical state for those tests performed at the same confining pressure, but different suctions. This figure also shows the numerical (N) SWRCs at wetting for the different confining pressures. The numerical curves were fitted to the experimental points by successively modifying an initially proposed PSD according to the procedure outlined in the previous chapter. In order to produce complete curves, it was necessary to estimate the values of the residual and the saturated degree of saturation according to the tendency of the experimental points. The first parameter was assessed as 0.05 for all tests, while the second was estimated as 0.91, 0.96, and 0.97 for the confining pressures of 0.1, 0.2, and 0.3 MPa, respectively.

Fig. (1c) shows the PSD obtained from mercury intrusion porosimetry (MIP) tests carried out on a sample prepared according to the aforementioned procedure. This curve shows a bimodal distribution with two peaks: one at approximately 0.45 μm and the other at approximately 4.5 μm , corresponding to the size distribution of

micro and macrocavities, respectively. The same figure shows the PSDs obtained by fitting the numerical and the experimental SWRC at wetting for the three different confining stresses. Although the experimental and the numerical curves show similar shapes, two main differences between them emerge: the first one is that the numerical PSD is displaced to the left with respect to the experimental results. The second one is that the numerical maximum relative volume of macropores is much smaller than the experimental value. The reason for these differences can be explained by the fact that MIP tests were performed in “as compacted” soil samples before the equalization stage, where the confining pressure and the increase in water content produced a volumetric reduction in the sample that affects mainly the size of macropores as has already been discussed in Chapters 3 and 5. This same deviation of the numerical PSD with respect to the experimental results was observed when a computational network model was used to simulate the SWRC of this material [115].

Once the PSD for each confining pressure has been established, the parameters required by the porous-solid model can be determined. Table 1 shows the parameters obtained for a confining pressure of 0.1 MPa. Notice that cavities and bonds needed a double logarithmic distribution to correctly simulate the SWRCs.

Table 1. Parameters of the model for a confining pressure of 0.1 MPa.

Parameter	mC	MC	mB	MB	Sol ₁	Sol ₂
\bar{R} (μm)	0.05	0.8	0.008	0.13	0.02	1.1
δ	1.7	1.4	1.7	1.4	3.8	1.1
q	0.01		0.01		0.005	

Notes: mC = mesocavities, MC = macrocavities, mB = microbonds, MB = macrobonds, Sol₁ = solids (1), Sol₂ = solids (2), q = relative volume factor.

For the confining pressures of 0.2 and 0.3 MPa all parameters included in Table 1 remain the same except for the mean size of macropores which takes the values of 0.83 μm and 0.75 μm , respectively. The connectivity considered in the porous solid model for this case was 4. Finally, a value of 0.25 for the shape factor allowed matching the numerical and experimental voids ratio for the different confining pressures as shown in Table 2.

Once all parameters of the porous-solid model have been defined, it is possible to simulate a wetting process and obtain the values of f^s , f^u , S_w^u and χ for the full range of suction and for each confining pressure. These results are presented in Fig. (2). In Figs. (2a and c), it can be seen that both parameters f^s and S_w^u increase

Tensile Strength

Abstract: In this chapter, the probabilistic porous-solid model is used to simulate the tensile strength of unsaturated soils tested at different water contents. The strength of unsaturated soils can be split into two parts: one related to the net stress and the other to suction stress. The strength generated by suction has its origin in the additional contact stresses induced to solid particles by water meniscus. This additional contact stress is called matric suction stress when it is solely related to matric suction. In such a case, the tensile strength of soils represents the matric suction stress of the material at that particular water content. The numerical and experimental comparisons of the tensile strength of unsaturated soils tested at different water contents show that the probabilistic porous-solid model can simulate this phenomenon quite accurately.

Keywords: Direct tensile test, Water meniscus, Tensile stress, Suction, Matric suction Stress, Additional contact stress, Tensile strength, Probabilistic porous-solid model, Effective stress, Net stress, Suction, Cohesion, Water menisci, Homogenous material, Retention curves.

7.1. INTRODUCTION

Eq. (2.18) in Chapter 2, represents the shear strength of an unsaturated soil subjected to a certain suction. This equation can also be rewritten as:

$$\tau = \sigma'_n \tan \varphi = (\bar{\sigma}_n + \sigma_s^*) \tan \varphi = \bar{\sigma}_n \tan \varphi + c$$

where c represents the cohesion of the soil. If osmotic suction is neglected, the matric suction stress represents additional contact stresses induced by water meniscus to solid particles (Lu, 2008). According to Eq. (2.15) in Chapter 2, the matric suction stress is given by the relationship:

$$\sigma_s^* = \chi s = [f^s + S_w^u f^u] s \quad (7.1)$$

Among the considerations made to obtain this equation is that the soil is a homogeneous isotropic material and in that sense, the matric suction stress represents an isotropic stress. During a tensile test, the maximum strength reached by a soil sample represents the bonding stress between solid particles, and therefore, it also represents the matric suction stress of the material at that particular water content [122]. Thus, tensile tests represent a direct measurement of the matric suction stress of soils. In that sense, the probabilistic porous-solid model can be

used to determine the matric suction stress of soils, and, therefore, their tensile strength.

7.2. TENSILE TESTS

Vesga and Vallejo [122] performed a series of direct tensile tests on kaolin samples with different degrees of saturation following a drying path. At the same time, these researchers reported the drying soil-water retention curve (SWRC) of the material.

The tensile tests were performed on flat bowtie-shaped samples. In this way, the samples could be fixed at their extremes, and the failure always occurred at their centers. The samples were 7 cm long, 2.2 cm thick, with a central neck 2.5 cm wide. These samples were cast in a flat mold where the material was placed at a water content close to the liquid limit (40%). Then a vertical load of 0.03 MPa was applied for 24 hours. Once the loading stage was finished, the sample was subjected to a drying process in controlled humidity conditions up to the point where it reached a water content previously specified. Finally, the sample was placed in a membrane for 48 hours to allow the homogenization of the humidity before the test was performed.

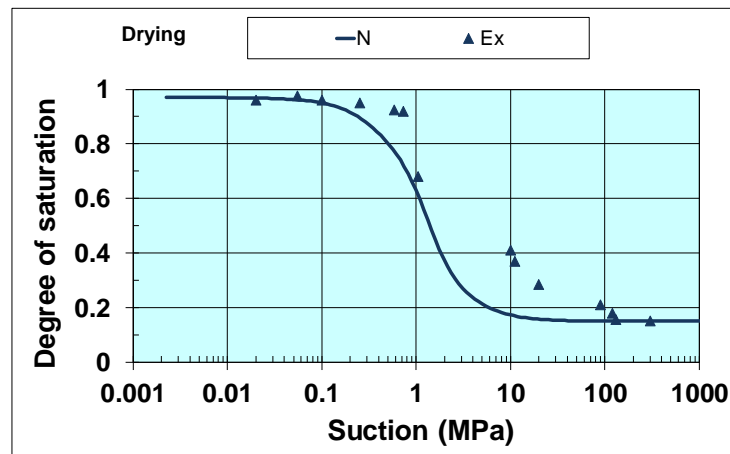
Unfortunately, all these tests were performed following a drying path, and there is no information related to the wetting path. Nevertheless, the porous-solid model was used to simulate the SWRC of the material by successively adjusting an initially proposed pore size distribution (PSD), as already explained in Chapter 5. Fig. (1a) shows the experimental SWRC obtained by Vesga and Vallejo [122] using the filter paper method. This figure also shows the fitted numerical SWRC obtained with the porous-solid model. In this case, a double logarithmic function was considered for both cavities and bonds to achieve the best fit for the SWRC. The required data for each distribution are the mean radius, the standard deviation, and the relative volume factor. The values obtained for these parameters are presented in Table 1.

Table 1. Parameters of the model.

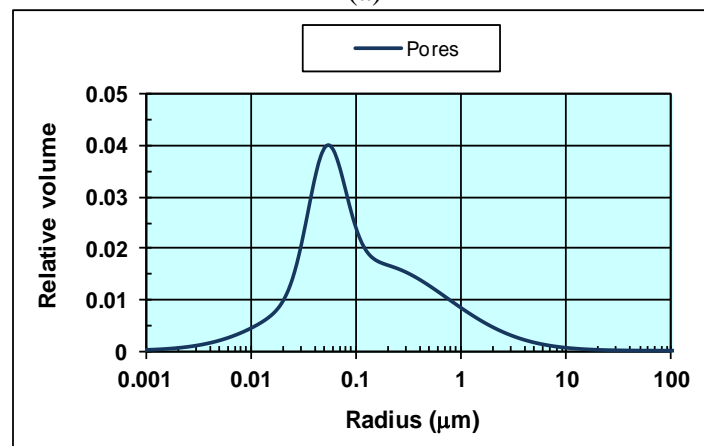
Parameter	mC	MC	mB	MB
\bar{R} (μm)	0.0014	0.075	0.0009	0.03
δ	5.1	1.5	7	3.5
ϱ	0.02		0.1	

Note: mC = microcavities, MC = macrocavities, mB = microbonds, MB = macrobonds, ϱ = relative volume factor.

These parameters establish the frequency of the different sizes of pores in the porous network. With this data and the size of the pores, it is possible to determine the numerical relative volume for each size, as shown in Fig. (1b). Fig. (1c) shows the values of parameters f^s , f^u , f^d and S_w^u obtained from the porous-solid model when the sample follows a drying path. Finally, Fig. (1d) shows the values for parameter χ versus the value of suction. By comparing Figs. (1a and d), it can be observed that the values of parameter χ are slightly smaller than those represented by the degree of saturation (S_w). Greater variations between χ and S_w can be observed when the difference in the mean size of micro and macrocavities is larger (double structured soils). All these parameters were obtained only for the drying condition as no information was provided for the wetting branch of the SWRC, as already mentioned.



(a)



(b)

(Fig. 1) contd....

Volumetric Behavior

Abstract: In this chapter, an equation to account for the volumetric behavior of unsaturated soils is proposed. This equation is based on the effective stress principle and results in a unifying framework for the volumetric behavior of both saturated and unsaturated soils. The numerical results of the proposed equation are compared with experimental results published by different researchers. These comparisons show that the equation is adequate to account for wetting-drying and net stress loading-unloading paths. This analysis confirms that the effective stress principle can be applied to the volumetric behavior of unsaturated soils.

Keywords: Volumetric behavior, Effective stress principle, Isotropic triaxial test, Controlled suction test, Effective stress, Compression index, Unloading-reloading index, Unsaturated soils, Collapse, Elastoplastic framework, Hydro-mechanical coupling, Water menisci, Macropores shrinkage, Suction hardening, Yield surface.

8.1. INTRODUCTION

Different approaches have been proposed to simulate the volumetric behavior of unsaturated soils. Two of the main trends are, on one side, the independent stress variables approach and, on the other, the single stress variable approach. In the first one, two different coefficients are used to account for the contribution of net stress and suction on the volumetric behavior. In the second case, a single volumetric coefficient is related to a single stress variable (in most cases referred to as the effective stress) to simulate the volumetric behavior.

One of the main advantages of using the single stress approach is that the hydro-mechanical coupling observed in unsaturated soils is implicit in the formulation. On the contrary, the difficulties in finding a correct explanation for the phenomenon of collapse upon wetting were one of the main objections to this approach. However, it is presently acknowledged that the simulation of this phenomenon requires, in addition to the effective stress equation, an appropriate elastoplastic framework. In contrast, the independent stress variables models seem to clearly explain the phenomenon of collapse upon wetting, while the implementation of the hydro-mechanical coupling has been included in different degrees, as can be observed in references [27, 28, 128, 129].

The first approach has the following general form for the elastoplastic volumetric strain increment $d\varepsilon_v$:

$$d\varepsilon_v = \frac{1}{v} \left(\lambda_{vp} \frac{d\bar{p}}{\bar{p}} + \lambda_{vs} \frac{ds}{(s + p_{atm})} \right)$$

Where v is the specific volume of the soil, \bar{p} and $d\bar{p}$ represent the apparent preconsolidation mean net stress at the current suction and its increment, respectively, s and ds are the maximum previous suction and its increment, p_{atm} is the atmospheric pressure, λ_{vp} and λ_{vs} are the slopes of the compression curves due to increases of the mean net stress and suction, respectively, in a semilogarithmic plane. Both slopes show negative values meaning that negative volumetric strains indicate volumetric reduction. This expression allows great flexibility in the simulation of the volumetric behavior of unsaturated soils. It is common to express λ_{vp} as a function of suction while λ_{vs} is considered constant. However, the experimental results indicate that λ_{vp} must also depend on the mean net stress while λ_{vs} must depend on both the mean net stress and suction (see for example [130, 131]). In that sense, the above expression becomes more complicated than it seems. Another disadvantage of this expression is that under zero suction, the equation for the volumetric behavior of saturated soils is not recovered, and therefore the transition from unsaturated to saturated states and *vice-versa*, is not smooth [132]. Examples of this approach are given in the models developed by Alonso, Gens and Josa [7], Wheeler and Sivakumar [111], and Thu, Rahardjo and Leong [133], among others.

The second approach uses the same equation as for saturated soils, written in the following general form:

$$d\varepsilon_v = \frac{\lambda_v}{v} \frac{dp'}{p'}$$

where p' and dp' represent the preconsolidation mean effective stress and its increment, respectively and λ_v represents the slope of the compression curve in the axes of the logarithm of the mean effective stress *versus* specific volume. For the most general case, λ_v can be written as a function of the mean net stress, the preconsolidation stress, and suction. Another possibility is to write λ_v as a function of the degree of saturation [132]. The effective stress approach has been used in the models proposed by Sheng, Sloan and Gens [30], Sun, Cui, Matsuoka and Sheng [129], Khogo, Nikano and Miyazaky [134], Loret and Khalili [135], Kholer and Hofstetter [136] and Koliji, Laloui and Vulliet [137] among others.

Recently Sheng, Fredlund and Gens [138] proposed a combination of these two trends writing the suction volumetric index as a function of the mean stress index, in the form:

$$d\varepsilon_v = \lambda_{vp} \frac{d\bar{p}}{\bar{p}+s} + \lambda_{vs} \frac{ds}{\bar{p}+s} \quad (8.1)$$

where the volumetric suction index λ_{vs} depends on the value of λ_{vp} according to the following relationship:

$$\lambda_{vs} = \begin{cases} \lambda_{vp} & s < s_a \\ \lambda_{vp} \frac{s_a+1}{s+1} & s > s_a \end{cases} \quad (8.2)$$

where s_a represents the saturation suction [138]. In this case, the volumetric strain by net stress or suction increase depends on both the current net stress and the current suction; therefore, Eq. (8.1) is able to reproduce quite accurately the volumetric response of unsaturated soils reported in the international literature.

One of the most important features of this equation is the introduction to some extent of the hydro-mechanical coupling through parameter s_a . In addition, although the two compression indexes λ_{vs} and λ_{vp} can be related using Eq. (8.2), different approaches can be used for more general cases. When plotted in the mean net stress axis *versus* suction, the yield surface generated with Eq. (8.1) shows a concavity. In fact, most constitutive models for unsaturated soils show a concavity at the transition between saturated and unsaturated states (see for example [139-142]). Although this concavity poses some difficulties in obtaining a unique response, this can be numerically solved. Moreover, Eq. (8.1) cannot be integrated and therefore requires special treatment in the stress integration for the constitutive model.

In contrast, the effective stress approach shows important advantages over the others because it uses a single compression index, shows a smooth transition between saturated and unsaturated states, and the proposed equation can be integrated. In addition, with a proper elastoplastic framework, this approach correctly explains the phenomenon of collapse upon wetting (see Chapter 9) and results in a unifying volumetric framework for saturated and unsaturated soils. This approach is developed in the next sections.

Collapse Upon Wetting

Abstract: This chapter presents the modeling of the phenomenon of collapse upon wetting using the effective stress approach established in Chapter 2 and the elastoplastic framework for the volumetric behavior of soils proposed in the previous chapter. Using the probabilistic porous-solid model, Bishop's parameter χ can be obtained to determine the current effective stress. The proposed framework includes the hysteresis of the SWRC and, to some extent, the hydro-mechanical coupling of unsaturated soils. This model is able to reproduce some particularities of the phenomenon of collapse upon wetting that other models cannot simulate.

Keywords: Collapse upon wetting, Unsaturated soils, effective stress, Elastoplastic framework, Yield surface, Suction hardening, Soil-water retention curve, Hysteresis, Hydro-mechanical coupling, Porous-solid model, Bishop's effective stress equation, Compacted soils, Neutral loading, Suction controlled tests, Preconsolidation stress.

9.1. INTRODUCTION

The Barcelona Basic Model (BBM) [7] has been able to reproduce the main aspects of the phenomenon of collapse upon wetting using the independent stress variables approach formally established by Fredlund and Morgenstern [5]. The key point for the simulation of the phenomenon of collapse upon wetting in this model is the consideration that the apparent preconsolidation stress increases with suction (Fig. 1). This feature is introduced into the model through the loading collapse yield surface (LCYS), which adopts the geometry shown in Fig. (1b). By analyzing the volumetric behavior of a soil sample subject to a drying-wetting cycle, the equation relating the yield stress in unsaturated (p_0) and saturated (p_0^*) conditions can be written as a function of the slopes of the loading ($\lambda(0)$ and $\lambda(s)$) and unloading-reloading (κ and κ_s) compression curves of the soil at saturated and unsaturated conditions, respectively. This equation writes:

$$\frac{p_0}{p^r} = \left(\frac{p_0^*}{p^r} \right)^{\frac{\lambda(0) - \kappa}{\lambda(s) - \kappa_s}}$$

where p^r represents a reference pressure. In general, it can be considered that $\kappa = \kappa_s$ as their values are relatively small. In turn, $\lambda(s)$ depends on the values of $\lambda(0)$ and suction. This equation represents the shape of the LCYS, as shown in Fig. (1b).

Eduardo Rojas

All rights reserved-© 2022 Bentham Science Publishers

When an increment of the net stress is applied to an initially saturated sample that has been dried to suction s_1 , as indicated by the stress path AA'BD in Fig. (1b), the initial LCYS_i displaces on the mean net stress axis reaching the position LCYS_f. Then, the elastic zone is bounded by the suction increase yield surface (SIYS), the suction decrease yield surface (SDYS), and the LCYS.

The volumetric compression of the material during a net stress increase (dv_p) beyond the yield stress is given by:

$$dv_p = -\lambda(s) \frac{d\bar{p}}{\bar{p}}$$

In the same way, the volumetric response of the soil during a suction increase (dv_s) beyond the SIYS is given by:

$$dv_s = \lambda_s \frac{ds}{s + p_{at}}$$

where λ_s represents the slope of the virgin compression line (VCL) during suction increase, ds is the increment in suction and p_{at} is the atmospheric pressure. In the case when both net stress and suction are increased, the total volumetric response of the material (dv) is given by the addition of the volumetric behavior during mean net stress increase and suction increase, in the form:

$$dv = dv_p + dv_s$$

This model has been widely employed to reproduce the volumetric behavior of unsaturated soils with great success.

Other models have been formulated based on the effective stress concept. See, for example, Bolzon, Schrefler and Zienkiewics [161], Vaunat, Romero and Jommi [128], Loret and Khalili [135], Karube and Kawai [162], Gallipoli, Gens, Sharma and Vaunat [28], Wheeler, Sharma and Buisson [27]. These models make use of Bishop's [14] effective stress σ'_{ij} :

$$\sigma'_{ij} = \sigma_{ij} - \delta_{ij}[u_a - \chi(u_a - u_w)]$$

The Bishop parameter χ can be written as a function of the degree of saturation, suction or both. For example, the model proposed by Gallipoli, Gens, Sharma and

Vaunat [28] considers that χ is equal to the degree of saturation. To account for the volumetric behavior of unsaturated soils, the model includes the constitutive parameter ξ which represents the bonding and debonding stress produced by water menisci. This parameter is written as a function of the degree of saturation S_r in the form:

$$\xi = f(s)(1 - S_r)$$

where $f(s)$ is a function of suction representing interparticle forces. Considering that e and e_s represent the void ratio in unsaturated and saturated conditions, respectively, when the soil is subject to the same Bishop stress, the relationship between the ratio e/e_s with parameter ξ , has been proposed as:

$$\frac{e}{e_s} = 1 - a[1 - \exp(b\xi)]$$

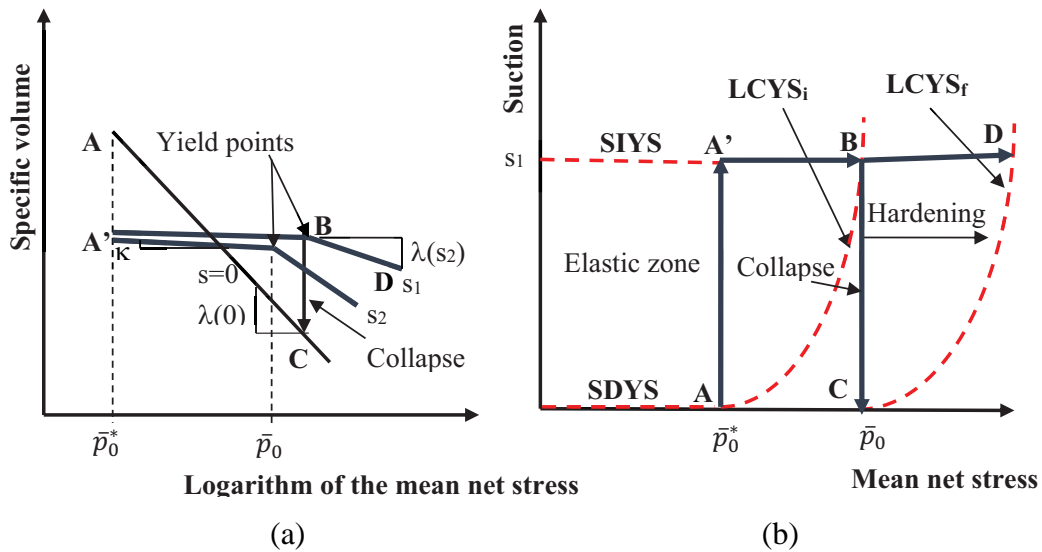


Fig. (1). (a) Volumetric behavior and (b) hardening of the LCYS in the BBM.

This model simulates the volumetric response of soils subjected to increments of the mean net stress and/or wetting-drying cycles, including the phenomenon of collapse upon wetting.

Another variation for the value of parameter χ is presented by Alonso, Pereira, Vaunat and Olivella [163]. In this case, the global degree of saturation (S_w) of the

Expansive Soils

Abstract: In this chapter, the elastoplastic framework for the volumetric behavior of soils developed in Chapters 8 and 9 is extended to account for the case of expansive soils. The hydraulic behavior of the soil is simulated using the porous-solid model developed in Chapter 4. The result is an elastoplastic framework where the value and sign of the expansion index depend on the density of the soil as well as the state of stresses and the direction of the increment of the effective stress with respect to the yield surfaces in the plane of effective mean stress against suction. Experimental and numerical comparisons show the ability of the model to simulate the behavior of expansive soils under different stress paths.

Keywords: Expansive soils, Effective stresses, Elastoplasticity, Compression index, Unloading-reloading index, Compression-expansion index, Relative density, Collapse upon loading, Loading collapse yield Surface, Suction increase yield surface, Wetting path, Drying path, Loading path, Unloading path.

10.1. INTRODUCTION

It is known that montmorillonite is one of the most active clays in nature. It appears as equidimensional flakes with a maximum length of 1 or 2 μm and a medium thickness of 0.001 μm for a single platelet or basic unit. Each basic unit is formed by one octahedral sheet packed between two silica sheets. The octahedral sheet may contain aluminum, magnesium, iron, zinc, nickel, lithium, or other cations (Mitchell [176]). These sheets are bonded together in a basic unit by primary valence links, which are very strong and hard to destroy. A certain number of basic units can be piled together by electrical forces forming a single clay particle. In general, positive cations and molecules of water can make the link between basic units. Their secondary specific surface (*i.e.*, the one that considers the interlayer surface) may be as large as 800 m^2/g . This means that electrical forces are of great importance for the behavior of these materials. Due to the bipolar characteristics of the molecule of water and depending on its availability, additional layers of water can intrude the link between the different platelets of a particle. When this happens, particles increase their volume, and clay exhibits expansion. This phenomenon is called crystalline swelling. If salt is diluted in the invading water, a double layer develops between particles, and repulsive forces appear. This phenomenon is called osmotic or double-layer swelling (Anandarajah and Amarasinghe [177]). In this paper, only the case of crystalline swelling is considered.

It is also known that many natural fine materials and dry of optimum compacted soils show a bimodal structure formed by a microstructure and a macrostructure. The microstructure is represented by the arrangement of small particles forming aggregates with pores of small size. These pores are called intra-aggregated pores or micropores. The relative arrangement of aggregates constitutes the macrostructure which exhibits larger pores. These pores are called inter-aggregated pores or macropores. The microstructure and the macrostructure become apparent through the pore size distribution (PSD) of the soil, which can be obtained from mercury intrusion porosimetry (MIP) tests like those performed by Simms and Yanful [55]. These researchers also observed that the relative volume of macropores reduces while that of intra-aggregated pores increases in relation to the total volume of pores when a soil sample is loaded or dried (Simms and Yanful [55, 56]).

This chapter is organized as follows: first, some of the most successful models for expansive soils are revised. Subsequently, the elastoplastic framework developed in Chapters 8 and 9 is extended for the case of expansive soils. Later, some comparisons between numerical and experimental results are presented.

10.2. BACKGROUND

One of the most successful models to simulate the behavior of expansive soils was proposed by Gens and Alonso [178] and later improved by Alonso, Vaunat and Gens [179]. These authors developed an elastoplastic framework for the behavior of expansive soils based on the independent stress variables approach [5]. This model includes the behavior of the two structural levels: the microstructure and the macrostructure. The microstructure is represented by swelling aggregates. This microstructure remains mostly saturated, and its behavior is governed by the effective stress obtained from the addition of net stress and pore water pressure. In that sense, a change in suction or net stress of the same quantity results in the same volumetric strain of the microstructure. The macrostructure is represented by the particular arrangement of aggregates and coarse material. These elements form the inter-aggregated pores where major structural rearrangements occur during loading or suction increase. However, the volumetric response of the macrostructure has a low direct influence on the microstructure. In contrast, the volumetric behavior of the microstructure greatly affects the macrostructure. When an expansive soil is subjected to wetting–drying cycles, the volume of its microstructure alternatively increases and reduces, and this volumetric behavior is partially transmitted to the macrostructure. Therefore, it can be said that there is a single-direction coupling between microstructure and macrostructure. Gens and Alonso [178] consider that

this coupling between micro and macrostructure depends on the overconsolidation ratio of the sample. Also, these authors consider microstructural deformations as largely reversible while irreversible behavior is attributed to the macrostructure.

The modeling of the macrostructure is described in the original Barcelona Basic Model (BBM) by Alonso, Gens and Josa [7]. The elastic region of the macrostructure in the plane of mean net stress (\bar{p}) versus suction (s) is bounded by the loading collapse yield surface (LCYS) as indicated in Fig. (1a). In order to include the behavior of expansive soils in this model, an expansive yield surface is added. This surface is called the Neutral Line (NL) and is represented by a straight line forming 135° with the horizontal in the plane formed by net stress and suction (Fig. 1a). When this yield surface is crossed by a suction or stress reduction path, the microstructure expands. A related movement between the NL and the LCYS takes into account the coupling between microstructure and macrostructure during expansion.

In order to include the macrostructural elastoplastic volumetric strains generated by the reversible microstructural strains, the suction increase yield surface (SIYS) and the suction decrease yield surface (SDYS) are included in the mean net stress-suction plane as indicated in Fig. (1a). These surfaces run parallel to the NL; the former is located above while the latter is located below the NL. The SIYS and the SDYS bound the macrostructural elastic volumetric strains during shrinkage and swelling of the microstructure, respectively. In addition, the dependency of the volumetric elastoplastic strains of the macrostructure on the elastic strains of the microstructure is included by means of two functions: f_D and f_I for suction decrease or increase, respectively. These functions depend on the ratio \bar{p}/\bar{p}_0 (where \bar{p}_0 represents the apparent preconsolidation net stress) for isotropic stresses, and their shape is plotted in Fig. (1b). This ratio has the same meaning as the overconsolidation ratio for saturated soils. A possible choice for these functions is given by Alonso, Vaunat and Gens [179]:

$$f_I = f_{I0} + f_{I1} \left(\frac{\bar{p}}{\bar{p}_0} \right)^{n_I} \quad \text{and} \quad f_D = f_{D0} + f_{D1} \left(1 - \frac{\bar{p}}{\bar{p}_0} \right)^{n_D}$$

CHAPTER 11**Hydro-Mechanical Coupling**

Abstract: The phenomenon of hysteresis during wetting-drying cycles can be simulated using the porous-solid model developed in Chapter 3. This model employs the current pore-size distribution of the material. The term “current pore-size distribution” means that the size of pores can be updated as the soil deforms. In that sense, the porous-solid model can be used advantageously for the development of fully coupled hydro-mechanical constitutive models, as the influence of the volumetric deformation on the retention curves and effective stresses can be easily assessed. By including some experimental observations related to the behavior of the pore size distribution of soils subjected to loading or suction increase, volume change can be related to the reduction in the size of macropores. This methodology avoids the necessity of any additional parameter or calibration procedure for the hydromechanical coupling of unsaturated soils.

Keywords: Hydro-mechanical coupling, Unsaturated soils, Porous-solid model, Pore size distribution, Soil-water retention curves, Hysteresis, Effective stresses, Macropores, Volumetric strain, Mean size of pores, Volumetric reduction, Evolution of pore size distribution, Loading, Suction increase.

11.1. INTRODUCTION

The aim of this chapter is to reproduce the shift of the soil-water retention curve (SWRC) generated by plastic volumetric deformations. To this purpose, the porous-solid model developed in Chapter 4 is coupled to the elastoplastic framework developed in Chapter 8, to build up fully coupled constitutive models for unsaturated soils. The idea is to take advantage of the fact that the porous-solid model is based on the current pore size distribution (PSD) of the material. Then, by making some assumptions on the way the PSD changes with volumetric deformations, an analytical expression can be derived. Using this procedure, no additional parameters nor fitting process are required for the porous-solid model to account for hydromechanical coupling.

This chapter starts with a brief description of some of the most relevant models used to include the hydro-mechanical coupling in unsaturated soils. Afterward, some assumptions regarding the way in which the PSD changes with the volumetric response of the material are considered, and an analytical equation is derived. Finally, this proposal is evaluated by making some numerical and experimental comparisons.

Eduardo Rojas

All rights reserved-© 2022 Bentham Science Publishers

The hydro-mechanical coupling in unsaturated soils was probably first mentioned by Wheeler [206]. This researcher stated that complete constitutive models for unsaturated materials should include information on the water content or degree of saturation. For that purpose, this author proposed the use of the specific water volume (v_w) as a second volumetric state variable. This variable comes in addition to the specific volume ($v = 1 + e$), generally treated as the first volumetric state variable. The specific water volume is defined as:

$$v_w = 1 + S_w e$$

where S_w and e represent the degree of saturation and the void ratio of the material, respectively. Wheeler [206] also indicated that fully coupled models should incorporate the hydraulic hysteresis and the effect of the state of stresses on the hydraulic behavior. The hysteresis of the SWRC causes the water content to be dependent not only on the value of suction but also on the wetting-drying path followed by the material. In addition, the volumetric deformation of the soil produces a shift of the SWRC in the axes of suction.

It is presently acknowledged that the best way to develop fully coupled hydro-mechanical models is on the basis of the effective stress principle. In recent years, several effective stress constitutive models that take account of the hysteresis of the SWRC have been developed. Among the most remarkable are the models by Vaunat, Romero and Jommi [128], Jommi [207], Buisson and Wheeler [208], Wheeler, Sharma and Buisson [27], Gallipoli, Gens, Sharma and Vaunat [28], Sheng, Sloan and Gens [30], Tamagnini [29] and Sun, Sheng and Sloan [209]. Different solutions have been proposed by earlier researchers to include the influence of the volumetric deformation on the SWRC (Vaunat, Romero and Jommi [128], Kawai, Kato and Karube [210], Gallipoli, Wheeler and Karstunen [211], Wheeler, Sharma and Buisson [27], Simms and Yanful [102], Koliji, Laloui and Vuillet [116], Sun, Sheng, Cui, Sloan [165], Nuth and Laloui [212], Tarantino [213], Mâsín [214], Sheng and Zhou [215], Gallipoli [216], Salager, Nuth, Ferrari and Laloui [217], Zhou and Ng [218] among others). Some of these models include the shift of the SWRC dependent on the volumetric deformation ([128, 216, 218]). The different solutions adopted by some of these models on this issue are reviewed below.

Vaunat, Romero and Jommi [128], adopted the elastoplastic framework of the Barcelona Basic Model (Alonso, Gens and Josa [7]) and included the effect of hysteresis and the state of stresses on the hydraulic behavior of the material. The last was considered by establishing all possible hydraulic states of the sample in the

void ratio-water ratio-suction space. The water ratio was defined as the ratio between the volume of water and the volume of solids. These researchers also considered that macropores are the only pores responsible for the volumetric deformation of soils. By including the void ratio in a modified van Genuchten formulation of the SWRCs, the influence of the irreversible deformation on the hydraulic behavior of soils is taken into account. For example, the water ratio $e_{wD,W}$ at drying (D) or wetting (W) was expressed as:

$$e_{wD,W} = e_{wm} + (e - e_{wm}) \left[1 + (\alpha_{D,W} s)^{n_{D,W}} \right]^{-m_{D,W}} \left[1 - \frac{\ln \left(1 + \frac{s}{s_{mD,W}} \right)}{2} \right]$$

where e_{wm} is the water ratio of micropores. The values of soil parameters $\alpha_{D,W}$, $s_{mD,W}$, $m_{D,W}$ and $n_{D,W}$ also depend on the path followed by suction: drying (D) or wetting (W). A similar approach to include the influence of void ratio on the SWRC was proposed by Della Vecchia, Jommi and Romero [164].

Khalili, Habte and Zargarbashi [219], simulated the SWRC using a modified Brooks and Corey [220] equation written as a function of the effective degree of saturation (S_{we}), defined as:

$$S_{we} = \frac{S_w - S_{wr}}{1 - S_{wr}}$$

where S_{wr} represents the residual degree of saturation. Therefore the main curves are simulated in terms of the air entry (s_{ae}) or the air expulsion (s_{ex}) value for the drying or wetting curve, respectively, in the form:

$$S_{we} = \begin{cases} 1 & \text{for } s < s_e \\ \left(\frac{s_b}{s} \right)^{\lambda_p} & \text{for } s \geq s_e \end{cases}$$

where s represents the current suction of the material and s_b takes the value of s_{ae} or s_{ex} for the main drying or wetting curve, respectively. Parameter λ_p is called the pore size distribution index and controls the slope of the main retention curves. For the case of wetting-drying cycles, parameter S_{we} depends on the value of suction at

A Fully Coupled Critical State Model

Abstract: In previous chapters, it has been shown that the principle of effective stresses can be applied to the shear strength, the tensile strength, and the volumetric behavior of unsaturated soils. This chapter shows that the critical state line for unsaturated soils shifts with respect to the saturated critical state line in a quantity that depends on the suction stress. Taking into account this phenomenon and the influence of hydro-mechanical coupling on the behavior of unsaturated soils, a fully coupled general constitutive model for soils is developed. This model is based on the modified Cam-Clay model but includes a yield surface with anisotropic hardening that takes into account the shift of the critical state line with suction. The result is a very simple model with symmetric stiffness matrix that can be used for the case of saturated, unsaturated, and compacted materials.

Keywords: Critical state concept, Critical void ratio, Effective stress, Virgin consolidation line, Elastoplastic framework, Elastic zone, Constitutive models, Tensile strength, Volumetric behavior, Effective stress, Yield surface, Plastic deformations, Suction hardening, Failure surface, Preconsolidation stress.

12.1. BACKGROUND

In the last twenty years, many hydro-mechanical coupled models for unsaturated soils have been developed using the effective stress concept. Some recent examples of models developed to solve different problems can be found in references [232 - 236]. Some models use non-normal flow rules requiring a plastic potential function in addition to a yield surface. Others use elaborated hardening coefficients to reproduce the volumetric behavior of unsaturated soils. Some others include fitting parameters for hydro-mechanical coupling. Models based on the modified Cam-Clay model (MCCM) have been largely used with fair results [30, 164, 237-243]. Other approaches have also been used with similar precision, for example, hypoplastic ([244, 245]), generalized plasticity [246], hydromechanical energy dissipation [247], bonding fabric ([137, 248]), among others. The hydraulic behavior is generally included by employing the simple elastoplastic model proposed by Wheeler [27]. Others use the van Genuchten [84] or the Fredlund, Wilson and Fredlund [249] equations for single or double porosity soils to simulate the main wetting and drying curves. Then, with the aid of some analytical relationships, wetting-drying cycles can be simulated.

Some of the most representative models are those proposed by Russell and Khalili [250], Zhou and Sheng [242] and Ma, Wei, Wei and Li [243]. These models are reviewed herein. The model by Russell and Khalili [250] uses Bishop's effective stress equation with Bishop's parameter-dependent solely on suction. This model uses the bounding surface concept to generate a smooth transition between elastic and elastoplastic behavior. The loading and the bounding surface show the same shape and are represented by a logarithmic function with isotropic hardening dependent on the volumetric strain. A simple radial mapping rule with the center at the origin, is used to define the projection of the state of stresses on the bounding surface. Additionally, a non-associated flow rule is used with a plastic potential obtained from the integration of a dilation rule. The flow rule is dependent on the position of the stress state with respect to the critical state line (CSL) as well as the direction of the normal vector of the plastic potential. This feature ensures contraction or dilatation when the stress state is located below or above the CSL, respectively. The hardening modulus is split into two parts, one for the bounding surface and the other dependent on the distance between the loading and the bounding surface. This last hardening modulus can be defined arbitrarily provided that it becomes null at the bounding surface and uses a parameter that depends on the initial conditions. The model includes the effect of particle crushing for the case of sands tested at large mean stresses. It also considers the shift of both the CSL and the isotropic consolidation line (VCL) due to suction hardening by means of an analytical equation written in terms of suction and the volumetric plastic strain of the sample. This model requires several fitting parameters and functions such as the exponent of the yield surface ($1/N$), an initial state or changing conditions parameter k_m , a function defining energy dissipation k_d , a function defining the slope of the isotropic compression line dependent on suction $\lambda(s)$ and a function defining the shift of the VCL with suction. In addition, as the plastic potential does not cross the mean effective stress axis at a straight angle, deviatoric strains appear during isotropic loading.

The model by Zhou and Sheng [242] uses Bishop's equation and the effective degree of saturation takes the value of Bishop's parameter. Contrary to common models where suction is used as the third axis in addition to mean effective stress and deviator stress, this model uses the effective degree of saturation as the third axis. It employs a bounding and a subloading surface as well as a unified hardening parameter in addition to a hydraulic model to build up a coupled hydro-mechanical model. It includes a loading collapse yield surface (LCYS) similar in shape to the Barcelona Basic Model but written in terms of the effective degree of saturation. The compression index also depends on the effective degree of saturation of the soil. A common isotropic hardening rule is used for the yield surface. A modified

van Genuchten equation, which includes the influence of plastic volume changes on the soil-water retention curves (SWRCs), is employed for the hydraulic model. Wetting-drying cycles can be simulated using the Sheng and Zhou [215] hydraulic model. The initial void ratio is considered a key variable for the behavior of the soil. It requires two fitting parameters for hydro-mechanical coupling. The phenomena of suction hardening and the shift of the VCL and CSL with suction are not included directly in the model. This model requires in total 13 parameters.

The model by Ma, Wei, Wei and Li [243] uses Bishop's equation and the degree of saturation as Bishop's parameter to compute effective stresses. This model is based on the elliptic yield surface of the MCCM and couples hydraulic and mechanical behavior. The Feng and Fredlund [251] hydraulic model is used to simulate wetting-drying cycles and includes the dependency of the SWRCs on the plastic volumetric strains. The constitutive model uses a non-associated flow rule through a dilatancy term. The hardening rule considers the effect of volumetric and deviatoric plastic strains. The influence of deviatoric plastic strains is included by means of a parameter dependent on the degree of saturation and suction. It also considers a correction function that accounts for the hardening effect of a non-saturated material which depends on the current value of several parameters such as suction, the degree of saturation, and the plastic volumetric strain of the sample. This model does not consider the shift of the VCL or CSL due to suction hardening.

This chapter shows that constitutive models based on the Critical State theory for saturated soils can be easily adapted as fully coupled models for unsaturated soils when the phenomena of suction hardening, hydraulic hysteresis, and dependency of SWRCs on plastic volumetric strains are properly considered. Specifically, this chapter shows that the MCCM can properly simulate the behavior of unsaturated soils with minor changes. In this way, very simple fully coupled constitutive models for soils can be generated with similar precision to other models.

12.2. CRITICAL STATE

One issue that requires reviewing, is the critical state concept for soils tested at different suctions. Wheeler and Sivakumar [111] performed a series of triaxial tests on samples of unsaturated compacted speswhite kaolin. These samples were prepared by static compaction in a mold at 25% water content. The tests were conducted in double-walled triaxial cells designed to accurately measure the volume change of the samples during the test. In Chapter 6, the compression strength of unsaturated samples subjected to different suctions was predicted using the concept of effective stress. These simulations showed that a unique failure

Retention Curves in Deforming Soils

Abstract: During the determination of the main drying curve, the soil is subjected to high suctions, which induce important volumetric deformations. These volumetric deformations modify the pore size distribution of the sample affecting both the drying and the wetting branch of the retention curves. Although most deformation occurs at drying, this branch is only slightly affected by soil deformation. In contrast, the wetting branch shows important shifting when volume change is considered. A porous-solid model based on the grain and pore size distributions of the soil is coupled with a mechanical model to simulate the soil-water retention curves while the material is deforming.

Keywords: Soil-water retention curves, Suction, Deforming soils, Macropores, Micropores, Coupled models, Effective stresses, Porous models, Hydromechanical coupling, Elastoplasticity, Plastic strains, Pore size distribution, Volumetric strains, Degree of saturation, Unsaturated soils.

13.1. INTRODUCTION

Different models have been proposed to account for the density of soils during the determination of the soil-water retention curves (SWRCs). See for example [211, 213, 214, 262-266], among others. Some of the more representative models are reviewed herein.

From a series of experimental results, Tarantino [213] observed that at a high suction range, the water ratio ($e_w = V_w/V_s$) can be expressed as a power function of suction. In addition, the degree of saturation in the van Genuchten equation [84] can be written in terms of the water ratio and void ratio ($e = V_v/V_s$). By performing some substitutions in these equations, the SWRC can be expressed in terms of the void ratio. In addition, with the inclusion of different parameters for the drying and wetting curve, the phenomenon of hysteresis can be considered and scanning behavior can be modeled. Three parameters are required for each branch, two of which are directly obtained from the data of the corresponding retention curve of the soil. The third is determined by the best fit with the corresponding curve.

The model developed by Hu *et al.* [264] also considers the van Genuchten equation to simulate the SWRCs. These authors use a logarithmic relationship between the mean size of pores with the mean stress. With this relationship, they could assess the variation in the mean size of pores through the variation in the void ratio of the

soil using a proportional parameter. Therefore, the air entry value for the retention curve is written as a function of the current void ratio. Hysteresis is included by considering different air entry values for the drying and wetting curves. This equation of the SWRC dependent on the void ratio shows similarities to the equation proposed by Gallipoli *et al.* [211]. However, the last relates the air entry value to void ratio using an empirical power function, while Hu *et al.* [264] derive their equation from the change in the pore size distribution (PSD). In addition, all seven parameters required by Hu's model, show a clear physical meaning. However, two of these parameters are related to the scanning behavior and need to be determined from hydro-mechanical scanning, which represents an important drawback. A correction factor, similar to that proposed by Fredlund and Xing [53], is included for the high suction range of the SWRC. This model requires the variation in the void ratio of the sample during wetting-drying cycles to simulate the shift of the retention curves in the axis of suction. Wetting-drying cycles are simulated following the procedure proposed by Gallipoli [216] who assumes similar shapes between the scanning curves and the main curves.

The model by Della Vecchia *et al.* [265] includes the evolution of the pore size distribution of soils during hydro-mechanical loading through the progress of parameters of the soil-water retention curves. Double structured soils can be considered by introducing the porosity of both the micro and the macrostructure and adopting a van Genuchten's equation for each structural level, resulting in bimodal retention curves. These authors have established some relationships between the air entry value with the void ratio of the micro and macrostructure. In turn, the void ratio of the microstructure is related to the water ratio. As a normalized relationship relating the void ratio of the macrostructure with the air entry value could not be established, they have proposed a general equation. However, this equation requires a previous calibration to define some parameters which represents an important disadvantage. This model requires, in total, eight parameters for double structured soils. The influence of pore size distribution on the retention curves as well as the evolution of water ratio with suction can be fairly simulated with this model, which can even simulate the retention curve as the soil is deforming.

In a similar way, the model by Gao and Sun [266], simulates the effect of the void ratio on the retention curves through the air entry value. These authors use the Fredlund and Xing [53] equation to represent the retention curves and write the air entry value as a function of the saturated water content (or saturated void ratio) through a semilogarithmic relationship requiring two parameters. These parameters are determined using the retention curves in terms of both water content and degree

of saturation. They include the saturated water content, the residual suction, the main slope of the curve, and the value of suction at the inflexion point. The model predicts fairly well the shift of the retention curve for different densities of soil.

The main drawback of the above methods is that none of them consider full hydro-mechanical coupling. When an increment in suction is applied, the soil deforms and the SWRC modifies. This in turn, affects the value of the effective stress parameter χ used to calculate the next volumetric strain. As Della Vecchia [265] points out, the resulting SWRC is not the same when the retention curve is simulated using the final PSD. In addition, none of these models includes simultaneously the case for double structured soils along with the simulation of scanning curves during wetting-drying cycles.

In this chapter, the porous-solid model based on the grain size distribution (GSD) and current PSD of the soil (Chapter 3), is used to simulate the evolution of retention curves while the soil is deforming. This porous-solid model is coupled with an effective stress mechanical model to determine the volumetric strains with suction. Some numerical and experimental results are compared and some conclusions are withdrawn. These results show important differences from previously published models.

13.2. PROCEDURE

The porous-solid model can be used advantageously to include hydromechanical coupling in constitutive formulations as no additional parameters or fitting processes are required. According to the experimental results reported by Simms and Yanful [55], only the volume of macropores reduces when soils show plastic volumetric strains during compression. Therefore, these plastic volumetric strains represent the reduction in the volume of macrocavities as the volume of macrobonds is negligible, as stated in Chapter 3. This reduction in the volume of macrocavities can be included in the model in three different ways: by a reduction in the number of macrocavities, by a reduction in the mean size of macrocavities or by a combination of both. The first method has been used in Chapter 11, to simulate the evolution of initially known SWRCs when the soil undergoes volumetric deformations. In such a case, the relative volume factor for macrocavities was related to the plastic volumetric strain of the material. In this chapter, the second procedure is adopted.

To that purpose, the whole process of drying and wetting to obtain the SWRCs is simulated with a coupled model, resulting in PSDs that adjust better to experimental

Undrained Tests

Abstract: When undrained triaxial tests are performed, two main phenomena occur. First, the compression of the sample produces an increase in the degree of saturation and therefore, a reduction in the value of suction. Second, with the reduction in the sizes of pores, the retention curves shift on the axis of suction. Thereafter, the simulation of undrained triaxial tests requires the correct simulation of the hydromechanical coupling phenomenon. A fully coupled constitutive model for unsaturated soils is used herein to simulate the behavior of unsaturated soils subjected to undrained conditions. The mechanical model is based on the modified Critical State model and the effective stress concept. The hydraulic model uses the grain and pore size distributions to approximately reproduce the structure of soils. This model is able to simulate the soil-water retention curves during wetting-drying cycles. Plastic volumetric strains modify the pore size distribution of the soil, which in turn affects the retention curves and, therefore, the current effective stress. Some comparisons between numerical and experimental results of undrained triaxial tests show the adequacy of the model.

Keywords: Effective stresses, Undrained tests, Constant water tests, Constitutive model, Unsaturated soils, Elastoplasticity, Suction stress, Net stress, Yield surface, Anisotropic hardening, Preconsolidation stress, Critical state, Suction hardening, Triaxial tests, Isotropic compression.

14.1. INTRODUCTION

One of the most representative models to simulate the behavior of unsaturated soils under undrained conditions was proposed by Sun *et al.* [267]. It is based on the modified Cam-Clay model and uses some aspects of the Barcelona Basic Model (BBM). It considers the strain tensor (ε_{ij}) and the degree of saturation (S_w) as the strain-state variables while suction (s) and Bishop's effective stress tensor (σ'_{ij}) represent the stress-state variables. Parameter χ is equalized to the degree of saturation S_w . The hydraulic model is similar to the one proposed by Wheeler *et al.* [27], except that the air entry and air expulsion values are expressed as a function of the void ratio of the sample. In this way, the hydromechanical coupling is included in the model. It considers a loading collapse yield surface (LCYS) represented by the same equation as proposed by Alonso *et al.* [7] for the BBM, except that it is written in terms of the effective mean stress in the form:

$$p'_0 = p'_n \left(\frac{p_0^{*'}}{p'_n} \right)^{\frac{\lambda(0)-\kappa}{\lambda(s)-\kappa}}$$

where p'_0 and $p_0^{*'}$ represent the apparent preconsolidation stress at certain suction and the saturated preconsolidation stress, respectively, while p'_n is an isotropic stress at which no collapse occurs during wetting. κ is the unloading-reloading index while $\lambda(0)$ and $\lambda(s)$ represent the compression indexes in saturated and unsaturated conditions, respectively. Similar to the BBM, the compression index for unsaturated materials $\lambda(s)$, depends on the compression index of the saturated material $\lambda(0)$ and suction, in the form:

$$\lambda(s) = \lambda(0) + \frac{\lambda_s s}{(p_{at} + s)}$$

where λ_s is a soil parameter while p_{at} is the atmospheric pressure. The value $\lambda(0) + \lambda_s$ represents the compression index of the soil when subjected to large values of suction. The yield surface f is an ellipse similar to the modified Cam-Clay model given by the equation:

$$f = q^2 + M^2 p'(p' - p'_0)$$

The critical state line is represented by the Mohr-Coulomb failure condition irrespective of the value of suction. Finally, the hardening of the yield surface is included through the saturated preconsolidation stress in the form:

$$dp_0^{*'} = \frac{1 + e_0}{\lambda(0) - \kappa} p_0^{*' } d\varepsilon_v^p$$

where e_0 and $d\varepsilon_v^p$ represent the initial void ratio and the increment of the volumetric plastic strain. The model considers the associated flow rule and requires five parameters: $\lambda(0)$, λ_s , κ , p'_n and M , while the hydraulic model requires three parameters: the slopes of the retention curve before and after the air entry value (κ_s and λ_{sr} , respectively) and the slope of the variation of void ratio with the degree of saturation.

The model proposed herein shows some of the characteristics of this model although, in addition, it shows the following features which are not included in the model above:

- a. The apparent preconsolidation stress increases twice the value of the suction stress during drying due to the phenomenon of suction hardening.
- b. Due to this same phenomenon, the yield surface shows anisotropic hardening.
- c. The yield surface can adopt different shapes.
- d. The position of the critical state point on the yield surface depends on the value of the suction stress.
- e. The hydromechanical coupling due to the shift of the retention curves with plastic volumetric strains, requires no additional parameters or fitting process.

Features (a) to (d) were explained in Chapter 12 while feature (e) was explained in Chapters 11 and 13. Undrained tests can be simulated by computing the volumetric strain produced by a small increment of load. This volumetric strain generates a variation in the degree of saturation of the material which in turn affects the value of suction. This change in suction is simulated by the porous-solid model assuming that the material follows a wetting or drying path depending if the soil compresses or dilates, respectively. The wetting or drying paths depart from the initial condition of the sample. This means that initially, a wetting or drying path can follow a scanning or a main curve depending on the initial condition of the sample. Finally, the change in suction obtained from the variation in the degree of saturation is used for the next increment of load. This procedure has been used herein to simulate the behavior of two different types of soil as shown below.

According to Tarantino and De Col [167] and Li *et al.* [268], when soil is compacted, its initial state appears close to the main drying curve. If this sample is compressed in undrained conditions, it follows a scanning path to reach the primary wetting curve. On the contrary, if the sample is unloaded, it follows a scanning path to reach the drying branch. In addition, when the soil is wetted before loading, as for the two series of tests simulated herein, the material is considered to be already placed on the main wetting curve.

14.2. NUMERICAL AND EXPERIMENTAL COMPARISONS

14.2.1. Tests by Jotisankasa *et al.*

These authors [269] performed triaxial tests on a mixture of 70% silt, 20% kaolin, and 10% London clay. These materials were mixed at a water content 1.5 times the liquid limit. Then the slurry was dried at 70^o C, grounded, and passed through sieve No. 40. This material shows a liquid limit of 28%, and plasticity index of 18%. This mixture was hydrated to reach a water content of 10.1%, and statically compacted

Compacted Soils

Abstract: When unsaturated soils are subjected to drained or undrained compression tests, they approach the saturated compression line with different slopes. This difference in slopes is produced by the amount of collapse of each path. During compression, four main phenomena occur in these materials: first, with the reduction in volume, the degree of saturation increases; second, with the reduction in the size of pores, the soil-water retention curve shifts on the suction axis; third, these two phenomena produce an increase in the suction stress and, finally, this increase in suction stress produces a certain amount of collapse on the sample. In this chapter, a coupled model is employed to simulate the volumetric behavior of compacted soils under different stress paths. The comparison between experimental and numerical results shows the pertinence of the model.

Keywords: Compression, static compaction, Collapse upon wetting, Effective stresses, Coupled model, Undrained tests, Elastoplasticity, Unsaturated soils, Hydromechanical coupling, Retention curves, Suction stress, degree of saturation, Preconsolidation stress, Volumetric behavior, Saturated compression line.

15.1. INTRODUCTION

The volumetric behavior of unsaturated soils has been profusely studied in the last twenty years, but doubts still subsist on the best way to model this behavior. It is well known that the previous stress history and the current stress path greatly influence the behavior of soils. Also, phenomena such as suction hardening, hysteresis, and hydromechanical coupling affect the behavior of these materials. For example, on one hand, soil samples that have been dried from the saturated condition show an apparent preconsolidation stress dependent on the maximum value of the suction stress applied during drying. When these materials are compressed at constant suction (drained tests), they present an initial elastic behavior up to the apparent preconsolidation stress. When the preconsolidation stress is surpassed, their paths approach, and sometimes cross, the virgin consolidation line (VCL) for saturated materials when plotted on the axes of the logarithm of the mean net stress *vs.* void ratio. See for example the experimental results reported by Futai and Almeida [130]; Thu *et al.* [252]; Cunningham *et al.* [150]. When these paths are replotted using the logarithm of the mean effective stress, they run quasi-parallel to the VCL as the apparent preconsolidation stress appears above this line. These results indicate that the compression index is the same for both cases (see Chapter 8). This behavior is indicated as path 1 in Fig. (1).

On the other hand, when a soil sample is prepared by compaction of a disaggregated mixture of solid particles with water, and this sample is loaded beyond the apparent preconsolidation stress under undrained conditions (constant water conditions), it shows larger compressibility than a saturated sample. This behavior is presented as path 2 in Fig. (1). See, for example, the experimental results by Sivakumar [114], Sharma [272], Sivakumar and Wheeler [49], Toll and Ong [156].

The difference in the behavior of these samples lies basically in their previous loading history, their current loading path, and their hydraulic behavior. Different loading histories produce diverse shapes for the loading-collapse yield surface (LCYS) which in turn, affect the volumetric behavior of the soil. In addition, the main soil-water retention curves (SWRCs) for each case are different: for the case of drained tests, in order to keep suction constant during compression, the soil drains a certain amount of water. Instead, in the case of undrained tests, the sample maintains the same water content but reduces the value of suction when the degree of saturation increases. The combination of these elements generates variations on the value of the suction stress which has a fundamental role in the volumetric behavior of soils. By making an analogy, it can be said that suction stress for unsaturated soils is to pore water pressure for saturated materials.

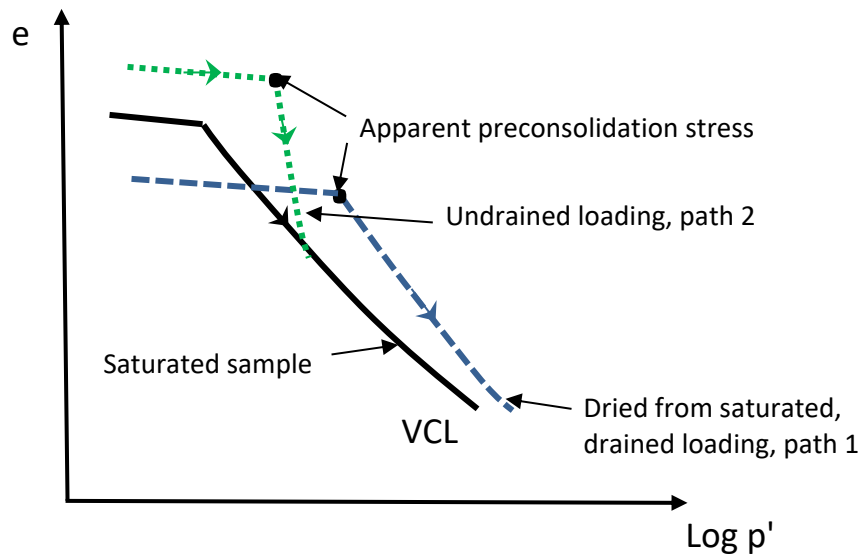


Fig. (1). General paths during drained and undrained compression tests.

Several researchers have studied the volumetric behavior of unsaturated soils subjected to different stress paths see for example, Thu *et al.* [252], Jotisankasa

et al. [273], Cui *et al.* [159], Casini [172], Zhou *et al.* [274], Mihalache and Buscamera [275], Mun and McCartney [146], Lloret *et al.* [276], Zhang *et al.* [277], Pedroti and Tarantino [278]. Some of the most representative models to simulate the volumetric behavior of unsaturated soils are those proposed by Tarantino and De Col [167], Zhou *et al.* [279] and Alonso *et al.* [221]. These models are discussed below.

The model by Tarantino and De Col [167] considers the average skeleton stress given by the relationship $\sigma_n^v = \sigma_n + s S_r$, where σ_n represents the net stress, s is suction and S_r the degree of saturation. The SWRCs for a constant void ratio e , were obtained by interpolating the results of compaction tests at different initial water contents. Then, the equation for the main wetting curves for different voids ratios is proposed according to Gallipoli *et al.* [28], as $S_r = \left[\frac{1}{1 + (\phi e^\psi s)^r} \right]^m$ where ϕ , ψ , m and r are fitting parameters. The void ratio in saturated conditions is represented by the equation $e_s = (N - 1) - \lambda \ln \sigma_n^v$, while for unsaturated materials, they propose the following relationship obtained from their experimental results $e = e_s \left[1 - a \left(\frac{s^*}{\sigma_n^v} \right)^b \right]$, where $s^* = n s$ is the modified suction, n is the porosity of the material and a and b represent two fitting parameters that require calibration with experimental results. This in fact, represents an important inconvenience for the practical application of the model. This last equation uses the values of suction from a SWRC obtained from the interpolation of results of samples tested at different water contents. This model correctly simulates the behavior of one-dimensional statically compacted samples. In total, the model requires 10 parameters, five of which correspond to the retention curve.

The model by Zhou *et al.* [279] considers that mean effective stress is given by the relationship $p' = p_n + s S_e$, where p_n represents the mean net stress. S_e is the effective degree of saturation given by the relationship $S_e = (S_w - S_w^r) / (S_w^0 - S_w^r)$, where S_w , S_w^0 and S_w^r represent the current, the saturated, and the residual degree of saturation of the material. These authors also define an apparent preconsolidation stress for unsaturated soils using the equation $p'_0 = (p'_0)^{\beta}$, where p'_0 represent the saturated preconsolidation stress and $\beta = (\lambda_0 - \kappa) / (\lambda(S_e) - \kappa)$ where λ_0 and κ represent the compression indexes for loading and unloading in saturated conditions, respectively, while the compression index for any degree of saturation is represented by the equation $\lambda(S_e) = \lambda_0 - (1 - S_e)^{\alpha_1} (\lambda_0 - \lambda_d)$ where λ_d represents the compression index under the condition of residual degree of saturation. If this last parameter is not available, it

REFERENCES

- [1] E.L. Matyas, and H.S. Radhakrishna, "Volume change characteristics of partially saturated soils", *Geotechnique*, vol. 18, no. 4, pp. 432-448, 1968.
<http://dx.doi.org/10.1680/geot.1968.18.4.432>
- [2] V.Q. Hung, D.G. Fredlund, and J.H.F. Pereira, "Coupled solution for the prediction of volume change in expansive soils", *Proceedings of the Third International Conference on Unsaturated Soils*, vol. 1, pp. 181-186, 2002. Recife Brazil.
- [3] J.A. Jiménez, *Hacia una mecánica de suelos no saturados.. Décima Conferencia Nabor Carrillo, Sociedad Mexicana de Mecánica de Suelos: México*, 1990.
- [4] X. Zhang, and R.L. Lytton, "Modified state-surface approach to the study of unsaturated soil behavior. Part I: Basic concept", *Can. Geotech. J.*, vol. 46, no. 5, pp. 536-552, 2009.
<http://dx.doi.org/10.1139/T08-136>
- [5] D.G. Fredlund, and N.R. Morgenstern, "Stress state variables for unsaturated soils", *J. Geotech. Eng. Div.*, vol. 103, no. 5, pp. 447-466, 1977.
<http://dx.doi.org/10.1061/AJGEB6.0000423>
- [6] A.W. Bishop, and I.B. Donald, "The experimental study of partly saturated soil in the triaxial apparatus", *Proc. 5th Int. Conf. Soil Mech.*, vol. I, Paris. , pp. 13-21, 1961.
- [7] E.E. Alonso, A. Gens, and A. Josa, "A constitutive model for partially saturated soils", *Geotechnique*, vol. 40, no. 3, pp. 405-430, 1990.
<http://dx.doi.org/10.1680/geot.1990.40.3.405>
- [8] K.H. Roscoe, and J.B. Burland, "On the generalized stress-strain behaviour of wet clay", In: L. De Heyman, Ed., *Engineering Plasticity*. Cambridge University Press, 1968, pp. 535-609.
- [9] K. Terzaghi, "The shearing resistance of saturated soils and the angle between the planes of shear", *Proc. 1st Int. Conf. Soil Mech., Int. Soc. Soil Mech. Found. Engrng*, vol. 1, 1936pp. 54-56
- [10] A.W. Skempton, Terzaghi's discovery of effective stress. *From theory to practice in soil mechanics..* John Wiley: New York, USA, 1960.
- [11] P.V. Lade, and R. De Boer, "The concept of effective stress for soil, concrete and rock", *Geotechnique*, vol. 47, no. 1, pp. 61-78, 1997.
<http://dx.doi.org/10.1680/geot.1997.47.1.61>
- [12] J.E.B. Jennings, "Discussion on M.S. Youssef's paper", *Proc. 4th Int. Conf. on Soil Mech., Int. Soc. Soil Mech. Found. Engrng.*, vol. vol. 3, 1957p. 168
- [13] D. Croney, J.D. Coleman, and W.P.M. Black, "Movement and distribution of water in soil in relation to highway design and performance", *Highway Research Board, Spec.*, vol. 40, 1958.
- [14] A.W. Bishop, "The principle of effective stress", *Tek. Ukebl.*, vol. 39, pp. 859-863, 1959.
- [15] G.D. Aitchison, *Relationships of moisture stress functions in unsaturated soils..* Buttherworths: London, U.K., 1960.*Conf. Pore Pressures, Institution of Civil Engineering.* Buttherworths: London, U.K., 1960.
- [16] G.E. Blight, "Effective stress evaluation for unsaturated soils", *J. Soil Mech. Div*, vol. 93, pp. 125-148, 1967.
- [17] N. Khalili, and M.H. Khabbaz, "A unique relationship for χ for the determination of the shear strength of unsaturated soils", *Geotechnique*, vol. 48, no. 5, pp. 681-687, 1998.

- <http://dx.doi.org/10.1680/geot.1998.48.5.681>
- [18] A-L. Öberg, and G. Sällfors, "A rational approach to the determination of the shear strength parameters of unsaturated soils", *Proceedings 1st Int. Conf. on Unsaturated Soils*, Alonso & Delage eds, vol. 1, 1995pp. 151-158 Paris, France.
- [19] E.A. Garven, and S.K. Vanapalli, "Evaluation of empirical procedures for predicting the shear strength of unsaturated soils", *Proceedings 5th International Congress on Unsaturated Soil Mechanics*, 2006 Arizona, USA.
[http://dx.doi.org/10.1061/40802\(189\)219](http://dx.doi.org/10.1061/40802(189)219)
- [20] J.E.B. Jennings, and J.B. Burland, "Limitations to the Use of Effective Stresses in Partly Saturated Soils", *Geotechnique*, vol. 12, no. 2, pp. 125-144, 1962.
<http://dx.doi.org/10.1680/geot.1962.12.2.125>
- [21] S.K. Vanapalli, D.G. Fredlund, D.E. Pufahl, and A.W. Clifton, "Model for the prediction of shear strength with respect to soil suction", *Can. Geotech. J.*, vol. 33, no. 3, pp. 379-392, 1996.
<http://dx.doi.org/10.1139/t96-060>
- [22] G.T. Houlsby, "The work input to an unsaturated granular material", *Geotechnique*, vol. 47, no. 1, pp. 193-196, 1997.
<http://dx.doi.org/10.1680/geot.1997.47.1.193>
- [23] X.S. Li, "Thermodynamics-based constitutive framework for unsaturated soils. 1: Theory", *Geotechnique*, vol. 57, no. 5, pp. 411-422, 2007.
<http://dx.doi.org/10.1680/geot.2007.57.5.411>
- [24] X.S. Li, "Thermodynamics-based constitutive framework for unsaturated soils. 2: A basic triaxial model", *Geotechnique*, vol. 57, no. 5, pp. 423-435, 2007.
<http://dx.doi.org/10.1680/geot.2007.57.5.423>
- [25] E. Nikooee, G. Habibagahi, S.M. Hassanizadeh, and A. Ghahramani, "Effective stress in unsaturated soils: A thermodynamic approach based on the interfacial energy and hydromechanical coupling", *Transp. Porous Med.*, vol. 96, pp. 369-396, 2013.
- [26] O. Coussy, "Revisiting the constitutive equations of unsaturated porous solids using a Lagrangian saturation concept", *Int. J. Numer. Anal. Methods Geomech.*, vol. 31, no. 15, pp. 1675-1694, 2007.
<http://dx.doi.org/10.1002/nag.613>
- [27] S.J. Wheeler, R.S. Sharma, and M.S.R. Buisson, "Coupling of hydraulic hysteresis and stress-strain behaviour in unsaturated soils", *Geotechnique*, vol. 53, no. 1, pp. 41-54, 2003.
<http://dx.doi.org/10.1680/geot.2003.53.1.41>
- [28] D. Gallipoli, A. Gens, R. Sharma, and J. Vaunat, "An elasto-plastic model for unsaturated soil incorporating the effects of suction and degree of saturation on mechanical behaviour", *Geotechnique*, vol. 53, no. 1, pp. 123-135, 2003.
<http://dx.doi.org/10.1680/geot.2003.53.1.123>
- [29] R. Tamagnini, "An extended Cam-clay model for unsaturated soils with hydraulic hysteresis", *Geotechnique*, vol. 54, no. 3, pp. 223-228, 2004.
<http://dx.doi.org/10.1680/geot.2004.54.3.223>
- [30] D. Sheng, S.W. Sloan, and A. Gens, "A constitutive model for unsaturated soils: Thermomechanical and computational aspects", *Comput. Mech.*, vol. 33, no. 6, pp. 453-465, 2004.
<http://dx.doi.org/10.1007/s00466-003-0545-x>
- [31] C.S. Desai, and Z. Wang, "Disturbed state model for porous saturated materials", *Int. J. Geomech.*, vol. 3, no. 2, pp. 260-265, 2003.
[http://dx.doi.org/10.1061/\(ASCE\)1532-3641\(2003\)3:2\(260\)](http://dx.doi.org/10.1061/(ASCE)1532-3641(2003)3:2(260))

- [32] A. Sridharan, A.G. Altschaeffl, and S. Diamond, "Pore size distributions studies", *J. Soil Mech. Found. Div.*, vol. 97, no. 5, pp. 771-787, 1971.
<http://dx.doi.org/10.1061/JSFEAQ.0001595>
- [33] W.B. Haines, "The hysteresis effect in capillary properties and the mode of moisture distribution associated therewith", *J. Agric. Sci.*, vol. 20, p. 7, 1929.
- [34] E.J. Murray, "An equation of state for unsaturated soils", *Can. Geotech. J.*, vol. 39, no. 1, pp. 125-140, 2002.
<http://dx.doi.org/10.1139/t01-087>
- [35] C.S. Desai, and Z. Wang, "Disturbed state model for porous saturated materials", *Int. J. Geomech.*, vol. 3, no. 2, pp. 260-265, 2003.
[http://dx.doi.org/10.1061/\(ASCE\)1532-3641\(2003\)3:2\(260\)](http://dx.doi.org/10.1061/(ASCE)1532-3641(2003)3:2(260))
- [36] A-L. Öberg, Stability of sand and silt slopes. *Internal report.*. Department of Geotechnical Engineering, Chalmers University of Technology: Gothenburg, Sweden, 1995.
- [37] M.A. Biot, "Theory of elasticity and consolidation for a porous anisotropic solid", *J. Appl. Phys.*, vol. 26, no. 2, pp. 182-185, 1955.
<http://dx.doi.org/10.1063/1.1721956>
- [38] W.B. Haines, "Studies in the physical properties of soils: II. A note on the cohesion developed by capillary forces in an ideal soil", *J. Agric. Sci.*, vol. 15, no. 4, pp. 529-535, 1925.
<http://dx.doi.org/10.1017/S0021859600082460>
- [39] X. Chateau, and L. Dormieux, "Micromechanics of saturated and unsaturated porous media", *Int. J. Numer. Anal. Methods Geomech.*, vol. 26, no. 8, pp. 831-844, 2002.
<http://dx.doi.org/10.1002/nag.227>
- [40] E.E. Alonso, J.M. Pereira, J. Vaunat, and S. Olivella, "A microstructurally based effective stress for unsaturated soils", *Geotechnique*, vol. 60, no. 12, pp. 913-925, 2010.
<http://dx.doi.org/10.1680/geot.8.P.002>
- [41] I. Vlahinić, H.M. Jennings, J.E. Andrade, and J.J. Thomas, "A novel and general form of effective stress in a partially saturated porous material: The influence of microstructure", *Mech. Mater.*, vol. 43, no. 1, pp. 25-35, 2011.
<http://dx.doi.org/10.1016/j.mechmat.2010.09.007>
- [42] W. Fuentes, and T.H. Triantafyllidis, "On the effective stress for unsaturated soils with residual water", *Geotechnique*, vol. 63, no. 16, pp. 1451-1455, 2013.
<http://dx.doi.org/10.1680/geot.13.T.013>
- [43] J.M. Konrad, and M. Lebeau, "Reply to the discussion by Mesri and Kane on "Capillary-based effective stress formulation for predicting shear strength of unsaturated soils"", *Can. Geotech. J.*, vol. 53, no. 9, pp. 1562-1564, 2016.
<http://dx.doi.org/10.1139/cgj-2016-0216>
- [44] V. Escario, J.F.T. Jucá, and M.S. Coppe, "Strength and deformation of partly saturated soils", *Proceedings of the 12th International Conference of Soil Mechanics and Foundation Engineering*, vol. 1, International Society of Soil Mechanics and Foundation Engineering: Rio de Janeiro, pp. 43-49, 1989. Rio de Janeiro, Brazil.
- [45] J.K. Gan, and D.G. Fredlund, "Shear strength characteristics of two saprolitic soils", *Can. Geotech. J.*, vol. 25, pp. 500-510, 1996.
<http://dx.doi.org/10.1139/t88-055>
- [46] A.W. Bishop, and G.E. Blight, "Some aspects of effective stress in saturated and partly saturated soils", *Geotechnique*, vol. 13, no. 3, pp. 177-197, 1963.
<http://dx.doi.org/10.1680/geot.1963.13.3.177>

- [47] M.M. Allam, and A. Sridharan, "Effect of wetting and drying on shear strength", *J. Geotech. Eng. Div.*, vol. 107, no. 4, pp. 421-438, 1981.
<http://dx.doi.org/10.1061/AJGEB6.0001117>
- [48] T. Nishimura, Y. Hirabayashi, D.G. Fredlund, and J.K.M. Gan, "Influence of stress history on the strength parameters of an unsaturated statically compacted soil", *Can. Geotech. J.*, vol. 36, no. 2, pp. 251-261, 1999.
<http://dx.doi.org/10.1139/t98-098>
- [49] V. Sivakumar, and S.J. Wheeler, "Influence of compaction procedure on the mechanical behaviour of an unsaturated compacted clay (Part 1 and 2)", *Geotechnique*, vol. 50, pp. 359-376, 2000.
<http://dx.doi.org/10.1680/geot.2000.50.4.359>
- [50] G. Klubertanz, L. Laloui, L. Vulliet, and P. Gachet, "Experimental validation of the hydromechanical modeling of unsaturated soils", *Proceedings Workshop Chemo-mechanical coupling in clays*, pp. 223-230, 2002.
- [51] V. Mayagoitia, F. Rojas, and I. Kornhauser, "Domain complexions in capillary condensation. Part 1.—The ascending boundary curve", *J. Chem. Soc., Faraday Trans. I*, vol. 84, no. 3, p. 785, 1988.
<http://dx.doi.org/10.1039/f19888400785>
- [52] V. Mayagoitia, and I. Kornhauser, "Fundamentals of adsorption IV", In: M. Suzuki, Ed., *The Engineering Foundation*. New York, USA, 1990.
- [53] D.G. Fredlund, and A. Xing, "Equations for the soil-water characteristic curve", *Can. Geotech. J.*, vol. 31, no. 4, pp. 521-532, 1994.
<http://dx.doi.org/10.1139/t94-061>
- [54] P.H. Simms, and E.K. Yanful, "Pore network modelling for unsaturated soils", *Geotech. Conf.*, 2003. Winnipeg, Canada.
- [55] P.H. Simms, and E.K. Yanful, "Measurement and estimation of pore shrinkage and pore distribution in a clayey till during soil-water characteristic curve tests", *Can. Geotech. J.*, vol. 38, no. 4, pp. 741-754, 2001.
<http://dx.doi.org/10.1139/t01-014>
- [56] P.H. Simms, and E.K. Yanful, "A discussion of the application of mercury intrusion porosimetry for the investigation of soils, including an evaluation of its use to estimate volume change in compacted clayey soils", *Geotechnique*, vol. 54, no. 6, pp. 421-426, 2004.
<http://dx.doi.org/10.1680/geot.2004.54.6.421>
- [57] N.R. Morrow, "Physics and thermodynamics of capillary action in Porous media", *Ind. Eng. Chem.*, vol. 62, no. 6, pp. 32-56, 1970.
<http://dx.doi.org/10.1021/ie50726a006>
- [58] D.H. Everet, "The solid-gas interface", *Edisson Flood, Dekker, New York, USA*, vol. II, pp. 1005-1010, 1967.
- [59] R.P. Ray, and K.B. Morris, "Automated laboratory testing for soils-water characteristic curves", *Proc. 1st Int. Conf. Unsat. Soils*, vol. 1, Elsevier, pp. 547-552, 1995. Paris, France.
- [60] P.A. Cundall, and O.D.L. Strack, "The development of constitutive laws for soil using the Distinct Element Method", *Proceedings Int. Conf. Num. Meth. Geomech*, vol. 1, pp. 289-298, 1979.
- [61] J.A. Gili, and E.E. Alonso, "Microstructural deformation mechanisms of unsaturated granular soils", *Int. J. Numer. Anal. Methods Geomech.*, vol. 26, no. 5, pp. 433-468, 2002.
<http://dx.doi.org/10.1002/nag.206>
- [62] E.E. Alonso, E. Rojas, and N.M. Pinyol, "Unsaturated soil mechanics", In: *Reunión Nacional de Mecánica de Suelos. Especial: Aguascalientes, Mexico*, 2008, pp. 117-205.

- [63] C.R.I. Clayton, M.B. Hababa, N.E. Simons, Y.E. Mohamedzein, J.C. Santamarina, S. Thevanayagam, J.E. Tomaz, and J.E. Tyree, "Discussion: Dynamic penetration resistance and the prediction of the compressibility of a fine-grained sand—a laboratory study", *Geotechnique*, vol. 36, no. 2, pp. 275-281, 1986.
<http://dx.doi.org/10.1680/geot.1986.36.2.275>
- [64] J. Horta, E. Rojas, M. L. Pérez, T. López-Lara, and J. B. Hernández, "A random porous model to simulate the retention curve of soils", *Int. J. Num. Anal. Meth. Geomech.*, 2012.
<http://dx.doi.org/10.1002/nag.1133>
- [65] F.A.L. Dullien, *Porous media, fluid transport and pore structure..* Academic Press: USA, 1992.
- [66] B.V. Enustun, and M. Enuysal, "Determination of the Pore Size Distribution by Direct Methods", *Middle East Tech. Univ. J. Pure Applied Sci.*, vol. 3, pp. 81-88, 1970.
- [67] A.J. Brown, "The thermodynamics and hysteresis of adsorption", *PhD thesis*, University of Bristol: England, 1963.
- [68] D.W. Taylor, *Fundamentals of soil mechanics*. John Wiley: New York, USA, 1954.
- [69] X. Li, and L. Zhang, "Characterization of dual-structure pore-size distribution of soil", *Can. Geotech. J.*, vol. 46, pp. 129-141, 2009.
<http://dx.doi.org/10.1139/T08-110>
- [70] J.R. Nimmo, "Semiempirical model of soil water hysteresis", *Soil Sci. Soc. Am. J.*, vol. 56, no. 6, pp. 1723-1730, 1992.
<http://dx.doi.org/10.2136/sssaj1992.03615995005600060011x>
- [71] X. Li, L.M. Zhang, and L.Z. Wu, "A framework for unifying soil fabric, suction, void ratio and water content during the dehydration process", *Soil Sci. Soc. Am. J.*, vol. 78, no. 2, pp. 387-399, 2014.
<http://dx.doi.org/10.2136/sssaj2013.08.0362>
- [72] K. Collins, and A. McGown, "The form and function of microfabric features in a variety of natural soils", *Geotechnique*, vol. 24, no. 2, pp. 223-254, 1974.
<http://dx.doi.org/10.1680/geot.1974.24.2.223>
- [73] M. He, A. Szuchmacher Blum, D.E. Aston, C. Buenviaje, R.M. Overney, and R. Luginbühl, "Critical phenomena of water bridges in nanoasperity contacts", *J. Chem. Phys.*, vol. 114, no. 3, pp. 1355-1360, 2001.
<http://dx.doi.org/10.1063/1.1331298>
- [74] N. Lu, B.D. Zeidman, M.T. Lusk, C.S. Willson, and D.T. Wu, "A Monte Carlo paradigm for capillarity in porous media", *Geophys. Res. Lett.*, vol. 37, no. 23, p. n/a, 2010.
<http://dx.doi.org/10.1029/2010GL045599>
- [75] S. Gao, J.N. Meegoda, and L. Hu, "Two methods for pore network of porous media", *Int. J. Numer. Anal. Methods Geomech.*, vol. 36, no. 18, pp. 1954-1970, 2012.
<http://dx.doi.org/10.1002/nag.1134>
- [76] A. Rostami, G. Habibagahi, M. Ajdari, and E. Nikooee, "A pore network investigation on hysteresis phenomena and influence of stress state on SWRC", *Int. J. Geomech.*, vol. 15, no. 5, p. 04014072, 2015.
[http://dx.doi.org/10.1061/\(ASCE\)GM.1943-5622.0000315](http://dx.doi.org/10.1061/(ASCE)GM.1943-5622.0000315)
- [77] X. Li, and L.M. Zhang, "Characterization of dual-structure pore-size distribution of soil", *Can. Geotech. J.*, vol. 46, no. 2, pp. 129-141, 2009.
<http://dx.doi.org/10.1139/T08-110>
- [78] M. Xiao, L.N. Reddi, and S.L. Steinberg, "Variation of water retention characteristics due to particle rearrangement under zero gravity", *Int. J. Geomech.*, vol. 9, no. 4, pp. 179-186, 2009.
[http://dx.doi.org/10.1061/\(ASCE\)1532-3641](http://dx.doi.org/10.1061/(ASCE)1532-3641)

- [79] E. Rojas, J. Horta, T. López-Lara, and J.B. Hernández, "Probabilistic porous model to simulate the retention curves of soils", *J. Geotech. Geoenviron. Eng.*, vol. 139, no. 2, pp. 320-329, 2013.
[http://dx.doi.org/10.1061/\(ASCE\)GT.1943-5606.0000763](http://dx.doi.org/10.1061/(ASCE)GT.1943-5606.0000763)
- [80] G. Mason, "Determination of the pore size distribution and pore-space interconnectivity of vycor porous glass from adsorption-desorption hysteresis capillary condensation isotherms", *Proc. of the Royal Society*, vol. 415, pp. 453-486, 1988.
- [81] D. Penumadu, and J. Dean, "Compressibility effect in evaluating the pore-size distribution of kaolin clay using mercury intrusion porosimetry", *Can. Geotech. J.*, vol. 37, no. 2, pp. 393-405, 2000.
<http://dx.doi.org/10.1139/t99-121>
- [82] E. Rojas, and F. Rojas, "Modeling hysteresis of the soil-water characteristic curve", *Jiban Kogakkai Ronbun Hokokushu*, vol. 45, no. 3, pp. 135-145, 2005.
http://dx.doi.org/10.3208/sandf.45.3_135
- [83] W.B. Haines, "Studies in the physical properties of soils: IV. A further contribution to the theory of capillary phenomena in soil", *J. Agric. Sci.*, vol. 17, no. 2, pp. 264-290, 1927.
<http://dx.doi.org/10.1017/S0021859600018499>
- [84] M.T. van Genuchten, "A closed form equation for predicting the hydraulic conductivity of unsaturated soils", *Soil Sci. Soc. Am. J.*, vol. 44, no. 5, pp. 892-898, 1980.
<http://dx.doi.org/10.2136/sssaj1980.03615995004400050002x>
- [85] E. Perrier, M. Rieu, G. Sposito, and G. de Marsily, "Models of the water retention curve for soils with a fractal pore size distribution", *Water Resour. Res.*, vol. 32, no. 10, pp. 3025-3031, 1996.
<http://dx.doi.org/10.1029/96WR01779>
- [86] A. Hunt, R. Ewing, and B. Ghanbarian, "Pressure saturation curves and the critical volume fraction for percolation: Accessibility function of percolation theory", *Lecture Notes in Physics*, vol. 880, pp. 273-296, 2014.
http://dx.doi.org/10.1007/978-3-319-03771-4_8
- [87] L. Wang, L. Tang, Z. Wang, H. Liu, and W. Zhang, "Probabilistic characterization of the soil-water retention curve and hydraulic conductivity and its application to slope reliability analysis", *Comput. Geotech.*, vol. 121, p. 103460, 2020.
<http://dx.doi.org/10.1016/j.compgeo.2020.103460>
- [88] C.F. Chiu, W.M. Yan, and K-V. Yuen, "Estimation of water retention curve of granular soils from particle-size distribution — a Bayesian probabilistic approach", *Can. Geotech. J.*, vol. 49, no. 9, pp. 1024-1035, 2012.
<http://dx.doi.org/10.1139/t2012-062>
- [89] E. Romero, A. Gens, and A. Lloret, "Water permeability, water retention and microstructure of unsaturated compacted Boom clay", *Eng. Geol.*, vol. 54, no. 1-2, pp. 117-127, 1999.
[http://dx.doi.org/10.1016/S0013-7952\(99\)00067-8](http://dx.doi.org/10.1016/S0013-7952(99)00067-8)
- [90] A.B. Abell, K.L. Willis, and D.A. Lange, "Mercury intrusion porosimetry and image analysis of cement-based materials", *J. Colloid Interface Sci.*, vol. 211, no. 1, pp. 39-44, 1999.
<http://dx.doi.org/10.1006/jcis.1998.5986> PMID: 9929433
- [91] S. Roels, J. Elsen, J. Carmeliet, and H. Hens, "Characterisation of pore structure by combining mercury porosimetry and micrography", *Mater. Struct.*, vol. 34, no. 2, pp. 76-82, 2001.
<http://dx.doi.org/10.1007/BF02481555>

- [92] A. Sawangsuriya, T.B. Edil, and P.J. Bosscher, "Modulus-suction-moisture relationship for compacted soils in postcompaction state", *J. Geotech. Geoenviron. Eng.*, vol. 135, no. 10, pp. 1390-1403, 2009.
[http://dx.doi.org/10.1061/\(ASCE\)GT.1943-5606.0000108](http://dx.doi.org/10.1061/(ASCE)GT.1943-5606.0000108)
- [93] L.F. Vesga, "Equivalent effective stress and compressibility of unsaturated kaolinite clay subjected to drying", *J. Geotech. Geoenviron. Eng.*, vol. 134, no. 3, pp. 366-378, 2008.
[http://dx.doi.org/10.1061/\(ASCE\)1090-0241\(2008\)134:3\(366\)](http://dx.doi.org/10.1061/(ASCE)1090-0241(2008)134:3(366))
- [94] D.G. Fredlund, A. Xing, M.D. Fredlund, and S.L. Barbour, "The relationship of the unsaturated soil shear strength to the soil-water characteristic curve", *Can. Geotech. J.*, vol. 33, no. 3, pp. 440-448, 1996.
<http://dx.doi.org/10.1139/t96-065>
- [95] M.D. Fredlund, D.G. Fredlund, and G. Wilson, "Prediction of the soil-water characteristic curves from grain-size distribution and volume-mass properties", *Proc. Third Brazilian Symp. Unsat. Soils*, vol. 1, pp. 13-23, 1997. Rio de Janeiro, Brazil.
- [96] M. Aubertin, J-F. Ricard, and R.P. Chapuis, "A predictive model for the water retention curve: Application to tailings from hard-rock mines", *Can. Geotech. J.*, vol. 35, no. 1, pp. 55-69, 1998.
<http://dx.doi.org/10.1139/t97-080>
- [97] J.S.C. Mbagwu, and C.N. Mbah, "Estimating water retention and availability in Nigerian soils from their saturation percentage", *Commun. Soil Sci. Plant Anal.*, vol. 29, no. 7-8, pp. 913-922, 1998.
<http://dx.doi.org/10.1080/00103629809369995>
- [98] L.M. Arya, and J.F. Paris, "Physicoempirical model to predict the soil moisture characteristic from particle-size distribution and bulk density", *Soil Sci. Soc. Am. J.*, vol. 45, no. 6, pp. 1023-1030, 1981.
<http://dx.doi.org/10.2136/sssaj1981.03615995004500060004x>
- [99] L.M. Arya, and T.S. Dierolf, "Predicting soil moisture characteristics from particle size distributions: An improved method to calculate pore radii from particle radii", *Proc. Int. Workshop Indirect Meth. Estim. Hydraulic Prop. Unsat. Soils*, University of California, Riverside, pp. 115-124, 1992.
- [100] A. Basile, and G. D'Urso, "Experimental corrections of simplified methods for predicting water retention curves in clay-loamy soils from particle-size determination", *Soil Technol.*, vol. 10, no. 3, pp. 261-272, 1997.
[http://dx.doi.org/10.1016/S0933-3630\(96\)00020-7](http://dx.doi.org/10.1016/S0933-3630(96)00020-7)
- [101] P.H. Simms, and E.K. Yanful, "Predicting soil—water characteristic curves of compacted plastic soils from measured pore-size distributions", *Geotechnique*, vol. 52, no. 4, pp. 269-278, 2002.
<http://dx.doi.org/10.1680/geot.2002.52.4.269>
- [102] P.H. Simms, and E.K. Yanful, "A pore-network model for hydromechanical coupling in unsaturated compacted clayey soils", *Can. Geotech. J.*, vol. 42, no. 2, pp. 499-514, 2005.
<http://dx.doi.org/10.1139/t05-002>
- [103] G.P. Androusoopoulos, and R. Mann, "Evaluation of mercury porosimeter experiments using a network pore structure model", *Chem. Eng. Sci.*, vol. 34, no. 10, pp. 1203-1212, 1979.
[http://dx.doi.org/10.1016/0009-2509\(79\)85151-9](http://dx.doi.org/10.1016/0009-2509(79)85151-9)
- [104] L.M. Zhang, and X. Li, "Microporosity structure of coarse granular soils", *J. Geotech. Geoenviron. Eng.*, vol. 136, no. 10, pp. 1425-1436, 2010.
[http://dx.doi.org/10.1061/\(ASCE\)GT.1943-5606.0000348](http://dx.doi.org/10.1061/(ASCE)GT.1943-5606.0000348)

- [105] J. Bear, "Hydraulic of Groundwater", In: *Series of Water Resources and Environmental Eng.*, McGraw-Hill, 1979.
- [106] A. Anandarajah, and P.M. Amarasinghe, "Microstructural investigation of soil suction and hysteresis of fine-grained soils", *J. Geotech. Geoenviron. Eng.*, vol. 138, no. 1, pp. 38-46, 2012.
[http://dx.doi.org/10.1061/\(ASCE\)GT.1943-5606.0000555](http://dx.doi.org/10.1061/(ASCE)GT.1943-5606.0000555)
- [107] R.P. Chen, P. Liu, X.M. Liu, P.F. Wang, and X. Kang, "Pore-scale model for estimating the bimodal soil–water characteristic curve and hydraulic conductivity of compacted soils with different initial densities", *Eng. Geol.*, vol. 260, p. 105199, 2019.
<http://dx.doi.org/10.1016/j.enggeo.2019.105199>
- [108] P. Chen, N. Lu, and C. Wei, "General scanning hysteresis model for soil-water retention curves", *J. Geotech. Geoenviron. Eng.*, vol. 145, no. 12, p. 04019116, 2019.
[http://dx.doi.org/10.1061/\(ASCE\)GT.1943-5606.0002184](http://dx.doi.org/10.1061/(ASCE)GT.1943-5606.0002184)
- [109] Z. Han, S.K. Vanapalli, and W. Zou, "Simple approaches for modeling hysteretic soil-water retention behavior", *J. Geotech. Geoenviron. Eng.*, vol. 145, no. 10, p. 04019064, 2019.
[http://dx.doi.org/10.1061/\(ASCE\)GT.1943-5606.0002148](http://dx.doi.org/10.1061/(ASCE)GT.1943-5606.0002148)
- [110] X.S. Li, "Modelling of hysteresis response for arbitrary wetting/drying paths", *Comput. Geotech.*, vol. 32, no. 2, pp. 133-137, 2005.
<http://dx.doi.org/10.1016/j.compgeo.2004.12.002>
- [111] S.J. Wheeler, and V. Sivakumar, "An elasto-plastic critical state framework for unsaturated soil", *Geotechnique*, vol. 45, no. 1, pp. 35-53, 1995.
<http://dx.doi.org/10.1680/geot.1995.45.1.35>
- [112] R. Thom, R. Sivakumar, V. Sivakumar, E.J. Murray, and P. Mackinnon, "Pore size distribution of unsaturated compacted kaolin: The initial states and final states following saturation", *Geotechnique*, vol. 57, no. 5, pp. 469-474, 2007.
<http://dx.doi.org/10.1680/geot.2007.57.5.469>
- [113] J. Espitia, "Micromechanical model to reproduce the soil-water retention curve of soils", s *Master thesis*, University of Queretaro: Mexico, 2005.
- [114] V. Sivakumar, "A critical state framework for unsaturated soils", *PhD thesis*, University of Sheffield, UK, 1993.
- [115] E. Rojas, "An Equivalent stress equation for unsaturated soils, II: Solid-porous model", *Int. J. Geomech.*, vol. 8, no. 5, pp. 291-299, 2008.
[http://dx.doi.org/10.1061/\(ASCE\)1532-3641\(2008\)8:5\(291\)](http://dx.doi.org/10.1061/(ASCE)1532-3641(2008)8:5(291))
- [116] A. Koliji, L. Laloui, O. Cusinier, and L. Vulliet, "Suction induced effects on the fabric of a structured soil", *Transp. Porous Media*, vol. 64, no. 2, pp. 261-278, 2006.
<http://dx.doi.org/10.1007/s11242-005-3656-3>
- [117] S.K. Vanapalli, D.G. Fredlund, and D.E. Pufahl, "The relationship between the soil-water characteristic curve and unsaturated shear strength of a compacted glacial till", *Geotech. Test. J.*, vol. 19, p. GTJ10351J, 1996.
- [118] Q. Wang, D.E. Pufahl, and D.G. Fredlund, "A study of critical state on an unsaturated silty soil", *Can. Geotech. J.*, vol. 39, no. 1, pp. 213-218, 2002.
<http://dx.doi.org/10.1139/t01-086>
- [119] O.M. Vilar, "A simplified procedure to estimate the shear strength envelope of unsaturated soils", *Can. Geotech. J.*, vol. 43, no. 10, pp. 1088-1095, 2006.
<http://dx.doi.org/10.1139/t06-055>
- [120] J. Chae, B. Kim, S. Park, and S. Kato, "Effect of suction on unconfined compressive strength in partly saturated soils", *KSCE J. Civ. Eng.*, vol. 14, no. 3, pp. 281-290, 2010.
<http://dx.doi.org/10.1007/s12205-010-0281-7>

- [121] R. Schnellmann, H. Rahardjo, and H.R. Schneider, "Unsaturated shear strength of a silty sand", *Eng. Geol.*, vol. 162, pp. 88-96, 2013.
<http://dx.doi.org/10.1016/j.enggeo.2013.05.011>
- [122] L.F. Vesga, and L.E. Vallejo, "Direct and indirect tensile tests for measuring the equivalent effective stress in a kaolinite clay", *Proceedings Fourth Int. Conf. Unsat. Soils*, vol. 1, pp. 1290-13, 2006. Arizona, USA.
[http://dx.doi.org/10.1061/40802\(189\)106](http://dx.doi.org/10.1061/40802(189)106)
- [123] J. Lechman, and N. Lu, "Capillary force and water retention between two uneven sized particles", *J. Geotech. Eng.*, vol. 134, pp. 374-384, 2008.
- [124] R.B. Goulding, "Tensile strength shear strength and effective stress for unsaturated sand", *PhD Thesis*, University of Missouri: Columbia, USA, 2006.
- [125] N. Lu, T.H. Kim, S. Sture, and W.J. Likos, "Tensile strength of unsaturated sand", *J. Eng. Mech.*, vol. 135, no. 12, pp. 1410-1419, 2009.
[http://dx.doi.org/10.1061/\(ASCE\)EM.1943-7889.0000054](http://dx.doi.org/10.1061/(ASCE)EM.1943-7889.0000054)
- [126] B. Narvaez, M. Aubertin, and F. Saleh-Mbemba, "Determination of the tensile strength of unsaturated tailings using bending tests", *Can. Geotech. J.*, vol. 52, no. 11, pp. 1874-1885, 2015.
<http://dx.doi.org/10.1139/cgj-2014-0156>
- [127] C-S. Tang, X-J. Pei, D-Y. Wang, B. Shi, and J. Li, "Tensile strength of compacted clayey soil", *J. Geotech. Geoenviron. Eng.*, vol. 140, pp. 1-8, 2015.
- [128] J. Vaunat, E. Romero, and C. Jommi, "An elastoplastic hydromechanical model for unsaturated soils", *Experimental Evidence and Theoretical Approaches in Unsaturated Soils*, Balkema Rotterdam, pp. 121-138, 2000.
- [129] D.A. Sun, H.B. Cui, H. Matsuoka, and D.C. Sheng, "A three-dimensional elastoplastic model for unsaturated compacted soils with hydraulic hysteresis", *Soil Found.*, vol. 47, no. 2, pp. 253-264, 2007.
<http://dx.doi.org/10.3208/sandf.47.253>
- [130] M.M. Futai, and M.S.S. Almeida, "An experimental investigation of the mechanical behaviour of an unsaturated gneiss residual soil", *Geotechnique*, vol. 55, no. 3, pp. 201-213, 2005.
<http://dx.doi.org/10.1680/geot.2005.55.3.201>
- [131] J.M. Fleureau, S. Kheirbek-Saoud, R. Soemitro, and S. Taibi, "Behavior of clayey soils on drying-wetting paths", *Can. Geotech. J.*, vol. 30, no. 2, pp. 287-296, 1993.
<http://dx.doi.org/10.1139/t93-024>
- [132] D. Sheng, "Review of fundamental principles in modelling unsaturated soil behaviour", *Comput. Geotech.*, vol. 38, no. 6, pp. 757-776, 2011.
<http://dx.doi.org/10.1016/j.compgeo.2011.05.002>
- [133] T.M. Thu, H. Rahardjo, and E.C. Leong, "Elastoplastic model for unsaturated soil with incorporation of the soil-water characteristic curve", *Can. Geotech. J.*, vol. 44, no. 1, pp. 67-77, 2007.
<http://dx.doi.org/10.1139/t06-091>
- [134] Y. Kohgo, M. Nakano, and T. Miyazaki, "Theoretical aspects of constitutive modeling for unsaturated soils", *Soil Found.*, vol. 33, no. 4, pp. 49-63, 1993.
http://dx.doi.org/10.3208/sandf1972.33.4_49
- [135] B. Loret, and N. Khalili, "A three-phase model for unsaturated soils", *Int. J. Numer. Anal. Methods Geomech.*, vol. 24, no. 11, pp. 893-927, 2000.
[http://dx.doi.org/10.1002/1096-9853\(200009\)24:11<893::AID-NAG105>3.0.CO;2-V](http://dx.doi.org/10.1002/1096-9853(200009)24:11<893::AID-NAG105>3.0.CO;2-V)

- [136] R. Kohler, and G. Hofstetter, "A cap model for partially saturated soils", *Int. J. Numer. Anal. Methods Geomech.*, vol. 32, no. 8, pp. 981-1004, 2008.
<http://dx.doi.org/10.1002/nag.658>
- [137] A. Koliji, L. Laloui, and L. Vulliet, "Constitutive modeling of unsaturated aggregated soils", *Int. J. Numer. Anal. Methods Geomech.*, vol. 34, no. 17, pp. 1846-1876, 2010.
<http://dx.doi.org/10.1002/nag.888>
- [138] D. Sheng, D.G. Fredlund, and A. Gens, "A new modelling approach for unsaturated soils using independent stress variables", *Can. Geotech. J.*, vol. 45, no. 4, pp. 511-534, 2008.
<http://dx.doi.org/10.1139/T07-112>
- [139] D. Sun, D. Sheng, and Y. Xu, "Collapse behaviour of unsaturated compacted soil with different initial densities", *Can. Geotech. J.*, vol. 44, no. 6, pp. 673-686, 2007.
<http://dx.doi.org/10.1139/t07-023>
- [140] R.I. Borja, "Cam-Clay plasticity. Part V: A mathematical framework for three-phase deformation and strain localization analyses of partially saturated porous media", *Comput. Methods Appl. Mech. Eng.*, vol. 193, no. 48-51, pp. 5301-5338, 2004.
<http://dx.doi.org/10.1016/j.cma.2003.12.067>
- [141] L.R. Hoyos, and P. Arduino, "Implicit algorithms in modeling unsaturated soil response in three-invariant stress space", *Int. J. Geomech.*, vol. 8, no. 4, pp. 266-273, 2008.
[http://dx.doi.org/10.1061/\(ASCE\)1532-3641\(2008\)8:4\(266\)](http://dx.doi.org/10.1061/(ASCE)1532-3641(2008)8:4(266))
- [142] H.W. Zhang, and L. Zhou, "Implicit integration of a chemo-plastic constitutive model for partially saturated soils", *Int. J. Numer. Anal. Methods Geomech.*, vol. 32, no. 14, pp. 1715-1735, 2008.
<http://dx.doi.org/10.1002/nag.690>
- [143] E. Juárez-Badillo, "Constitutive relationships for soils", *Proceedings of the Symposium on Recent Developments in the Analysis of Soil Behavior and their Application to Geotechnical Structures*, University of New South Wales: NSW, Australia., pp. 231-257, 1975.
- [144] R. Butterfield, "A natural compression law for soils (an advance on $e - \log p$)", *Geotechnique*, vol. 29, no. 4, pp. 469-480, 1979.
<http://dx.doi.org/10.1680/geot.1979.29.4.469>
- [145] W. Mun, and J.S. McCartney, "Compression mechanisms of unsaturated clay under high stresses", *Can. Geotech. J.*, vol. 52, no. 12, pp. 2099-2112, 2015.
<http://dx.doi.org/10.1139/cgj-2014-0438>
- [146] W. Mun, and J.S. McCartney, "Roles of particles breakage and drainage in the isotropic compression of sand to high pressures", *J. Geotech. Geoenviron. Eng.*, vol. 143, no. 10, p. 04017071, 2017.
[http://dx.doi.org/10.1061/\(ASCE\)GT.1943-5606.0001770](http://dx.doi.org/10.1061/(ASCE)GT.1943-5606.0001770)
- [147] D. Sheng, Y. Yao, and J.P. Carter, "A volume–stress model for sands under isotropic and critical stress states", *Can. Geotech. J.*, vol. 45, no. 11, pp. 1639-1645, 2008.
<http://dx.doi.org/10.1139/T08-085>
- [148] J.A. Infante Sedano, and S.K. Vanapalli, "The relationship between the critical state shear strength of unsaturated soils and the soil-water characteristic curve", *Proceedings of the Fifth International Conference on Unsaturated Soils*, vol. 1, pp. 253-258, 2010. Barcelona, Spain.
<http://dx.doi.org/10.1201/b10526-31>
- [149] E. Romero, A. Gens, and A. Lloret, "Suction effects on a compacted clay under non-isothermal conditions", *Geotechnique*, vol. 53, no. 1, pp. 65-81, 2003.
<http://dx.doi.org/10.1680/geot.2003.53.1.65>
- [150] M.R. Cunningham, A.M. Ridley, K. Dineen, and J.B. Burland, "The mechanical behaviour of a reconstituted unsaturated silty clay", *Geotechnique*, vol. 53, no. 2, pp. 183-194, 2003.

- <http://dx.doi.org/10.1680/geot.2003.53.2.183>
- [151] N. Khalili, F. Geiser, and G.E. Blight, "Effective stress in unsaturated soils: Review with new evidence", *Int. J. Geomech.*, vol. 4, no. 2, pp. 115-126, 2004.
[http://dx.doi.org/10.1061/\(ASCE\)1532-3641\(2004\)4:2\(115\)](http://dx.doi.org/10.1061/(ASCE)1532-3641(2004)4:2(115))
- [152] I. Vlahinić, H.M. Jennings, and J.J. Thomas, "A constitutive model for drying of a partially saturated porous material", *Mech. Mater.*, vol. 41, no. 3, pp. 319-328, 2009.
<http://dx.doi.org/10.1016/j.mechmat.2008.10.011>
- [153] G.E. Blight, "Shrinkage during wetting of fined-pored materials. Does this accord with the principle of effective stress?", *Proceedings of the fifth International Conference on Unsaturated Soils*, vol. 1, pp. 205-209, 2010.
<http://dx.doi.org/10.1201/b10526-23>
- [154] A. Pereira, C. Feuerharmel, W.Y.Y. Gheleng, and A.V.D. Bica, "A study on the shear strength envelope of an unsaturated colluviums soil", *Proceedings of the Fourth International Conference on Unsaturated Soils*, vol. 1, pp. 1191-1199, 2006. Arizona, USA.
[http://dx.doi.org/10.1061/40802\(189\)97](http://dx.doi.org/10.1061/40802(189)97)
- [155] D. Sheng, A. Zhou, and D.G. Fredlund, "Shear strength criteria for unsaturated soils", *Geotech. Geol. Eng.*, vol. 29, no. 2, pp. 145-159, 2011.
<http://dx.doi.org/10.1007/s10706-009-9276-x>
- [156] D.G. Toll, and B.H. Ong, "Critical-state parameters for an unsaturated residual sandy clay", *Geotechnique*, vol. 53, no. 1, pp. 93-103, 2003.
<http://dx.doi.org/10.1680/geot.2003.53.1.93>
- [157] J.C.B. Benatti, M.G. Miguel, R.A. Rodriguez, and O.M. Vilar, "Collapsibility study for tropical soil profile using oedometric tests with controlled suction", *Proceedings of the fifth International Conference on Unsaturated Soils*, vol. 1, pp. 193-198, 2010. Barcelona, Spain.
<http://dx.doi.org/10.1201/b10526-21>
- [158] G.J. Burton, D. Sheng, and D. Airey, "Experimental study on volumetric behaviour of Maryland clay and the role of degree of saturation", *Can. Geotech. J.*, vol. 51, no. 12, pp. 1449-1455, 2014.
<http://dx.doi.org/10.1139/cgj-2013-0332>
- [159] K. Cui, P. Défossez, Y.J. Cui, and G. Richard, "Quantifying the effect of matric suction on the compressive properties of two agricultural soils using an osmotic oedometer", *Geoderma*, vol. 156, no. 3-4, pp. 337-345, 2010.
<http://dx.doi.org/10.1016/j.geoderma.2010.03.003>
- [160] J. Kodikara, "New framework for volumetric constitutive behaviour of compacted unsaturated soils", *Can. Geotech. J.*, vol. 49, no. 11, pp. 1227-1243, 2012.
<http://dx.doi.org/10.1139/t2012-084>
- [161] G. Bolzon, B.A. Schrefler, and O.C. Zienkiewicz, "Elastoplastic soil constitutive laws generalized to partially saturated states", *Geotechnique*, vol. 46, no. 2, pp. 279-289, 1996.
<http://dx.doi.org/10.1680/geot.1996.46.2.279>
- [162] D. Karube, and K. Kawai, "The role of pore water in the mechanical behavior of unsaturated soils", *Geotech. Geol. Eng.*, vol. 19, no. 3/4, pp. 211-241, 2001.
<http://dx.doi.org/10.1023/A:1013188200053>
- [163] E.E. Alonso, J.M. Pereira, J. Vaunat, and S. Olivella, "A microstructurally based effective stress for unsaturated soils", *Geotechnique*, vol. 60, no. 12, pp. 913-925, 2010.
<http://dx.doi.org/10.1680/geot.8.P.002>
- [164] G.D. Vecchia, and E. Romero, "A fully coupled elastic-plastic hydromechanical model for compacted soils accounting for clay activity", *Int. J. Numer. Anal. Methods Geomech.*, vol. 37, no. 5, pp. 503-535, 2013.

- <http://dx.doi.org/10.1002/nag.1116>
- [165] D.A. Sun, D.C. Sheng, H.B. Cui, and S.W. Sloan, "A density-dependent elastoplastic hydro-mechanical model for unsaturated compacted soils", *Int. J. Numer. Anal. Methods Geomech.*, vol. 31, no. 11, pp. 1257-1279, 2007.
<http://dx.doi.org/10.1002/nag.579>
- [166] R.A. Rodrigues, and O.M. Volar, "Experimental study of the collapsible behavior of a tropical unsaturated soil", *Proceedings 5th Int. Conf. Unsat. Soils*, vol. 1, pp. 353-357, 2010. Barcelona, Spain.
<http://dx.doi.org/10.1201/b10526-47>
- [167] A. Tarantino, and E. De Col, "Compaction behaviour of clay", *Geotechnique*, vol. 58, no. 3, pp. 199-213, 2008.
<http://dx.doi.org/10.1680/geot.2008.58.3.199>
- [168] B. Caicedo, J. Tristanchó, L. Thorel, and S. Leroueil, "Experimental and analytical framework for modeling soil compaction", *Eng. Geology*, 2014.
<http://dx.doi.org/10.1016/j.enggeo.2014.03.014>
- [169] D.A. Sun, H. Matsuoka, and Y. Xu, "Collapse of compacted clay in suction-controlled triaxial cell", *Geotech. Test. J.*, vol. 27, pp. 362-370, 2004.
- [170] J.H. Pereira, D.G. Fredlund, M.P. Cardão Neto, and G.F. Gitirana Jr, "Hydraulic Behavior of Collapsible Compacted Gneiss Soil", *J. Geotech. Geoenviron. Eng.*, vol. 131, no. 10, pp. 1264-1273, 2005.
[http://dx.doi.org/10.1061/\(ASCE\)1090-0241\(2005\)131:10\(1264\)](http://dx.doi.org/10.1061/(ASCE)1090-0241(2005)131:10(1264))
- [171] L. Barden, A. McGown, and K. Collins, "The collapse mechanism in partly saturated soil", *Eng. Geol.*, vol. 7, no. 1, pp. 49-60, 1973.
[http://dx.doi.org/10.1016/0013-7952\(73\)90006-9](http://dx.doi.org/10.1016/0013-7952(73)90006-9)
- [172] F. Casini, "Deformation induced by wetting: A simple model", *Can. Geotech. J.*, vol. 49, no. 8, pp. 954-960, 2012.
<http://dx.doi.org/10.1139/t2012-054>
- [173] C. Choudhury, and T.V. Bharat, "Wetting-induced collapse behavior of kaolinite: Influence of fabric and inundation pressure", *Can. Geotech. J.*, vol. 55, no. 7, pp. 956-967, 2018.
<http://dx.doi.org/10.1139/cgj-2017-0297>
- [174] S. Singhal, R.S. Sharma, and B.R. Phanikumar, "A laboratory study of collapse behaviour of remoulded loess under controlled wetting and flooding", *Geomechanics and Geoen지니어ing*, vol. 11, no. 2, pp. 159-163, 2016.
<http://dx.doi.org/10.1080/17486025.2015.1057620>
- [175] D. Zhang, and S. Wang, "The compression and collapse behavior of intact loess in suction-monitored triaxial apparatus", *Acta Geotech.*, 2019.
<http://dx.doi.org/10.1007/s11440-019-00829-3>
- [176] J.K. Mitchell, *Fundamentals of soil behavior*. John Wiley and sons, 1993.
- [177] A. Anandarajah, and P.M. Amarasinghe, "Discrete-element study of the swelling behaviour of Na-montmorillonite", *Geotechnique*, vol. 63, no. 8, pp. 674-681, 2013.
<http://dx.doi.org/10.1680/geot.12.P.012>
- [178] A. Gens, and E.E. Alonso, "A framework for the behaviour of unsaturated expansive clays", *Can. Geotech. J.*, vol. 29, no. 6, pp. 1013-1032, 1992.
<http://dx.doi.org/10.1139/t92-120>
- [179] E.E. Alonso, J. Vaunat, and A. Gens, "Modelling the mechanical behaviour of expansive clays", *Eng. Geol.*, vol. 54, no. 1-2, pp. 173-183, 1999.
[http://dx.doi.org/10.1016/S0013-7952\(99\)00079-4](http://dx.doi.org/10.1016/S0013-7952(99)00079-4)

- [180] A. Lloret, M.V. Villar, M. Sánchez, A. Gens, X. Pintado, and E.E. Alonso, "Mechanical behaviour of heavily compacted bentonite under high suction changes", *Geotechnique*, vol. 53, no. 1, pp. 27-40, 2003.
<http://dx.doi.org/10.1680/geot.2003.53.1.27>
- [181] E.E. Alonso, E. Romero, and C. Hoffmann, "Hydromechanical behaviour of compacted granular expansive mixtures: Experimental and constitutive study", *Geotechnique*, vol. 61, no. 4, pp. 329-344, 2011.
<http://dx.doi.org/10.1680/geot.2011.61.4.329>
- [182] W. Sun, D. Sun, and J. Li, "Elastoplastic modeling of hydraulic and mechanical behavior of unsaturated expansive soil", *Proc. GeoShanghai 2010, Int. Conf.*, pp. 119-127, 2010.
[http://dx.doi.org/10.1061/41103\(376\)15](http://dx.doi.org/10.1061/41103(376)15)
- [183] W. Sun, and D. Sun, "Coupled modelling of hydro-mechanical behaviour of unsaturated compacted expansive soils", *Int. J. Numer. Anal. Methods Geomech.*, vol. 36, no. 8, pp. 1002-1022, 2012.
<http://dx.doi.org/10.1002/nag.1036>
- [184] D. Mašín, "Double structure hydromechanical coupling formalism and a model for unsaturated expansive clays", *Eng. Geol.*, vol. 165, pp. 73-88, 2013.
<http://dx.doi.org/10.1016/j.enggeo.2013.05.026>
- [185] J. Li, Z-H. Yin, Y. Cui, and Y. Hicher, "Work input analysis for soils with double porosity and application to the hydro-mechanical modeling of unsaturated clays", *Can. Geotech. J.*, 2016.
<http://dx.doi.org/10.1139/cgj-2015-0574>
- [186] G.E. Blight, "The time-rate of heave of structures on expansive clays", In: *Moisture equilibria and moisture changes in soils beneath covered areas.* Butterworths: Sydney, 1965, pp. 78-87.
- [187] G. Kassiff, and A.B. Shalom, "Experimental relationship between swell pressure and suction", *Geotechnique*, vol. 21, no. 3, pp. 245-255, 1971.
<http://dx.doi.org/10.1680/geot.1971.21.3.245>
- [188] D.G. Fredlund, J.U. Hasam, and H. Filson, "The prediction of total heave", *Proc. Fourth Int. Conf. Exp. Soils*, pp. 1-17, 1980. Denver, Colorado.
- [189] H.Q. Vu, and D.G. Fredlund, "Numerical modelling of two dimensional heave for slabs-on-ground and shallow foundations", *Proc. 56th Can. Geotech. Conf.*, pp. 220-227, 2003. Winnipeg.
- [190] H. Tu, and S.K. Vanapalli, "Prediction of the variation of swelling pressure and one dimensional heave of expansive soils with respect to suction using the soil-water retention curve as a tool", *Can. Geotech. J.*, 2016.
<http://dx.doi.org/10.1139/cgj-2015-0222>
- [191] R. Monroy, L. Zdravkovic, and A. Ridley, "Evolution of microstructure in compacted London Clay during wetting and loading", *Geotechnique*, vol. 60, no. 2, pp. 105-119, 2010.
<http://dx.doi.org/10.1680/geot.8.P.125>
- [192] C. Hoffmann, E.E. Alonso, and E. Romero, "Hydro-mechanical behaviour of bentonite pellet mixtures", *Phys. Chem. Earth Parts ABC*, vol. 32, no. 8-14, pp. 832-849, 2007.
<http://dx.doi.org/10.1016/j.pce.2006.04.037>
- [193] M.V. Villar, and A. Lloret, "Influence of dry density and water content on the swelling of a compacted bentonite", *Appl. Clay Sci.*, vol. 39, no. 1-2, pp. 38-49, 2008.
<http://dx.doi.org/10.1016/j.clay.2007.04.007>

- [194] H. Nowamooz, and F. Masroui, "Mechanical behaviour of expansive soils after several drying and wetting cycles", *Geomechanics and Geoengineering*, vol. 5, no. 4, pp. 213-221, 2010.
<http://dx.doi.org/10.1080/17486025.2010.521588>
- [195] E. Romero, G. Della Vecchia, and C. Jommi, "An insight into the water retention properties of compacted clayey soils", *Geotechnique*, vol. 61, no. 4, pp. 313-328, 2011.
<http://dx.doi.org/10.1680/geot.2011.61.4.313>
- [196] H. Arroyo, E. Rojas, M. de la Luz Pérez-Rea, J. Horta, and J. Arroyo, "A porous model to simulate the evolution of the soil–water characteristic curve with volumetric strains", *C. R. Mec.*, vol. 343, no. 4, pp. 264-274, 2015.
<http://dx.doi.org/10.1016/j.crme.2015.02.001>
- [197] S.A. Habib, "Lateral pressure of unsaturated expansive clay in looped stress path", *Proc. First Int. Conf. Unsat. Soils*, pp. 95-100, 1995.
- [198] E.E. Alonso, A. Lloret, A. Gens, and D.Q. Yang, "Experimental behavior of highly expansive double-structure clay", *Proc. First Int. Conf. Unsat. Soils*, vol. 1, pp. 11-16, 1995. Paris, France.
- [199] N. Lu, J.W. Godt, and D.T. Wu, "A closed-form equation for effective stress in unsaturated soil", *Water Resour. Res.*, vol. 46, no. 5, 2010.
<http://dx.doi.org/10.1029/2009WR008646>
- [200] E. Rojas, M.L. Pérez-Rea, T. López-Lara, J.B. Hernández, and J. Horta, "Use of effective stresses to model the collapse upon wetting of unsaturated soils", *J. Geotech. Geoenviron. Eng.*, vol. 141, no. 5, p. 04015007, 2015.
[http://dx.doi.org/10.1061/\(ASCE\)GT.1943-5606.0001251](http://dx.doi.org/10.1061/(ASCE)GT.1943-5606.0001251)
- [201] X. Bian, Y.J. Cui, and X.Z. Li, "Voids effect on the swelling behaviour of compacted bentonite", *Geotechnique*, vol. 69, no. 7, pp. 593-605, 2019.
<http://dx.doi.org/10.1680/jgeot.17.P.283>
- [202] Z.G. Yigzaw, O. Cuisinier, L. Massat, and F. Masroui, "Role of different suction components on swelling behavior of compacted bentonites", *Appl. Clay Sci.*, vol. 120, pp. 81-90, 2016.
<http://dx.doi.org/10.1016/j.clay.2015.11.022>
- [203] Y. Erzin, and O. Erol, "Swell pressure prediction by suction methods", *Eng. Geol.*, vol. 92, no. 3-4, pp. 133-145, 2007.
<http://dx.doi.org/10.1016/j.enggeo.2007.04.002>
- [204] A.R. Estabragh, B. Parsaei, and A.A. Javadi, "Laboratory investigation of the effect of cyclic wetting and drying on the behaviour of an expansive soil", *Soil Found.*, vol. 55, no. 2, pp. 304-314, 2015.
<http://dx.doi.org/10.1016/j.sandf.2015.02.007>
- [205] S. Kaufhold, W. Baille, T. Schanz, and R. Dohrmann, "About differences of swelling pressure — dry density relations of compacted bentonites", *Appl. Clay Sci.*, vol. 107, pp. 52-61, 2015.
<http://dx.doi.org/10.1016/j.clay.2015.02.002>
- [206] S.J. Wheeler, "Inclusion of specific water volume within an elasto-plastic model for unsaturated soil", *Can. Geotech. J.*, vol. 33, no. 1, pp. 42-57, 1996.
<http://dx.doi.org/10.1139/t96-023>
- [207] C. Jommi, "Remarks on the constitutive modelling of unsaturated soils. Experimental evidence and theoretical approaches in unsaturated soils", *Proc. of the Int. Workshop on Unsat. Soils*, pp. 139-153, 2000. Rotterdam.

- [208] M.S.R. Buisson, and S.J. Wheeler, "Inclusion of hydraulic hysteresis in a new elastoplastic framework for unsaturated soils", *Proc. of the Int. Workshop Unsat. Soils*, pp. 109-119, 2000. Rotterdam.
- [209] D. Sun, D. Sheng, and S.W. Sloan, "Elastoplastic modelling of hydraulic and stress-strain behaviour of unsaturated soils", *Mech. Mater.*, vol. 39, no. 3, pp. 212-221, 2007.
<http://dx.doi.org/10.1016/j.mechmat.2006.05.002>
- [210] K. Kawai, S. Kato, and D. Karube, "The model of water retention curve considering effects of void ratio", *Proc. of the Asian Conf. Unsat. Soils*, pp. 329-334, 2000. Singapore.
- [211] D. Gallipoli, S.J. Wheeler, and M. Karstunen, "Modelling the variation of degree of saturation in a deformable unsaturated soil", *Geotechnique*, vol. 53, no. 1, pp. 105-112, 2003.
<http://dx.doi.org/10.1680/geot.2003.53.1.105>
- [212] M. Maleki, and H. Pouyan, "A kinematic hardening based model for unsaturated soils considering different hydraulic conditions", *Int. J. Numer. Anal. Methods Geomech.*, vol. 40, no. 16, pp. 2271-2290, 2016.
<http://dx.doi.org/10.1002/nag.2539>
- [213] A. Tarantino, "A water retention model for deformable soils", *Geotechnique*, vol. 59, no. 9, pp. 751-762, 2009.
<http://dx.doi.org/10.1680/geot.7.00118>
- [214] D. Mašin, "Predicting the dependency of a degree of saturation on void ratio and suction using effective stress principle for unsaturated soils", *Int. J. Numer. Anal. Methods Geomech.*, vol. 34, no. 1, pp. 73-90, 2010.
<http://dx.doi.org/10.1002/nag.808>
- [215] D. Sheng, and A.N. Zhou, "Coupling hydraulic with mechanical models for unsaturated soils", *Can. Geotech. J.*, vol. 48, no. 5, pp. 826-840, 2011.
<http://dx.doi.org/10.1139/t10-109>
- [216] D. Gallipoli, "A hysteretic soil-water retention model accounting for cyclic variations of suction and void ratio", *Geotechnique*, vol. 62, no. 7, pp. 605-616, 2012.
<http://dx.doi.org/10.1680/geot.11.P.007>
- [217] S. Salager, M. Nuth, A. Ferrari, and L. Laloui, "Investigation into water retention behaviour of deformable soils", *Can. Geotech. J.*, vol. 50, no. 2, pp. 200-208, 2013.
<http://dx.doi.org/10.1139/cgj-2011-0409>
- [218] C. Zhou, and C.W.W. Ng, "A new and simple stress-dependent water retention model for unsaturated soil", *Comput. Geotech.*, vol. 62, pp. 216-222, 2014.
<http://dx.doi.org/10.1016/j.compgeo.2014.07.012>
- [219] N. Khalili, M.A. Habte, and S. Zargarbashi, "A fully coupled flow deformation model for cyclic analysis of unsaturated soils including hydraulic and mechanical hystereses", *Comput. Geotech.*, vol. 35, no. 6, pp. 872-889, 2008.
<http://dx.doi.org/10.1016/j.compgeo.2008.08.003>
- [220] R. Brooks, and A. Corey, "Hydraulic properties of porous media", In: *Hydrology Paper No. 3*. Colorado State University: Fort Collins, CO, 1964.
- [221] E.E. Alonso, N.M. Pinyol, and A. Gens, "Compacted soil behaviour: Initial state, structure and constitutive modelling", *Geotechnique*, vol. 63, no. 6, pp. 463-478, 2013.
<http://dx.doi.org/10.1680/geot.11.P.134>
- [222] S. Jayanth, K. Iyer, and D.N. Singh, "Influence of drying- and wetting- cycles on SWCC of fine-grained soils", *J. Test. Eval.*, vol. 40, no. 3, p. 104184, 2012.
<http://dx.doi.org/10.1520/JTE104184>
- [223] S. Jayanth, K. Iyer, and D.N. Singh, "Continuous determination of drying-path SWRC of fine-grained soils", *Geomechanics and Geoengineering*, vol. 8, no. 1, pp. 28-35, 2013.

- <http://dx.doi.org/10.1080/17486025.2012.727034>
- [224] C.F. Chiu, and C.W.W. Ng, "Coupled water retention and shrinkage properties of a compacted silt under isotropic and deviatoric stress paths", *Can. Geotech. J.*, vol. 49, no. 8, pp. 928-938, 2012.
<http://dx.doi.org/10.1139/t2012-055>
- [225] C.W.W. Ng, and Y.W. Pang, "Experimental investigations of the soil-water characteristics of a volcanic soil", *Can. Geotech. J.*, vol. 37, no. 6, pp. 1252-1264, 2000.
<http://dx.doi.org/10.1139/t00-056>
- [226] E. Rojas, and O. Chávez, "Volumetric behavior of unsaturated soils", *Can. Geotech. J.*, vol. 50, no. 2, pp. 209-222, 2013.
<http://dx.doi.org/10.1139/cgj-2012-0341>
- [227] W. Arairo, F. Prunier, I. Djeran-Maigre, and A. Millard, "On the use of effective stress in three-dimensional hydro-mechanical coupled model", *Comput. Geotech.*, vol. 58, pp. 56-68, 2014.
<http://dx.doi.org/10.1016/j.compgeo.2014.01.014>
- [228] Z. Bellia, M.S. Ghembaza, and T. Belal, "A thermo-hydro-mechanical model of unsaturated soils based on bounding surface plasticity", *Comput. Geotech.*, vol. 69, pp. 58-69, 2015.
<http://dx.doi.org/10.1016/j.compgeo.2015.04.020>
- [229] Z. Zhang, and X. Cheng, "A fully coupled THM model based on a non-equilibrium thermodynamic approach and its application", *Int. J. Numer. Anal. Methods Geomech.*, vol. 41, no. 4, pp. 527-554, 2017.
<http://dx.doi.org/10.1002/nag.2569>
- [230] Y. Zhang, and A. Zhou, "Explicit integration of a porosity-dependent hydro-mechanical model for unsaturated soils", *Int. J. Numer. Anal. Methods Geomech.*, vol. 40, no. 17, pp. 2353-2382, 2016.
<http://dx.doi.org/10.1002/nag.2533>
- [231] M. Lloret-Cabot, S.J. Wheeler, J.A. Pineda, D. Sheng, and A. Gens, "Relative performance of two unsaturated soil models using different constitutive variables", *Can. Geotech. J.*, vol. 51, no. 12, pp. 1423-1437, 2014.
<http://dx.doi.org/10.1139/cgj-2013-0462>
- [232] R. Hu, Y.F. Chen, H.H. Liu, and C-B. Zhou, "A coupled two-phase fluid flow and elastoplastic deformation model for unsaturated soils: Theory, implementation, and application", *Int. J. Numer. Anal. Methods Geomech.*, vol. 40, no. 7, pp. 1023-1058, 2016.
<http://dx.doi.org/10.1002/nag.2473>
- [233] E. Liu, H.S. Yu, G. Deng, J. Zhang, and S. He, "Numerical analysis of seepage–deformation in unsaturated soils", *Acta Geotech.*, vol. 9, no. 6, pp. 1045-1058, 2014.
<http://dx.doi.org/10.1007/s11440-014-0343-y>
- [234] J. Choo, J.A. White, and R.I. Borja, "Hydromechanical modeling of unsaturated flow in double porosity media", *Int. J. Geomech.*, vol. 16, 2016.
[http://dx.doi.org/10.1061/\(ASCE\)GM.1943-5622.0000558](http://dx.doi.org/10.1061/(ASCE)GM.1943-5622.0000558)
- [235] M. Lloret-Cabot, S.J. Wheeler, and M. Sánchez, "A unified mechanical and retention model for saturated and unsaturated soil behaviour", *Acta Geotech.*, vol. 12, no. 1, pp. 1-21, 2017.
<http://dx.doi.org/10.1007/s11440-016-0497-x>
- [236] X. Song, K. Wang, and M. Ye, "Localized failure in unsaturated soils under non-isothermal conditions", *Acta Geotech.*, vol. 13, no. 1, pp. 73-85, 2018.
<http://dx.doi.org/10.1007/s11440-017-0534-4>
- [237] B. Loret, and N. Khalili, "An effective stress elastic–plastic model for unsaturated porous media", *Mech. Mater.*, vol. 34, no. 2, pp. 97-116, 2002.

- [http://dx.doi.org/10.1016/S0167-6636\(01\)00092-8](http://dx.doi.org/10.1016/S0167-6636(01)00092-8)
- [238] D. Sun, D. Sheng, and S.W. Sloan, "Elastoplastic modelling of hydraulic and stress-strain behaviour of unsaturated soils", *Mech. Mater.*, vol. 39, no. 3, pp. 212-221, 2007.
<http://dx.doi.org/10.1016/j.mechmat.2006.05.002>
- [239] D. Sun, W. Sun, and L. Xiang, "Effect of degree of saturation on mechanical behaviour of unsaturated soils and its elastoplastic simulation", *Comput. Geotech.*, vol. 37, no. 5, pp. 678-688, 2010.
<http://dx.doi.org/10.1016/j.compgeo.2010.04.006>
- [240] W.T. Solowski, and S.W. Sloan, "Equivalent stress approach in creation of elastoplastic constitutive models for unsaturated soils", *Int. J. Geomech.*, 2013.
[http://dx.doi.org/10.1061/\(ASCE\)GM.1943-5622.0000368](http://dx.doi.org/10.1061/(ASCE)GM.1943-5622.0000368)
- [241] P. Sitarenios, and M. Kavvas, "A plasticity constitutive model for unsaturated, anisotropic, nonexpansive soils", *Int. J. Numer. Anal. Methods Geomech.*, vol. 44, no. 4, pp. 435-454, 2020.
<http://dx.doi.org/10.1002/nag.3028>
- [242] A. Zhou, and D. Sheng, "An advanced hydro-mechanical constitutive model for unsaturated soils with different initial densities", *Comput. Geotech.*, vol. 63, pp. 46-66, 2015.
<http://dx.doi.org/10.1016/j.compgeo.2014.07.017>
- [243] T. Ma, C. Wei, H. Wei, and W. Li, "Hydraulic and mechanical behavior of unsaturated silt: Experimental and theoretical characterization", *Int. J. Geomech.*, vol. 16, pp. 1-13, 2015.
- [244] D. Mašin, and N. Khalili, "A hypoplastic model for mechanical response of unsaturated soils", *Int. J. Numer. Anal. Methods Geomech.*, vol. 32, no. 15, pp. 1903-1926, 2008.
<http://dx.doi.org/10.1002/nag.714>
- [245] W. Fuentes, and T. Triantafyllidis, "Hydro-mechanical hypoplastic models for unsaturated soils under isotropic stress conditions", *Comput. Geotech.*, vol. 51, pp. 72-82, 2013.
<http://dx.doi.org/10.1016/j.compgeo.2013.02.002>
- [246] D. Manzanal, M. Pastor, and J. A. Fernández Merodo, "Generalized plasticity state parameter-based model for saturated and unsaturated soils. Part II: Unsaturated soil modeling", *Int. J. Num. Anal. Methods Geomech.*, pp. 1-19, 2010.
<http://dx.doi.org/10.1002/nag.983>
- [247] G.M. Rotisciani, G. Sciarra, F. Casini, and A. Desideri, "Hydro-mechanical response of collapsible soils under different infiltration events", *Int. J. Numer. Anal. Methods Geomech.*, vol. 39, no. 11, pp. 1212-1234, 2015.
<http://dx.doi.org/10.1002/nag.2359>
- [248] R. Hu, H.H. Liu, Y. Chen, C. Zhou, and D. Gallipoli, "A constitutive model for unsaturated soils with consideration of inter-particle bonding", *Comput. Geotech.*, vol. 59, pp. 127-144, 2014.
<http://dx.doi.org/10.1016/j.compgeo.2014.03.007>
- [249] M.D. Fredlund, G.W. Wilson, and D.G. Fredlund, "Use of the grain-size distribution for estimation of the soil-water characteristic curve", *Can. Geotech. J.*, vol. 39, no. 5, pp. 1103-1117, 2002.
<http://dx.doi.org/10.1139/t02-049>
- [250] A.R. Russell, and N. Khalili, "A unified bounding surface plasticity model for unsaturated soils", *Int. J. Numer. Anal. Methods Geomech.*, vol. 30, no. 3, pp. 181-212, 2006.
<http://dx.doi.org/10.1002/nag.475>
- [251] M. Feng, and D.G. Fredlund, "Hysteresis influence associated with thermal conductivity sensor measurements", *52nd Canadian Geotechnical Conference and Unsaturated Soil*

- Group, Proc. from Theory Practice Unsatur. Soil Mech.*, Canadian Geotechnical Society: Richmond BC, Canada, pp. 651-657, 1999.
- [252] T.M. Thu, H. Rahardjo, and E.C. Leong, "Soil-water characteristic curve and consolidation behavior for a compacted silt", *Can. Geotech. J.*, vol. 44, no. 3, pp. 266-275, 2007.
<http://dx.doi.org/10.1139/t06-114>
- [253] M. Nuth, and L. Laloui, "Effective stress concept in unsaturated soils: Clarification and validation of a unified framework", *Int. J. Numer. Anal. Methods Geomech.*, vol. 32, no. 7, pp. 771-801, 2008.
<http://dx.doi.org/10.1002/nag.645>
- [254] S. Oh, N. Lu, Y.K. Kim, S.J. Lee, and S.R. Lee, "Relationship between the soil-water characteristic curve and suction stress characteristic curve: Experimental evidence from residual soils", *J. Geotech. Geoenviron. Eng.*, vol. 138, no. 1, pp. 47-57, 2012.
[http://dx.doi.org/10.1061/\(ASCE\)GT.1943-5606.0000564](http://dx.doi.org/10.1061/(ASCE)GT.1943-5606.0000564)
- [255] Y.F. Dafalias, and L.R. Hermann, "Bounding surface plasticity I: Mathematical foundation and hypoplasticity", *J. Eng. Mech.*, vol. 112, no. 9, pp. 966-987, 1986.
[http://dx.doi.org/10.1061/\(ASCE\)0733-9399\(1986\)112:9\(966\)](http://dx.doi.org/10.1061/(ASCE)0733-9399(1986)112:9(966))
- [256] K. Hashiguchi, "Subloading surface model in unconventional plasticity", *Int. J. Solids Struct.*, vol. 25, no. 8, pp. 917-945, 1989.
[http://dx.doi.org/10.1016/0020-7683\(89\)90038-3](http://dx.doi.org/10.1016/0020-7683(89)90038-3)
- [257] K. Been, and M.G. Jefferies, "A state parameter for sands", *Geotechnique*, vol. 35, no. 2, pp. 99-112, 1985.
<http://dx.doi.org/10.1680/geot.1985.35.2.99>
- [258] S. Jocković, and M. Vukićević, "Bounding surface model for overconsolidated clays with new state parameter formulation of hardening rule", *Comput. Geotech.*, vol. 83, pp. 16-29, 2017.
<http://dx.doi.org/10.1016/j.compgeo.2016.10.013>
- [259] M.M. Futai, M.S.S. Almeida, and W.A. Lacerda, "Yield, strength, and critical state behavior of a tropical saturated soil", *J. Geotech. Geoenviron. Eng.*, vol. 130, no. 11, pp. 1169-1179, 2004.
[http://dx.doi.org/10.1061/\(ASCE\)1090-0241\(2004\)130:11\(1169\)](http://dx.doi.org/10.1061/(ASCE)1090-0241(2004)130:11(1169))
- [260] Y.J. Cui, and P. Delage, "Yielding and plastic behaviour of an unsaturated compacted silt", *Geotechnique*, vol. 46, no. 2, pp. 291-311, 1996.
<http://dx.doi.org/10.1680/geot.1996.46.2.291>
- [261] A.A. Garakani, S.M. Haeri, A. Khosravi, and G. Habibagahi, "Hydro-mechanical behavior of undisturbed collapsible loessial soils under different stress state conditions", *Eng. Geol.*, vol. 195, pp. 28-41, 2015.
<http://dx.doi.org/10.1016/j.enggeo.2015.05.026>
- [262] M. Mbonimpa, M. Aubertin, A. Maqoud, and B. Bussi ere, "Predictive model for the water retention curve of deformable clayey soils", *J. Geotech. Geoenviron. Eng.*, vol. 132, no. 9, pp. 1121-1132, 2006.
[http://dx.doi.org/10.1061/\(ASCE\)1090-0241\(2006\)132:9\(1121\)](http://dx.doi.org/10.1061/(ASCE)1090-0241(2006)132:9(1121))
- [263] M. Nuth, L. Laloui, and B.A. Schrefler, "Advances in modelling hysteretic water retention curve in deformable soils", *Comput. Geotech.*, vol. 35, no. 6, pp. 835-844, 2008.
<http://dx.doi.org/10.1016/j.compgeo.2008.08.001>
- [264] R. Hu, Y.F. Chen, H.H. Liu, and C.B. Zhou, "A water retention curve and unsaturated hydraulic conductivity model for deformable soils: Consideration of the change in pore-size distribution", *Geotechnique*, vol. 63, no. 16, pp. 1389-1405, 2013.
<http://dx.doi.org/10.1680/geot.12.P.182>

- [265] G. Della Vecchia, A.C. Dieudonné, C. Jommi, and R. Charlier, "Accounting for evolving pore size distribution in water retention models for compacted clays", *Int. J. Numer. Anal. Methods Geomech.*, vol. 39, no. 7, pp. 702-723, 2015.
<http://dx.doi.org/10.1002/nag.2326>
- [266] Y. Gao, and D. Sun, "Soil-water retention behavior of compacted soil with different densities over a wide range and its prediction", *Comp. Geotech.*, vol. 91, pp. 17-26, 2017.
<http://dx.doi.org/10.1016/j.compgeo.2017.06.016>
- [267] D.A. Sun, D. Sheng, L. Xiang, and S.W. Sloan, "Elastoplastic prediction of hydro-mechanical behaviour of unsaturated soils under undrained conditions", *Comput. Geotech.*, vol. 35, no. 6, pp. 845-852, 2008.
<http://dx.doi.org/10.1016/j.compgeo.2008.08.002>
- [268] Z.S. Li, J.M. Fleureau, and L.S. Tang, "Aspects of compaction and drying-wetting curves of a subgrade clayey soil", *Geotechnique*, vol. 67, pp. 1-7, 2017.
<http://dx.doi.org/10.1680/jgeot.16.T.010>
- [269] A. Jotisankasa, M. Coop, and A. Ridley, "The mechanical behaviour of an unsaturated compacted silty clay", *Geotechnique*, vol. 59, no. 5, pp. 415-428, 2009.
<http://dx.doi.org/10.1680/geot.2007.00060>
- [270] E.U. Klotz, and M.R. Coop, "On the identification of critical state lines for sand", *Geotech. Test. J.*, vol. 25, pp. 289-302, 2002.
- [271] D. Sun, J. Zhang, Y. Gao, and D. Sheng, "Influence of suction history on hydraulic and stress-strain behavior of unsaturated soils", *Int. J. Geomech.*, vol. 16, no. 6, p. D4015001, 2016.
[http://dx.doi.org/10.1061/\(ASCE\)GM.1943-5622.0000602](http://dx.doi.org/10.1061/(ASCE)GM.1943-5622.0000602)
- [272] R. Sharma, "Mechanical behavior of unsaturated highly expansive soil", *PhD thesis*, University of Oxford, UK, 1998.
- [273] A. Jotisankasa, A. Ridley, and M. Coop, "Collapse behavior of compacted silty clay in suction-monitored oedometer apparatus", *J. Geotech. Geoenviron. Eng.*, vol. 133, no. 7, pp. 867-877, 2007.
[http://dx.doi.org/10.1061/\(ASCE\)1090-0241\(2007\)133:7\(867\)](http://dx.doi.org/10.1061/(ASCE)1090-0241(2007)133:7(867))
- [274] A.N. Zhou, D. Sheng, S.W. Sloan, and A. Gens, "Interpretation of unsaturated soil behaviour in the stress – Saturation space, I: Volume change and water retention behaviour", *Comput. Geotech.*, vol. 43, pp. 178-187, 2012.
<http://dx.doi.org/10.1016/j.compgeo.2012.04.010>
- [275] C. Mihalache, and G. Buscarnera, "Is wetting collapse an unstable compaction process?", *J. Geotech. Geoenviron. Eng.*, vol. 141, no. 2, p. 04014098, 2015.
[http://dx.doi.org/10.1061/\(ASCE\)GT.1943-5606.0001226](http://dx.doi.org/10.1061/(ASCE)GT.1943-5606.0001226)
- [276] M. Lloret-Cabot, S.J. Wheeler, J.A. Pineda, E. Romero, and D. Sheng, "From saturated to unsaturated conditions and *vice versa*", *Acta Geotech.*, vol. 13, no. 1, pp. 15-37, 2018.
<http://dx.doi.org/10.1007/s11440-017-0577-6>
- [277] D. Zhang, J. Wang, C. Chen, and S. Wang, "The compression and collapse behaviour of intact loess in suction-monitored triaxial apparatus", *Acta Geotech.*, vol. 15, no. 2, pp. 529-548, 2020.
<http://dx.doi.org/10.1007/s11440-019-00829-3>
- [278] M. Pedrotti, and A. Tarantino, "A conceptual constitutive model unifying slurried (saturated), compacted (unsaturated) and dry states", *Geotechnique*, vol. 69, no. 3, pp. 217-233, 2019.
<http://dx.doi.org/10.1680/jgeot.17.P.133>
- [279] A.N. Zhou, D. Sheng, S.W. Scott, and A. Gens, "Interpretation of unsaturated soils behavior in the stress-saturation space. II: Constitutive relationships and validations", *Comput. Geotech.*, vol. 43, pp. 111-123, 2012.

- <http://dx.doi.org/10.1016/j.compgeo.2012.02.009>
- [280] A. Vatsala, and B.R. Srinivasa Murthy, "Suction in compacted states", *Geotechnique*, vol. 52, no. 4, pp. 279-283, 2002.
<http://dx.doi.org/10.1680/geot.2002.52.4.279>
- [281] A. Gens, E.E. Alonso, J. Suriol, and A. Lloret, "Effect of structure on the volumetric behavior of a compacted soil", *Proceedings 1st Int. Conf. on Unsaturated Soils, Alonso & Delage eds*, vol. 1, pp. 83-88, . Paris, France.
- [282] H. Hoffman-Riem, M.T. van Genuchten, and H. Flühler, "General model for hydraulic conductivity of unsaturated soils", F. J. Leij, and L. Wu, Eds., *Proceedings Int. Workshop on Characterization and Measurement of Hydraulic Properties of Unsaturated Porous Media*, University of California, Riverside: Calif., pp. 31-42, 1999.
- [283] N.T. Burdine, "Relative permeability calculation size distribution data", *Trans. Am. Inst. Min. Metall. Pet. Eng.*, vol. 198, pp. 71-78, 1953.
- [284] Y. Mualem, "A new model for predicting the hydraulic conductivity of unsaturated porous media", *Water Resour. Res.*, vol. 12, no. 3, pp. 513-522, 1976.
<http://dx.doi.org/10.1029/WR012i003p00513>
- [285] L. Alexander, and R.W. Skaggs, "Predicting unsaturated hydraulic conductivity from the soil-water characteristic", *Trans. ASAE*, vol. 29, no. 1, pp. 0176-0184, 1986.
<http://dx.doi.org/10.13031/2013.30123>
- [286] R.J. Kunze, G. Uehara, and K. Graham, "Factors important in the calculation of hydraulic conductivity", *Soil Sci. Soc. Am. J.*, vol. 32, no. 6, pp. 760-765, 1968.
<http://dx.doi.org/10.2136/sssaj1968.03615995003200060020x>
- [287] "Prediction of hydraulic properties of soils using particle-size distribution and bulk density data", *Proceedings of the Intenational Workshop on Indirect Methods for Estimating the Hydraulic Properties of Unsaturated Soils, Univ*, 1992pp. 317-328 California.
- [288] Y.Y. Mualem, "A catalog of the hydraulic properties of unsaturated soils", *Tech. Rep. Technion, Israel Inst. Technol.*, 1976.
- [289] R. Lenormand, "Liquids in porous media", *J. Phys. Condens. Matter*, vol. 2, no. S, pp. SA79-SA88, 1990.
<http://dx.doi.org/10.1088/0953-8984/2/S/008>
- [290] A. Peters, and W. Durner, "A simple model for describing hydraulic conductivity in unsaturated porous media accounting for film and capillary flow", *Water Resour. Res.*, vol. 44, no. 11, 2008.
<http://dx.doi.org/10.1029/2008WR007136>
- [291] M. Lebeau, and J.M. Konrad, "A new capillary and thin film flow model for predicting the hydraulic conductivity of unsaturated porous media", *Water Resour. Res.*, vol. 46, no. 12, 2010.
<http://dx.doi.org/10.1029/2010WR009092>
- [292] I. Fatt, "The network model of porous media, I. Capillary pressure characteristics", *Trans. Am. Inst. Metall. Pet. Eng*, vol. 207, pp. 144-159, 1956.
- [293] I. Chatzis, and F.A.L. Dullien, "Modelling pore structure by 2-D and 3-D networks with application to sandstone", *J. Can. Pet. Technol.*, vol. 16, no. 1, pp. 97-108, 1977.
<http://dx.doi.org/10.2118/77-01-09>
- [294] L.A. Ferrand, and M.A. Celia, "The effect of heterogeneity on the drainage capillary pressure-saturation relation", *Water Resour. Res.*, vol. 28, no. 3, pp. 859-870, 1992.
<http://dx.doi.org/10.1029/91WR02679>

- [295] G.R. Jerauld, and S.J. Salter, "The effect of pore-structure on hysteresis in relative permeability and capillary pressure: Pore-level modeling", *Transp. Porous Media*, vol. 5, no. 2, pp. 103-151, 1990.
<http://dx.doi.org/10.1007/BF00144600>
- [296] M.A. Ioannidis, I. Chatzis, and E.A. Sudicky, "The effect of spatial correlations on the accessibility characteristics of three-dimensional cubic networks as related to drainage displacements in porous media", *Water Resour. Res.*, vol. 29, no. 6, pp. 1777-1785, 1993.
<http://dx.doi.org/10.1029/93WR00385>
- [297] H. Rajaram, L.A. Ferrand, and M.A. Celia, "Prediction of relative permeabilities for unconsolidated soils using pore-scale network models", *Water Resour. Res.*, vol. 33, no. 1, pp. 43-52, 1997.
<http://dx.doi.org/10.1029/96WR02841>
- [298] B. Daneshian, G. Habibagahi, and E. Nikooee, "Determination of unsaturated hydraulic conductivity of sandy soils: A new pore network approach", *Acta Geotech.*, vol. 16, no. 2, pp. 449-466, 2021.
<http://dx.doi.org/10.1007/s11440-020-01088-3>
- [299] D.G. Fredlund, A. Xing, and S. Huang, "Predicting the permeability function for unsaturated soils using the soil-water characteristic curve", *Can. Geotech. J.*, vol. 31, no. 4, pp. 533-546, 1994.
<http://dx.doi.org/10.1139/t94-062>
- [300] T.F. Chiu, and C.D. Shackelford, "Unsaturated hydraulic conductivity of compacted sand-kaolin mixtures", *J. Geotech. Geoenviron. Eng.*, vol. 124, no. 2, pp. 160-170, 1998.
[http://dx.doi.org/10.1061/\(ASCE\)1090-0241\(1998\)124:2\(160\)](http://dx.doi.org/10.1061/(ASCE)1090-0241(1998)124:2(160))
- [301] R.E. Moore, "Water conduction from shallow water tables", *Hilgardia*, vol. 12, no. 6, pp. 383-426, 1939.
<http://dx.doi.org/10.3733/hilg.v12n06p383>
- [302] L.A. Richards, "Water conducting and retaining properties of soils in relation to irrigation", *Proc. of an International Symposium on Desert Research*, pp. 523-546, 1952. Jerusalem.
- [303] D.E. Elrick, and D.H. Bowman, "Note on an improved apparatus for soil moisture flow measurements", *Soil Sci. Soc. Am. J.*, vol. 28, no. 3, pp. 450-453, 1964.
<http://dx.doi.org/10.2136/sssaj1964.03615995002800030045x>
- [304] A. Nemes, M.G. Schaap, F.J. Leij, and J.H.M. Wösten, "Description of the unsaturated soil hydraulic database UNSODA version 2.0", *J. Hydrol. (Amst.)*, vol. 251, no. 3-4, pp. 151-162, 2001.
[http://dx.doi.org/10.1016/S0022-1694\(01\)00465-6](http://dx.doi.org/10.1016/S0022-1694(01)00465-6)

SUBJECT INDEX**A**

Adsorbed water 10, 45, 80, 141, 177
 Air phase 1, 2, 7, 8, 11, 12, 13, 15, 28, 38, 84
 dissolved 11
 water-dissolved 28
 Additional contact stress
 Analysis 2, 316
 sensitivity 316
 theoretical 2
 Axis translation technique 104, 130, 211, 238,
 247, 258, 265, 276

B

Bimodal structure 10, 11, 22, 40, 123, 172
 Bishop 1, 2, 6, 9, 10, 20, 22, 56, 57, 123, 124,
 147, 148, 223
 parameter 148
 Bishop's 4, 7, 8, 9, 18, 57, 150, 224
 equation 4, 7, 8, 9, 57, 224
 stress 18, 150
 Bonds 24, 54, 61, 71, 300, 315
 cavities 54
 converging 24, 61, 315
 dry 71
 macro 300
 micro 300
 Bounding surface 223, 232, 233, 234, 235,
 236, 237

C

Capillary 22, 206, 312
 bundle 312
 condensation 22
 phenomenon 206
 Cavities 47, 61, 64, 70, 315, 317
 contiguous 47
 dry 70
 proportion of 61, 317

spherical 315
 Clays 7, 26, 43, 45, 72, 91, 130, 132, 182,
 210, 214, 217, 258, 264, 296
 montmorillonite 130, 132
 plastic 72
 platelets 182
 silty 296
 Coarse kaolin 144, 146, 227 144
 Coefficients 28, 48, 118, 188, 192
 cluster 48
 contact friction 28
 lateral earth pressure 188, 192
 Collapse-expansion index 178
 Compaction 105, 156, 157, 160, 161, 184,
 188, 190, 211, 214, 218, 224, 275, 284,
 285, 293, 294, 295, 296, 303, 310 218
 mean stress 184
 process 156, 190
 static 105, 188, 190, 214, 224, 284, 293,
 294, 296, 303, 310
 stress 156, 160, 184, 296
 Compaction tests 286, 302
 static 302
 Compressibility index 287, 300
 Compression 123, 171, 183, 208, 247, 249,
 256, 258, 263, 264, 270, 284, 285, 288,
 289, 292, 293, 295
 expansion index 171
 isotropic 123, 247, 270, 289
 Compression indexes 118, 120, 121, 122, 175,
 177, 178, 179, 181, 183, 271, 258, 273,
 284, 286, 287, 288, 289, 296, 307
 effective 287
 elastic 287
 elastoplastic 258, 288, 289, 296
 global elastoplastic 183
 Compression line 4, 121, 284, 307
 saturated 4, 284, 307
 unsaturated 307
 Compression tests 175, 258, 284, 285, 288,
 300, 302
 drained 300

Eduardo Rojas

All rights reserved-© 2022 Bentham Science Publishers

Subject Index

undrained 284, 285
Compressive 125, 230
 behavior 230
 index 125
Computational constraints 30
Conditions 24, 33, 34, 38, 43, 46, 57, 60, 61,
 63, 67, 69, 77, 157, 188, 232, 290, 291,
 294
 drained 232, 290
 isothermal 77, 188
Confining 5, 29, 104, 105, 106, 107, 110, 121,
 211, 212, 240, 241, 242, 243, 246, 247,
 248, 273, 274, 277
 pressures 5, 104, 105, 106, 107, 110, 242
 stresses 29, 104, 110, 121, 211, 212, 240,
 241, 243, 246, 247, 248, 273, 274, 277
Connectivity 28, 37, 40, 60, 66, 71, 72, 77,
 106, 312, 315, 318
 matrices 28
Constant confining pressure 279
Constant suction 28, 122, 126, 129, 141, 152,
 161, 175, 284, 287, 288, 289
 stress 288
Constant volume 104, 176, 177, 179, 180,
 181, 184, 192, 194
 conditions 177
 swelling pressure test 180
 swelling tests 184
 test 104, 194
 wetting tests 179, 181
Constant water 188, 194, 270, 285, 288, 293,
 303
 conditions 285
 content 188, 194, 288, 293, 303
 tests 270
Constitutive 1, 256
 formulations 256
 surfaces 1
Construction principle 40, 43, 44, 50, 64
 angle, water-solid mineral 38
 forces 7, 27
Contact stresses 4, 8, 18, 26, 112, 122, 194
 additional 4, 18, 112, 122, 194
Controlled-suction tests 188
Correlation 24, 70, 88, 93, 101, 261, 315

Towards a Unified Soil Mechanics Theory 351

 statistical 24, 88
Coupled models, hydro-mechanical 221, 222,
 268
Coupling 9, 150, 172, 173, 176, 263
 function 176
 single-direction 172
Critical state theory 224, 225
 for saturated soils 224
Cycles 153, 174, 181, 182, 188, 221
 drying- loading 182
 drying-loading-wetting 153
 regular wetting-drying 181
 wetting-drying 188

D

Darcy's law 312
Deformable pore-network model 207
Deformation 8, 23, 26, 29, 151, 155, 205, 217,
 249, 254, 257, 283
 irreversible 29, 205
Dense sands 123
Densities 150, 151, 160, 161, 163, 164, 171,
 176, 177, 178, 182, 184, 186, 190, 192,
 197, 254, 256, 296, 297
 initial 160
 low 186
 relative 171, 176, 178, 182, 192, 197
Density functions 88, 317, 318
Deviator stress 19, 20, 104, 110, 111, 225,
 226, 229, 230, 234, 241, 242, 243, 244,
 245, 246
 numerical 241
Diameter oedometer 141
Direct 72, 112, 113
 porosimetry tests 72
 tensile test 112, 113
Distinct element models 26
Distribution 28, 29, 43, 44, 45, 57, 58, 69, 70,
 72, 86, 87, 99, 315
 adopted 87
 normal logarithmic 87
Drained 232, 235, 284, 285, 289, 293,
 295, 296, 299

- stress path 235
 - tests 232, 284, 285, 289, 293, 295, 296, 299
 - Dry 11, 105, 177, 180, 192, 194, 210, 211, 214
 - condition 11
 - density 105, 177, 180, 192, 194, 210, 211, 214
 - Drying 25, 29, 38, 57, 59, 63, 64, 65, 68, 69, 70, 71, 72, 73, 74, 84, 113, 115, 116, 125, 126, 127, 133, 141, 147, 153, 154, 156, 159, 179, 192, 193, 205, 211, 214, 218, 226, 229, 230, 254, 263, 289, 300
 - loading-wetting 154
 - path 141, 156
 - process 38, 63, 64, 65, 68, 69, 70, 71, 72, 73, 74, 84, 86, 113, 116
 - scanning path 159
 - wetting cycles 25, 29, 73, 147, 179, 192, 193, 214, 218
 - Drying path 141, 156
 - Dry volumetric weight 192
- E**
- Effect 62, 81, 190
 - boundary 62
 - combined 81
 - fading 190
 - Effective stress 1, 4, 6, 8, 10, 18, 56, 104, 110, 111, 118, 122, 129, 148, 151, 152, 156, 160, 175, 176, 179, 181, 182, 193, 204, 222, 225, 226, 270, 287, 291
 - concept 148, 175, 176, 222, 270
 - framework 179
 - plane 111, 152
 - principle 1, 118, 151, 204
 - tensor 8, 270
 - Elastic 125, 129, 141, 150, 153, 154, 160, 178, 181, 182, 183, 190, 237, 263, 295
 - behavior 129, 141, 153, 154, 178, 181, 190, 237
 - index 178, 183
 - recovery 125, 129, 160, 182, 263, 295
 - response 150
 - Elastic rebound 141, 164, 165, 230, 233
 - Elastoplastic 8, 27, 121, 141, 154, 155, 175, 190, 223, 230, 280, 287, 290
 - behavior 121, 155, 223, 230
 - contraction 190
 - deformation 280
 - model 175
 - Elastoplasticity 171, 254, 270, 284
 - Electron microscope 77
 - Equations 4, 5, 6, 7, 18, 57, 64, 65, 66, 68, 73, 75, 76, 118, 119, 147, 203, 206, 223, 255, 286, 312, 315, 323, 326
 - analytical 203, 223, 312
 - empirical 206
 - linear 315
 - probabilistic 57
 - Equilibrium 2, 10, 11, 14, 28, 105, 123, 174, 258, 293, 297, 315
 - forces 28
 - mass 315
 - vapor 258
 - Erratic behavior 262
 - Expansion 171, 173, 174, 176, 177, 178, 179, 181, 182, 183, 188, 192, 194, 196 188
 - index 171, 178, 179, 181, 182
 - pressure 194
 - tests 179, 192
 - Expansive 176, 178, 201
 - behavior 178, 201
 - pressure tests 176
 - Expansive soils 171, 172, 173, 175, 176, 182
 - behavior of 171, 172, 173, 175, 176, 182
 - Experimental SWRCs 87, 90, 91, 92, 99, 101, 106, 108, 113, 115, 195, 210, 239, 260, 315, 319
- F**
- Fabric 30, 222, 300
 - bonding 222
 - stress 300
 - Failure surface 2, 19, 20, 104, 107, 222

Subject Index

Flow 90, 175, 312, 314, 316, 318
 capillary 312, 316
 film 314, 316
 quasi-static 90
 rate, relative 318
 transient 175
Flow regime 326
 film 326
Forces 26, 27, 28, 141, 171
 capillary 27
 electrical 171
 electrical attraction 141
 repulsive 171
Framework 125, 129, 130, 134, 160, 161, 175,
 176, 183, 291, 293
 elastoplastic volumetric 183
Freeze-drying 84
Friction angle 2, 5, 104
Function of suction 20, 119, 130, 149, 164

G

Gas 11, 77
 phases 11
 xenon 77
Genetic algorithm 315
Grain size distribution 20, 22, 30, 71, 83, 104,
 123, 161, 183, 210, 237, 248, 256, 296,
 318

H

Hagen-Poiseuille 312, 316
 capillary flow 312
 equation 316
Hardening 126, 129, 149, 150, 151, 153, 159,
 165, 181, 190, 193, 222, 223, 228, 229,
 230, 270, 272
 anisotropic 222, 228, 229, 230, 270, 272
 isotropic 223
Hardening rule 223, 224
 common isotropic 223
Hoffman-Riem equation 313
Homogeneous isotropic material 15, 112
Hu's model 255

Towards a Unified Soil Mechanics Theory 353

Hydraulic 8, 56, 171, 204, 205, 222, 285
 behavior 8, 56, 171, 204, 205, 222, 285
Hydraulic conductivity 23, 312, 314, 315,
 316, 325, 326
 numerical 326
 of soils 312, 316
 predicted 325
 relative 23, 312, 314, 315
Hydromechanical coupling 56, 88, 104, 129,
 160, 175, 184, 254, 256, 270, 272, 284
 phenomenon 160, 270
Hydromechanical energy dissipation 222
Hydrometer test 72
Hysteresis 20, 23, 24, 56, 88, 147, 150, 152,
 203, 204, 207, 208, 224, 254
 hydraulic 20, 24, 204, 224
 phenomenon of 23, 203, 208, 254

I

Image processing 20
Intra-aggregated pores 172, 184
Isotherm generator 206
Isotropic 112, 118, 121, 134, 144, 161, 164,
 165, 168, 173, 211, 212, 213, 214, 218,
 223, 240, 273, 274, 280
 compression line 223
 compression tests 134, 240, 273, 274
 loading tests 144
 pressure 121
 stresses 112, 121, 161, 164, 165, 173, 211,
 212, 213, 214, 218
 triaxial test 118

K

Kaolin 319

L

Loading 23, 28, 29, 111, 121, 122, 123, 125,
 126, 127, 129, 134, 141, 142, 147, 150,
 151, 153, 156, 160, 164, 171, 173, 179,

- 181, 182, 183, 189, 190, 191, 194, 203, 208, 223, 227, 249, 255, 273, 289, 290, 291, 292, 293, 294, 295, 299, 302, 304
 - collapse yield surface (LCYS) 125, 126, 127, 147, 150, 153, 160, 164, 173, 179, 181, 182, 183, 189, 190, 191, 194, 227, 289, 290
 - compression index 191
 - drying tests 28
 - hydro-mechanical 255
 - isotropic 28, 121, 122, 123, 134, 141, 142, 208, 223
 - monotonic 249
 - path 126, 129, 151, 160, 171, 293, 295, 302
 - process 293
 - unloading semi-cycle 156
 - wetting tests 28
 - Loading collapse yield surface (LCYS) 151, 154, 183
 - compacted 183
 - hardened 151, 154
 - Loading stage 4, 28, 105, 113, 126, 151, 152, 164, 183, 188, 211, 299
 - drained 299
 - Loading surface 179, 235
 - neutral 179
 - Loading-unloading cycles 126, 191, 192, 229, 302, 306
 - cyclic 306
 - Local strain devices 273
 - Logarithmic 44, 80, 83, 86, 90, 91, 93, 99, 100, 104, 223, 257, 258, 260
 - distributions 86
 - function 223
 - normal distributions 44, 80, 83, 90, 91, 93, 99, 100, 104, 257, 258, 260
- M**
- Macrocavities 24, 43, 45, 46, 86, 88, 106, 113, 114, 123, 124, 209, 211, 218, 256, 257, 265, 299, 300
 - relative volume of 211, 265, 299, 300
 - Macropores 22, 23, 24, 71, 106, 118, 123, 124, 172, 174, 177, 203, 205, 208, 209, 254, 257, 260
 - relative volume of 106, 172, 209, 260
 - shrinkage of 23, 24, 118, 209
 - Macroporosity 150, 174
 - Macro-structural behavior 182
 - Mapping rule 234
 - Material 3, 208
 - collapsing 3
 - Matric suction 18, 26, 112, 177, 314
 - equivalent 177
 - Matric suction stress 18, 20, 107, 112, 113, 115, 116, 126, 130, 141, 142, 144
 - of soils 112, 113
 - Mechanisms of wetting and drying 46
 - Mercury 83, 84, 85, 90, 93
 - invasion 84, 85
 - pressure 84, 85
 - Mercury intrusion 72, 83, 84, 86, 87, 90, 94, 95, 96, 97, 98, 100, 102, 103, 105, 123, 172, 186, 207, 239
 - porosimetry (MIP) 72, 83, 87, 90, 94, 95, 96, 97, 98, 100, 102, 103, 105, 123, 172, 186, 207
 - porosimetry techniques 239
 - Mercury intrusion porosimetry (MIP) 83, 84, 85, 86, 87, 88, 90, 91, 92, 93, 99, 100, 102, 134, 184
 - method 86
 - tests 83, 84, 85, 86, 87, 88, 90, 91, 92, 93, 99, 100, 102, 134, 184
 - Microcavities 24, 43, 45, 46, 83, 86, 111, 113, 123, 124, 209, 211, 212, 218, 261, 263
 - Micrographs 72, 83, 86
 - scanning electron 83
 - Micropores 22, 23, 24, 71, 205, 208, 209, 215, 254, 261, 263
 - Microstructural behavior 182
 - Microstructure 10, 11, 172, 173, 175, 176, 177, 178, 179, 181, 182, 183, 186
 - shrink 182
 - swells 176, 177

Subject Index

Modeling 9, 27, 147, 150, 151, 173, 176, 178, 226, 232, 241, 257, 263, 264
 constitutive 9, 27
 micromechanical 27
 numerical 263
Modified Cam-clay model (MCCM) 3, 222, 224, 229, 232, 237, 270
Mohr-Coulomb failure condition 271
Monte Carlo procedure 43
Mualem's model 313

N

Net stress 2, 119, 104, 105, 122, 124, 125, 126, 127, 128, 133, 144, 148, 149, 150, 151, 156, 159, 164, 165, 166, 167, 169, 179, 181, 194, 290
 applied isotropic 164
 confining 2, 104
 isotropic 105, 144, 164, 165, 167, 169
 preconsolidated 133
 saturated preconsolidation 125
Net stress and suction 2, 118, 119, 148, 154, 173, 277
 combinations of 154, 227
Network 34, 40, 43, 44, 45, 49, 50, 51, 52, 56, 57, 62, 76, 77, 257, 312, 315, 316
 computational 49, 52, 56, 312
Network models 40, 43, 55, 56, 90, 92
 porous-solid 40
 probabilistic 55
Neutral Line (NL) 173, 174
Neutron tomography procedure 20
Nitrogen adsorption 72
Non-uniform connectivity 24
Normal distributions 44, 79, 80, 92, 105
 double logarithmic 105
 single logarithmic 80
Numerical 72, 88, 90, 91, 93, 94, 95, 96, 97, 98, 99, 102, 104, 106, 108, 110, 111, 114, 130, 132, 141, 163, 164, 165, 171, 183, 184, 188, 192, 194, 273, 274, 279, 280, 296, 297, 300, 314, 318, 325
 and experimental matric suction stress 111

Towards a Unified Soil Mechanics Theory 355

 comparisons 104, 164, 171, 183, 314
 PSD 88, 90, 91, 93, 94, 95, 96, 97, 98, 106, 108, 130, 132, 184, 297
 relative volume 114
 response 141
 simulations 99, 102, 163, 165, 188, 192, 194, 273, 274, 279, 280, 296, 300
 SWRCs 130, 297, 318, 325
 void ratio 72, 110
Numerical fitting 105, 141, 184, 185, 195, 211, 216, 239, 241, 247, 319, 325, 328

O

Oedometer cell 130, 188
Oedometric tests 188
Overconsolidated 122, 235, 248
 behavior 248
 materials 122, 235

P

Path 129, 130, 152, 154, 155, 156, 173, 179, 181, 205, 206, 230, 232, 284, 285, 290, 293
 drying-loading 129
 drying-wetting 130
 stress reduction 173
Percolation theory 79
Plastic 28, 183, 209, 214, 222, 223, 258
 deformations 222, 258
 expansion 183
Plasticity index 258, 272, 275
Pore(s) 1, 10, 15, 16, 22, 23, 24, 28, 34, 35, 36, 37, 38, 39, 45, 51, 52, 68, 73, 77, 83, 85, 87, 90, 123, 133, 172, 184, 185, 198, 206, 207, 280, 285, 312, 315
 connectivity of 37, 315
 cylindrical 90
 shrinkage of 22, 23, 206
 size-frequency functions 87
 space 315
 water pressure 1, 172, 280, 285

Pore size distribution (PSD) 23, 25, 30, 39, 49, 71, 72, 83, 88, 91, 92, 99, 104, 105, 123, 184, 186, 203, 205, 208, 211, 255
 bimodal 49, 123
 index 205
 monomodal 123
 tests 23
 trimodal 12

Porosimetry 80, 87, 111

Porosimetry tests 56, 57, 71, 72, 83, 84, 86, 89, 302, 306
 mercury intrusion 83, 84, 302, 306

Porous model 37, 38, 39, 86, 93, 316, 319, 321, 323, 325, 326, 328
 probabilistic 316

Porous network 23, 40, 43, 46, 59, 90, 114, 210, 312, 315, 316

Power function 254

Preconsolidation 119, 122, 126, 138, 142, 144, 147, 183, 229, 230, 231, 232, 236, 284
 stress 119, 122, 126, 138, 142, 144, 147, 183, 229, 230, 232, 236, 284

Pressure 1, 11, 12, 28, 83, 119, 148, 271, 280
 air and water 1, 11, 12
 atmospheric 119, 148, 271
 high mercury 83

Procedure 35, 65, 79, 203
 calibration 203
 reassemble 35

Process 28, 30, 33, 34, 36, 37, 39, 43, 46, 57, 59, 152, 154, 156, 161, 166, 207, 210, 256
 drainage 46
 drying-wetting 161
 fabric 30
 fabrication 166
 of drying and wetting 256
 transfer 28

Properties 6, 11, 20, 40, 44, 71
 geometrical 11
 mechanical 6

R

Recompression index 192

Relationship 7, 8, 23, 58, 61, 62, 68, 69, 88, 175, 177, 188, 206, 222, 254, 255, 286, 287, 290, 291, 313, 315
 analytical 222
 constitutive 8, 23
 elastic 8
 empirical 88
 linear 175, 177
 logarithmic 254
 semiempirical 206
 semilogarithmic 255

Relative 11, 44, 86, 93, 106, 113, 209, 212, 215, 218, 256, 312, 313, 314, 315, 316, 317
 humidity 11
 permeability of soils 314, 315, 316, 317
 volume factor 44, 86, 93, 106, 113, 209, 212, 215, 218, 256
 volumetric water content 312, 313

Relative conductivity 312, 314
 equation 312

Restrictions 24, 34, 39, 40, 44, 47
 additional 39
 geometrical 24, 40, 44

S

Sands 7, 10, 26, 43, 72, 91, 210, 214, 223, 232, 264, 269, 319
 clayey 264, 269
 graded 91
 silty 91

Saturated cavities 59, 61, 69, 70, 317
 volume of 61, 69

Saturated 1, 4, 6, 10, 11, 12, 15, 16, 17, 18, 19, 51, 52, 53, 57, 64, 65, 70, 71, 108, 116, 119, 121, 122, 123, 124, 125, 126, 133, 138, 149, 151, 152, 153, 175, 219, 224, 229, 231, 247, 248, 284, 286, 289, 291, 299, 307, 312, 317, 318

Subject Index

conditions 125, 126, 138, 149, 151, 152,
153, 284, 286, 289, 291, 307, 318
drained condition 299
elements 64, 65, 133, 312, 317
fraction 10, 11, 12, 15, 16, 17, 18, 51, 52,
70, 71, 108, 123, 124, 133
overconsolidated soil 231
permeabilities 175
permeability 312
pores 10, 51, 53, 57, 219
soils 1, 4, 6, 11, 18, 19, 116, 119, 121, 122,
224, 229
tests 18, 247, 248
Saturated material 2, 122, 123, 125, 154, 271,
284, 285, 289, 307
consolidated 125
Saturated preconsolidation 127, 129, 144, 157,
229, 271, 273, 286, 289, 295
stress 129, 144, 157, 229, 271, 273, 286,
289, 295
Saturation 6, 7, 8, 9, 10, 14, 16, 17, 18, 48, 56,
65, 105, 107, 120, 150, 175, 184, 199,
205, 223, 224, 270, 279, 286, 287
effective degree of 150, 199, 205, 223, 286,
287
suction 120
Scanning 42, 255, 272
hydro-mechanical 255
Scanning electron 86, 239
microscope 86
microscopy 239
Shear 18, 19, 111
strength equation 18, 19
test 111
Shrinkage 23, 122, 123, 173, 182, 209
progressive 23
Soil(s) 6, 7, 10, 11, 18, 22, 38, 46, 74, 83, 85,
86, 88, 91, 92, 104, 105, 113, 123, 124,
129, 142, 149, 177, 185, 188, 203, 204,
207, 208, 210, 211, 214, 218, 214, 221,
226, 229, 249, 254, 256, 257, 258, 272,
280, 295, 296, 301, 306, 312, 313, 316
bimodal 124
deformation 208, 254
expansion 188

Towards a Unified Soil Mechanics Theory 357

isotropic 11
mass 177
minerals 38, 85
plastic 86
porosity 6
properties 88
response 306
sandy 142
silty 229, 312, 316
swelling 185, 188
volumetric response of 123, 149, 296
water retention curve (SWRCs) 7, 22, 83,
88, 91, 92, 104, 105, 113, 129, 203, 204,
207, 211, 214, 221, 254, 257, 258, 313
Solids 11, 12, 15, 16, 24, 26, 28, 30, 33, 34,
35, 39, 43, 44, 45, 51, 52, 132, 133, 212,
215, 319, 321
neighboring 34
relative volume of 319, 321
Solid particles 4, 5, 6, 7, 8, 9, 10, 11, 12, 18,
22, 72, 83, 84, 112, 115, 116
Stiffness matrix 222, 237
symmetric 222
Strains 173, 177, 263
elastic 173, 263
reversible microstructural 173
Strength 1, 2, 6, 88, 104, 141, 142, 241, 246,
248, 249, 274, 279
behavior 6
equations 104
tensional 88
Stresses 1, 2, 5, 6, 8, 9, 112, 115, 116, 121,
127, 138, 151, 154, 156, 159, 171, 204,
223, 234, 226, 229, 231, 232, 234, 287,
306
artificial 6
bonding 112, 115
constitutive 287
equivalent states of 151, 154
state of 2, 151, 156, 159, 171, 204, 223, 234
tensile 112, 116
vertical effective 306
Stress 2, 6, 120, 151, 159, 223, 232
index 120
integration 120

state 151, 159, 223, 232
 variables 2, 6

Stress path(s) 104, 175, 177, 179, 181, 182, 193, 232, 233, 234, 235, 284, 285, 288, 290, 291
 mapping 235

Structure, solid-porous 39

Structured 44, 55, 123, 261, 312, 318
 material, double 55, 261
 soils 44, 123, 312, 318

Suction 19, 23, 46, 81, 87, 112, 120, 122, 125, 129, 133, 141, 142, 148, 154, 155, 173, 183, 193, 194, 227, 229, 247, 258, 262, 267, 273, 276, 280, 287, 293, 296, 302, 314
 controlled oedometer tests 194
 effective 287
 equalization 211
 equivalent 229
 inversion 183
 measurements 276, 302
 monitored oedometer test 273
 osmotic 112
 soil 19, 287

Suction hardening 118, 122, 126, 127, 129, 156, 222, 223, 224, 225, 226, 227, 229, 272, 273, 284, 289
 phenomenon of 156, 225, 226, 272, 273, 289

Suction stress 125, 155, 156, 159, 160, 179, 180, 181, 226, 227, 229, 262, 263, 268, 272, 284, 285, 287, 288, 289, 290, 291, 293, 294, 295, 299, 303, 306, 307
 effective 287
 equivalent 159
 evolution 263, 268
 variation 155, 160, 181, 262, 291, 294, 299, 303, 306

Swelling 171, 172, 173, 177, 178, 181, 184, 185
 aggregates 172
 crystalline 171
 double-layer 171
 index 177
 pressure 177

SWRC in wetting and drying 144

T

Techniques 20, 84, 86, 91, 130, 134, 141, 239, 241, 242, 258, 264, 265, 302
 air circulation 141
 fluid displacement 264
 fluid paraffin replacement 258
 freeze-drying 302
 image analysis 86
 osmotic 242
 psychrometer 91
 vapor circulation 130
 vapor equilibrium 258, 265

Tensile 112, 113, 116, 117, 141
 strength of soils 112, 141
 tests 112, 113, 116, 117

Tension 27, 83, 84
 air-water interfacial 27

Terzaghi's equation 18

Thermodynamics 17

Triaxial cell 105, 159, 211, 218, 224, 238, 247, 273, 275, 297
 double-walled 224
 suction-controlled 218

Triaxial tests 2, 7, 104, 160, 224, 227, 237, 242, 243, 246, 247, 251, 270, 275
 drained 237
 suction-controlled 160

U

Unified volumetric equation 125

Unloading 126, 130, 177, 182, 210, 273, 286, 304
 elastic 126

Unloading-reloading 118, 166, 171, 234, 235, 236, 271
 index 118, 171, 271
 line (URL) 166, 234, 235, 236

Unsaturated soils 1, 2, 8, 9, 18, 20, 22, 23, 26, 56, 112, 118, 125, 147, 165, 203, 222, 284, 285, 286

Subject Index

effective stress of 1, 18, 20
hydro-mechanical coupling of 147, 165
tensile strength of 112

V

Values, probability 75
Van Genuchten equation 224, 254, 323
Virgin compression line (VCL) 148, 153, 154,
223, 224, 225, 227, 228, 229, 235, 236,
284, 285, 291, 295
Void ratio 17, 30, 93, 121, 129, 130, 153, 154,
155, 164, 175, 177, 184, 192, 206, 215,
218, 222, 225, 235, 254, 255, 261, 262,
265, 268, 290
compactd 164, 184
critical 222, 225
global 17
Volume 44, 65, 71, 177, 209, 257, 276, 287
dry 65, 71
microvoid 287
proportional 44
Volume change 23, 104, 105, 182, 193, 203,
206, 211, 218, 224, 254, 273, 287
conditions 193
elastoplastic 287
global 273
Volumetric 106, 118, 119, 124, 125, 130, 148,
149, 151, 152, 175, 183, 203, 209, 219,
222, 223, 257, 271, 273, 284, 285, 286,
288, 296
behavior of unsaturated soils 118, 119,
124, 125, 130, 148, 149, 222, 284, 285,
286, 288
compression 148
dry 183
elastoplastic framework 151
plastic deformations 219
plastic strains 151, 152, 175, 209, 219, 223,
257, 271, 273
reduction 106, 119, 203, 296
Volumetric behavior of 6, 119, 121, 122, 231
overconsolidated soil 231
saturated soils 6, 119, 121, 122, 231

Towards a Unified Soil Mechanics Theory 359

soils 6, 119, 121, 122
Volumetric deformation 123, 125, 203, 204,
205, 206, 207, 209, 210, 215, 218, 219,
221, 254, 256
analytical 218
plastic 203, 210
Volumetric response 9, 27, 29, 123, 130, 133,
141, 144, 148, 164, 172, 176, 203, 249
numerical 130, 141
plastic 9
Volumetric strains 76, 126, 151, 164, 165,
166, 167, 168, 169, 173, 175, 182, 196,
241, 242, 246, 248, 249, 258, 262, 267,
272, 276, 279, 287, 289, 294
elastic 173, 289
elastoplastic 126, 182, 287, 294
influence of 76
macrostructural elastoplastic 173
numerical 165, 267

W

Waals interactions 45
Water 1, 2, 11, 12, 15, 16, 17, 18, 38, 47, 61,
62, 63, 85, 141, 207, 276, 280, 285, 300,
315
deionized 300
menisci forces 141
pressures 1, 2, 11, 12, 15, 276, 280
Wetting 46, 48, 49, 50, 51, 57, 58, 59, 61, 62,
72, 73, 79, 80, 104, 133, 144, 146, 147,
151, 155, 161, 163, 179, 183, 185, 190,
206, 211, 264, 272, 273, 291, 296, 300,
316
and drying 50, 57, 59, 79, 133, 144, 146,
183, 185, 296, 300
boundaries 51
conditions 316
cycle 73, 211
reversal 206
simulating 273
Wetting-drying 25, 57, 176, 181, 182, 183,
184, 188, 189, 190, 191, 192, 193, 196,
197, 198, 204, 255

paths 193, 204
processes 57
tests 176, 182
Wetting process 38, 46, 47, 51, 57, 59, 60, 61,
66, 75, 164, 317

X

X-ray tomography 20

Y

Yield surface
Young-Laplace equation 27, 38, 51, 83, 84,
90, 207, 312, 318



Eduardo Rojas

Eduardo Rojas graduated as Civil Engineer at the National Center of Technical and Industrial Education (CeNETI) in Mexico in 1980. He obtained his Master and PhD degrees in Soil Mechanics at the Institut de Mécanique de Grenoble (IMG), France, in 1982 and 1984, respectively. He was associate researcher at the Institute of Engineering (II) in the Universidad Nacional Autónoma de México (UNAM) from 1984 to 1996 and chairman of the Department of Soil Mechanics in the Postgraduate Division of the Faculty of Engineering, UNAM, from 1993 to 1996. He has been a research-professor at the Universidad Autónoma de Querétaro (UAQ) since 1996 where he teaches the courses of Geotechnical Engineering and Foundations at the undergraduate level and Unsaturated Soil Mechanics at postgraduate level. He was chairman of the Physics and Mathematics Research Center of the UAQ from 1998-2004. He has been awarded three times the Alejandrina award in Science and Technology for the years 2002, 2004 and 2018. He is currently a member of the National Research System (SNI). In combination with his academic activity at the university, he works as a consultant engineer and has participated in different engineering projects covering several topics from the underpinning of tilted buildings, stability of slopes during heavy rains, to the design of deep and shallow foundations on different types of soils including expansive, collapsing, dispersive and highly compressive materials. He has published 3 books, 9 chapters of books, 45 papers in international journals, and 102 papers in national and international congresses.